SAND77-8513
Unlimited Release

UC-62

Highlights Report
Solar Thermal Conversion Program
Central Power Projects

Prepared by Sandia Laboratories, Albuquerque, New Mexico 87115 and Livermore, California 94550 for the United States Department of Energy under Contract AT (29-1)-789.

Printed November 1977

Sandia Laboratories
energy report

Issued by Sandia Laboratories, operated for the United States Department of Energy by Sandia Corporation.

Printed in the United States of America
Available From
National Technical Information Service
U. S. Department of Commerce
5285 Port Royal Road
Springfield, VA 22161
Price: Printed Copy $6.75; Microfiche $3.00

SAND77-8513
Unlimited Release
Printed November 1977

UC-62

HIGHLIGHTS REPORT
SOLAR THERMAL CONVERSION PROGRAM
CENTRAL POWER PROJECTS

Sponsored by

Energy Research and Development Administration*
Division of Solar Energy
Washington, D. C.

ABSTRACT

This report presents the highlights of the Energy Research and Development Administration (ERDA) Solar Thermal Branch Semiannual Review held in Seattle, Washington, on August 23-24, 1977. The review covered status and and plans for Central Receiver Projects, the Solar Thermal Test Facility Project, and the related research and development activities.

*Effective October 1, 1977, the Energy Research and Development Administration became part of the Department of Energy.

ERDA SOLAR THERMAL CONVERSION PROGRAM
CENTRAL POWER PROJECTS SEMIANNUAL MEETING
SEATTLE, WASHINGTON - AUGUST 23-24, 1977

Agenda

(continued)

INTRODUCTION

ERDA, through its Division of Solar Energy, is engaged in research and development efforts leading to the commercialization of solar thermal power plants, which are expected to supply substantial quantities of the United States' future electric power needs during the post-1985 period. The objectives of these efforts are: (a) to verify the technical and economic feasibility and environmental acceptability of the solar energy power system concepts for intermediate load application and, (b) to provide the solar technology that will allow the solar plants to be economically competitive.

Elements of the solar thermal power plant projects include: (a) current technology systems, (b) advanced technology systems, (c) continuing analytical studies to provide guidelines in the planning of these programs, (d) a 50MW_t solar thermal test facility designed to assist in the evaluation of experimental receiver configurations, and (e) a 400-kW_t solar thermal test facility.

The current technology systems element is aimed at the introduction of competitive solar electric power with minimum risk. Of the possible solar power concepts, the point focus system, namely the central receiver, offers the promise of high performance with a reasonable cost of electricity if ERDA cost goals can be met. The central receiver concept is being developed through the construction of a pilot plant at an early date. To reduce risk, a steam receiver (boiler) with conventional electrical utility operating temperatures and pressures was selected for the preliminary design so that conventional electric power generation technology could be used.

The advanced technology systems element includes the definition and development of power plants which have the potential to produce electricity at costs substantially below those for current solar technology systems and which may also offer improvements in the operation, market potential, and environmental impact of the solar plants. System studies and large-scale experiments are planned for potentially attractive concepts, such as the Brayton and liquid metal Rankine cycle plants. Several research projects are currently funded to investigate alternate steam Rankine and advanced Brayton cycle receiver concepts. Additional advanced central solar plant concept system and advanced heliostat studies will be initiated in 1977.

Analytical support studies are conducted to evaluate various candidate solar thermal systems and applications and to assess their commercialization potential and their impact on environment and national resources. Previous studies of the central solar power plants for the southwestern U. S. have identified the intermediate load central receiver plant as the concept offering the greatest market penetration potential. Ongoing studies of this concept have extended these evaluations to other geographical locations in the U. S.

This report summarizes information presented at the ERDA Solar Thermal Projects Semiannual Review held August 23-24, 1977. Emphasized are results developed since the previous meeting was held in December 1976.

SOLAR CENTRAL RECEIVER PROGRAM ACCOMPLISHMENTS AND PLANS

G. Kaplan, ERDA

During fiscal year 1977, the following accomplishments were realized:

- Test Facilities

  - Construction began on the 5-MW solar thermal test facility in Albuquerque. The facility is scheduled to accept the first 5-MW pilot plant receiver in December 1977.

  - Construction of the Francia-type 400-kW solar steam generating plant at Georgia Institute of Technology is nearing completion. All major systems have been installed, and low-power startup of the system is scheduled for the middle of September 1977.

  - A Users Association has been formed in Albuquerque to provide an interface between potential industrial users and the solar test facilities at Sandia Laboratories and Georgia Institute of Technology.

- Research and Development

  - Overall system studies have been performed on the central receiver system.

  - Preliminary design studies have been performed on five heliostats, three receivers, and three thermal storage systems.

- Support to EPRI

  ERDA personnel have been providing analytical support to EPRI in connection with EPRI's development of the Brayton cycle receiver.

During fiscal 1977, the following activities were initiated:

- Public Service of New Mexico Retrofit Study

  A study has been initiated to determine the feasibility of using solar energy to supplement the fossil fuel supplies in existing Public Service of New Mexico (PSNM) plants.

- Low-Cost Heliostat

  Requests for proposals on low-cost heliostats were sent to prospective firms. The submitted proposals have been evaluated, and four of the proposals received have been recommended for funding.

- Advanced System Concept

  Studies of second-generation central receiver systems have been initiated. These advance systems include Brayton (air cycle), liquid metal, and molten salt receivers. These studies will continue through FY78.

For fiscal 1978, $60.1M have been budgeted for operations and $41.0M for construction in the solar thermal power program. Approximately 40-50% of these operating funds are dedicated to the central receiver pilot plant.

The following activities are scheduled for fiscal 1978:

- Operation of Solar Thermal Test Facility

  This facility is scheduled to begin operations in FY1978, with full operation scheduled for 1980.

- Issue RFPs

  Requests for proposals will be issued for development of water/steam receivers and for solar/fossil fuel hybrid systems.

- Sign International Energy Agency Implementing Agreement

  The purpose of this agreement will be a joint study of liquid metal central receiver systems and distributed systems in the 500-kW range.

- Low-Cost Heliostat RFP

  A second set of requests for proposals for low-cost heliostats will be distributed and the submitted proposals evaluated. The heliostat development initiated by the FY77 RFPs will also be continued.

OVERVIEW

A. C. Skinrood, Sandia Laboratories

A two-year research and development program to develop technology for a 10-megawatt electric (MW_e) solar central receiver pilot plant (Figure 1) has been completed. This represents a major milestone in the Energy Research and Development Administration's program to collect and use solar energy to produce electricity on a commercial scale. This plant, the first of its kind, will be built in Barstow, California, starting in 1978. It will provide direct operating costs and will aid in identifying solar plant operating unknowns and indirect costs, all of which must be known in order to assess the economic viability of a commercial central receiver power plant.

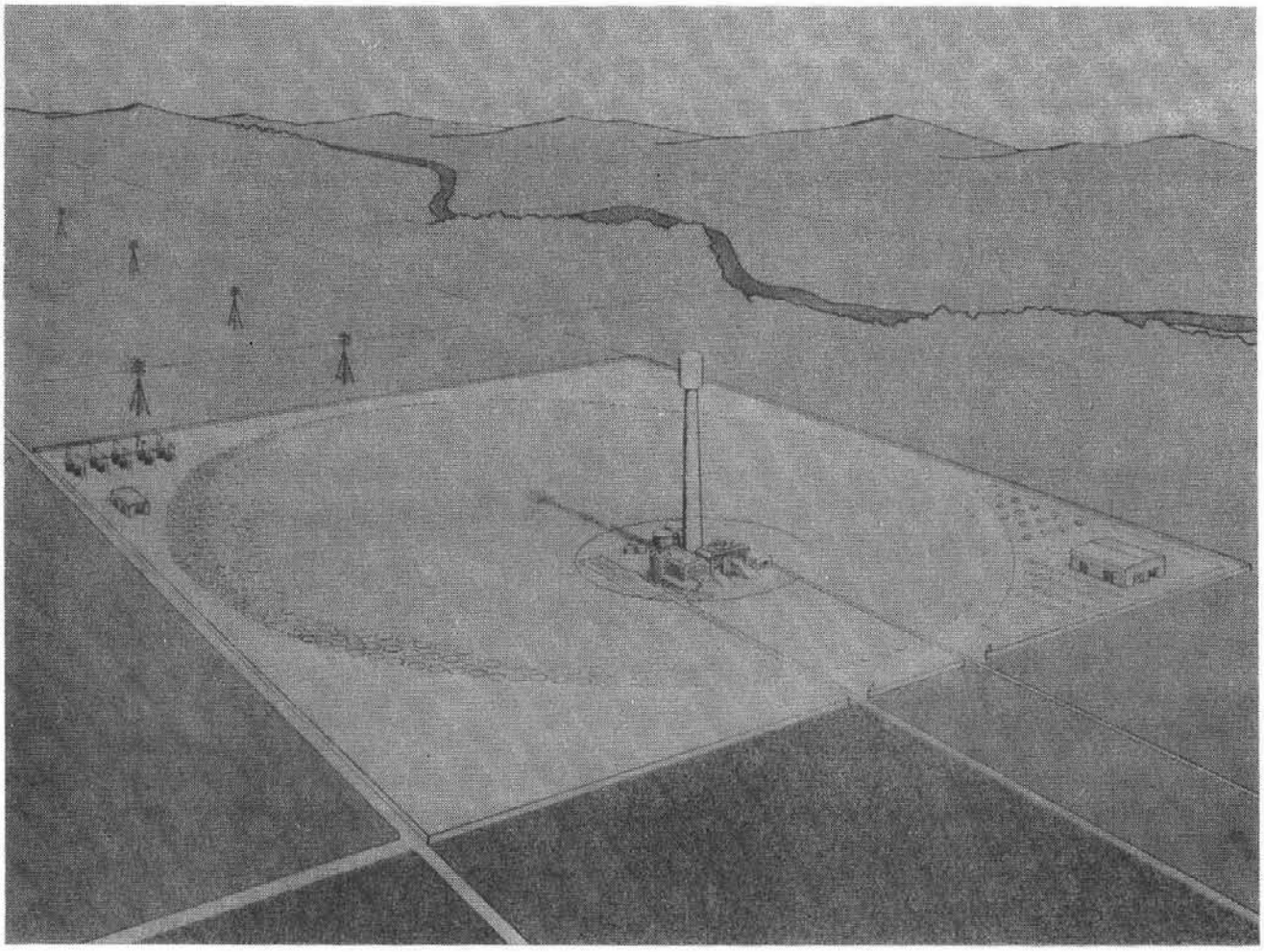

Figure 1. 10-Megawatt Solar-Electric Pilot Plant

Under the sponsorship of the Energy Research and Development Administration and the technical management of Sandia Laboratories, Livermore, California, three contract teams--headed by Honeywell, Martin Marietta, and McDonnell Douglas--have completed parallel and competing programs to develop conceptual designs for the pilot plant. Concurrent with these efforts, a fourth contractor, Boeing Engineering and Construction, designed a heliostat which could be incorporated into the three pilot plant designs. During this period, the contractors built and tested experimental collectors, receivers, and energy storage systems to assess the technical feasibility of these designs. In addition, materials testing has been done on adhesives, storage oil, glass, and other key elements of the designs.

Sandia Laboratories has completed an intensive three-month program to evaluate and analyze the results of the contractor's work and has recommended a conceptual design for the pilot plant to ERDA.

A workshop on collector computational methods was organized for Sandia by the University of Houston and held in August, 1977. The purpose was to disseminate analytical techniques to industry.

Extended heliostat testing has begun at Sandia for each of the four collector designs in order to gain continuous operating experience under identical operating conditions. Second-generation technology development has begun at Sanders and Dynatherm where ERDA-sponsored work is underway on receivers that use heat transport other than water/steam. Additional studies will be initiated in September, 1977, on receivers using sodium, molten salt, and air as the heat transport fluid. The study of receiver geometry will be continued; various configurations of both cavity and external receivers are being developed.

Second-generation heliostat development will be started through the placement of contracts at several companies in September, 1977. Although the present designs have excellent performance, much work remains to be done to achieve the ERDA goal of $65 per square meter of reflective surface.

The commercial acceptance of solar thermal electric power may be tied to the ability to store large quantities of thermal energy. Most of the storage concepts presently being pursued are relatively expensive, and therefore, additional energy storage research and development is needed.

FIELD PROGRAM MANAGEMENT

Jack Blasy, ERDA/SAN

The subject of Field Program Management for the Solar Thermal Program has been discussed before. However, I think it would be useful to discuss it briefly again for those who may be new to the program and also because of some recent changes, such as the establishment of a 10-MW Pilot Plant Project Office at SAN. As most of you know, the Central Power Systems Branch, headed by George Kaplan in the Division of Solar Energy, Headquarters, provides overall program direction. The San Francisco Operations Office and the Albuquerque Operations Office provide contract administration and program management. At present, SAN holds most of the contracts for the program except for Sandia Laboratories which is held by Albuquerque Operations Office.

It is important to understand the distinction between the 10 MW Project Office headed by Dick Schweinberg and the Solar Energy Division which I direct. Basically, Dick's project office will be responsible for seeing that the facility is built on time and within cost, and managing both the procurements required and the construction contractors' efforts. The contract administration and management of the four major design contractors, as well as the management of the low-cost heliostat and advanced receiver work, is handled by Bob Hughey, Doug Elliott, and Mark Schanfein in the Solar Energy Division.

Contract administration involves contract negotiation and execution as well as continuing administration of legal, safety, and financial requirements. Program management is a function performed for both the Headquarters Division of Solar Energy Program Director and for the Field Office Contracting Officer. Program management includes:

1. Finalizing and definitizing work statements, project milestones, and work products

2. Comparing actual progress versus milestones and cost projections

3. Anticipating problems and taking or recommending actions to resolve them

4. Certifying payment vouchers

5. Authorizing scope and schedule changes

6. Dealing with State Regional entities.

In all of the functions, SAN works closely with Sandia Laboratories and the Aerospace Corporation. Sandia Laboratories, Livermore (SLL) is the Technical Manager of the Central Receiver Program, acting for the Headquarters Solar Division Program Director. In this capacity, SLL:

1. Interprets, defines, and refines work statements and schedules

2. Maintains continuing technical surveillance over all contractor activities

3. Provides technical direction and guidance to the contractors to facilitate accomplishment of the work scope

4. Advises and assists ERDA in program planning.

The Aerospace Corporation provides overall planning and advice to the Headquarters Solar Program Director for the entire Solar Thermal Program, of which the Central Receiver is an important element. The Solar Thermal Program also includes total energy systems, distributed collectors, irrigation, and research projects. The Aerospace Corporation assists the Program Manager in assuring that all these elements fit into a consistent and comprehensive total program. The contractors perform what is the most important part of the program, the actual technical effort. Advisors from other Federal and State agencies and from the Electric Power Research Institute bring to bear important evaluations and guidance from their areas of responsibility and expertise.

10-MW SOLAR PILOT PLANT FROM A UTULITY POINT OF VIEW

J. Lynn Rasband, Southern California Edison

Daily Generation Planning Considerations

For a solar electric plant to be of value to a utility, it must be capable of generating electricity when the utility most needs the generating capacity, which is generally at the time of the daily peak load. Figures 2 and 3 illustrate a realistic peak load shape for an electric system and coincident collector output patterns for August (the summer peak month) and December (the winter peak month). The daily peak load and the sunfall, or solar energy input to the solar generating unit, are nearly coincident during the summertime. However, the sunfall is ended before the daily peak load occurs during the wintertime. The integration of an energy storage device into a solar generating unit would allow the production of electrical energy to be deferred until the time of the daily peak load. A solar unit with an energy storage capability would therefore have greater "capacity value" to the system than a solar unit with no energy storage capability.

System Operation Considerations

The introduction of solar generation into electric utility systems will affect four aspects of electric system operation: daily capacity planning, automatic generation control, spinning reserve, and maintenance.

Implementing a peak shaving dispatch strategy using solar energy complicates daily capacity planning and suggests that increased use of weather forecasts and telemetered sunfall data may be required. Similarly, computer programs to optimize combined solar and thermal generation may be necessary to assist operating personnel in optimizing the use of solar generation.

More complicated automatic generation control algorithms than are presently used by the utilities will be required to handle solar unit output variations that cannot be buffered effectively with storage. Adaptive Automatic Generation Controls for solar may be needed to anticipate collapses of solar input during cloudy periods and rapid recoveries thereafter. Telemetering of sunfall data may be required to dependably execute these algorithms.

Solar units with storage are likely to be subjected to the "spinning reserve" performance standards now applied to energy limited hydroelectric units. Such standards require that in order for a unit to be considered as on-line during any hour, it must have at least two hours of energy production capability in storage.

Optimal maintenance strategies for large solar systems will require a departure from present practice, and solar units will have to be designed so that outages can be deferred until noncritical hours.

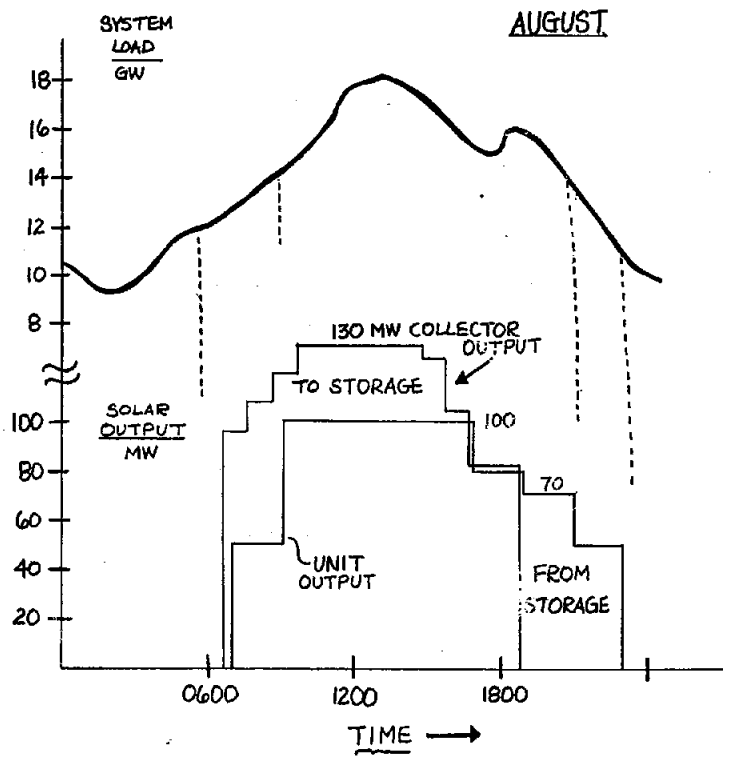

Figure 2. Peak Load Shape For an Electric System and Coincident Collector Output Patterns

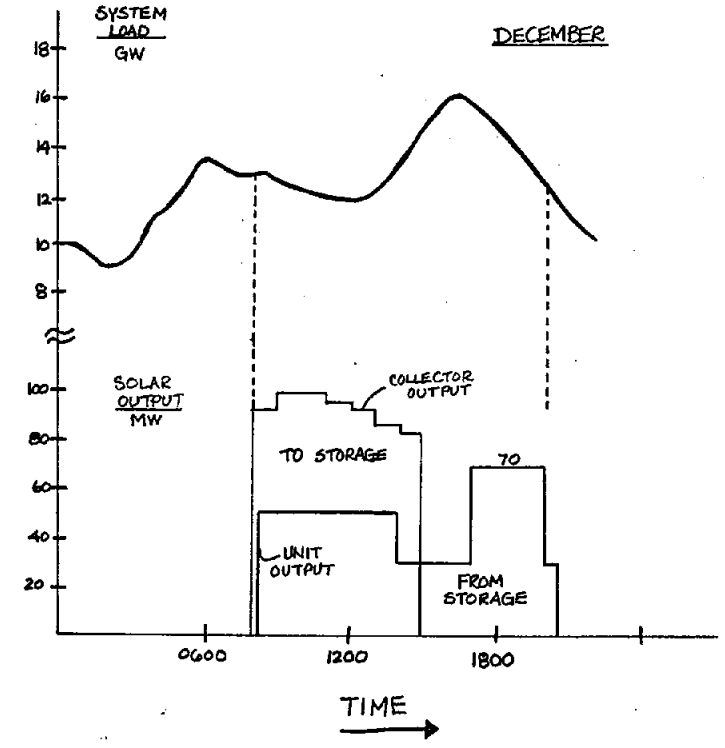

Figure 3. Peak Load Shape For an Electic System and Coincident Collector Output Patterns

In summary, as the amount of solar generation in an electric system increases, additional sophistication in system operation will be essential to fully benefit from its capabilities. In most cases, system operation computer programs and algorithms currently available or in effect can be adjusted and/or expanded to properly effect the integration of solar.

Reliability Considerations

Both the amount of solar generation included in the electric utility's aggregate resources and the amount of thermal energy storage associated with solar generating units have significant effects on the value of solar generating units to a utility.

Figure 4 illustrates the variation in reserve margin requirements as a function of solar penetration in the system. As illustrated, at any fixed amount of storage, the reserve margin requirements increase as the level of solar generation increases. Figure 3 also indicates that for a given level of solar penetration, margin requirements are reduced by an increase in the amount of thermal energy storage and the attendant increase in collector capability. Figure 5 shows that the effective load carrying capability of the solar generation is reduced as the solar penetration increases.

From Figure 5 it is apparent that the solar units can have significant load-carrying capability under certain conditions, but in all cases it is less than that of the average conventional unit. With modest amounts of storage, solar units have significant capacity value at low solar percentages, and with substantial amounts of storage the same is true at higher percentages. This suggests that the first solar units may require relatively little extended operation capability to achieve close to their full potential usefulness in a generating system.

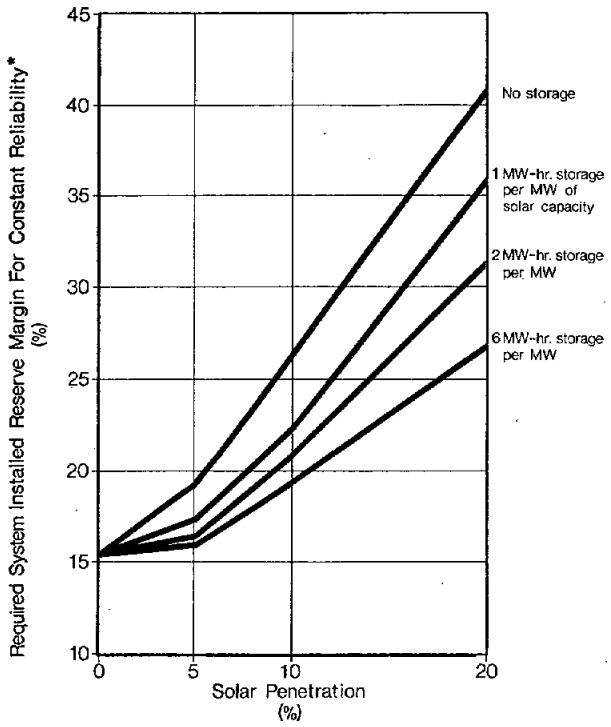

*Loss Of Load Probability Held Constant At 1 Hour Of Outage (Total) In 20 Years

Figure 4. Required Installed Reserve Margin Versus Solar Penetration

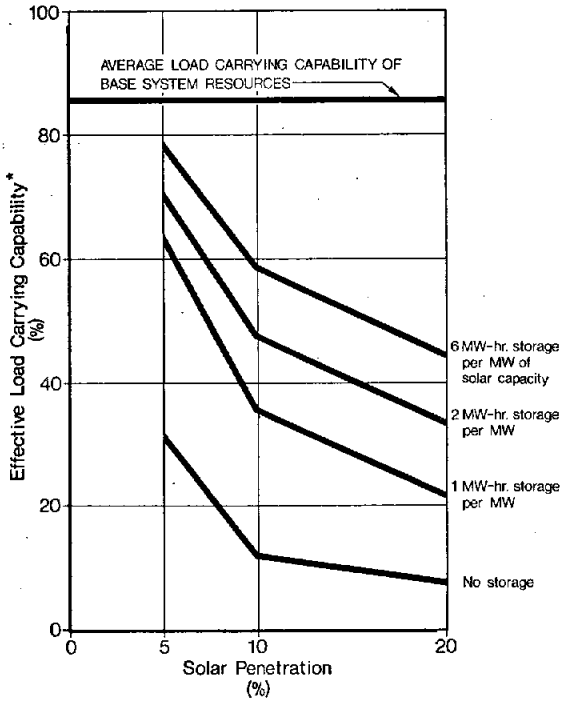

*Loss Of Load Probability Held Constant At 1 Hour Of Outage (Total) In 20 Years

Figure 5. Effective Load Carrying Capability of Solar Generation Versus Solar Penetration

ADVANCED CENTRAL POWER SYSTEMS ANALYSIS

Prem N. Mathur
The Aerospace Corporation

The Aerospace Corporation is conducting studies on advanced systems to assist ERDA in overall program planning and in formulating and directing the Advanced Central Receiver Power Systems Project. These efforts involve application analyses and other activities as outlined below in Table I.

TABLE I. ANALYSIS AND SUPPORT TASKS

1. Systems and Applications Analysis
   - Analysis and Evaluation of Advanced Options
   - Utility Application Studies
   - Advanced Systems Methodology Development
2. Storage Application Studies
   - On-Site Storage Analysis
   - Utility System Storage Analysis
3. Societal Impact Studies
4. Technical and Management Support

Study Objectives

The objectives of the systems and application analyses tasks are to define and analyze cost effective options, and evaluate their operating economics when integrated in a large electric utility. These studies will focus on parametric analysis as a function of various utility system parameters such as plant sites, insolation and load demand characteristics, reliability criteria and dispatch strategies. Major emphasis has been placed on the development of flexible methodology to conduct the application analyses for advanced systems involving different storage and power conversion subsystem characteristics.

The storage application studies are aimed at the definition of system requirements and evaluation of relative economics of solar plants involving two generic storage concepts. These are: on-site plant storage and central utility system storage. The utility system storage is an electric generation plant which utilizes storage techniques such as pumped hydro or advanced

batteries to supply electrical energy directly to the utility grid. The application analyses include the investigation of the use of various types of utility storage systems in conjunction with solar plants for peak shaving operations.

The objectives of the societal impact study are to develop data for supporting rationale for advanced solar electric plants in terms of their societal benefits or disbenefits over conventional power generation alternatives. The technical and management support task includes independent evaluations, reviews, specification updating, and industry study tasks to support ERDA/SAN and Sandia, Livermore in the management of industry studies.

System Analysis

An area of current interest is the identification and comparative evaluation of the various possible cost effective options for advanced systems. A preliminary analysis of this subject along with an analysis of a related issue of on-site storage performance requirements is presented below.

Table II presents a matrix of possible systems and subsystem options involving: (1) advanced steam cycles with higher operating steam temperatures and pressures than those used in current technology steam system, (2) improved steam reheat cycles and storage using liquid sodium (or molten salt) cooled receiver and storage, (3) various Brayton cycles including combined gas turbine-steam cycle, and (4) other binary cycles. An important variation of the water-steam or Brayton systems is the hybrid operation in which fossil combustion can be used in various ways to augment the solar energy. Examples of interest include: (1) a solar fossil hybrid system in which solar plant storage is replaced by fossil combustion equipment, and (2) hybrid systems in which the outlet fluid from a lower temperature (or technology) receiver or storage is boosted to higher temperatures by fossil combustion to enhance turbine, receiver, and system performance.

In order to make a comparative evaluation of the various advanced systems options on a uniform and consistent basis, the characteristics of current technology water-steam systems are used as reference and as a point of departure. Various systems are synthesized and integrated into a utility system using a consistent set of design criteria and assumptions as outlined in Table III. The particular comparison made in this analysis utilizes busbar energy cost as measure of merit. The results of some of these analyses are presented in Figure 6 for various levels of technology indicated by turbine inlet temperature. The energy costs for all system designs have been normalized with respect to that for current technology water-steam reference system to indicate relative improvements for different systems and technology levels.

TABLE II. ADVANCED SYSTEMS OPTIONS

- ALTERNATE SUBSYSTEM IMPLEMENTATION OPTIONS

SYSTEM CONCEPT (cycle)	DESIGN CONDITIONS	STORAGE	RECEIVER	OTHER
• ADVANCED WATER-STEAM	>950°F/1500 psia	• THERMAL	STEAM	• NO REHEAT
• SODIUM (or molten salt) STORAGE/RECEIVER	≥ 950°F/1500 psia	• Na/SALT SALT	Na SALT	REHEAT REHEAT • HYBRID
• BRAYTON SYSTEMS - OPEN-SIMPLE - OPEN-REGENERATIVE - CLOSED-REGENERATIVE - COMBINED CYCLE	• AIR OR GAS TURBINE INLET 1500°F-2250°F • AIR COOLED TURBINE	• SOLID/GAS • FOSSIL • OTHER	• AIR • HELIUM FOR CLOSED CYCLES	• FOSSIL BOOST • CERAMIC COATINGS
• BINARY CYCLES - GAS TURBINE/ORGANIC BOTTOMING - POTASSIUM TOPPING	• ORGANIC BOTTOMING • TOPPING 1500°F	• SOLID/GAS • LIQUID Na	• AIR • POTASSIUM	--

TABLE III. COMPARATIVE ANALYSIS ASSUMPTIONS

- CURRENT TECHNOLOGY WATER-STEAM REFERENCE
- ADVANCED SUBSYSTEMS/SYSTEMS PERFORMANCE AND COSTS BASED ON SCALING AND EXTRAPOLATION OF AVAILABLE DATA
  - INYOKERN SITE
  - 100 MW_e SIZE PLANTS
  - 6 hr THERMAL STORAGE
- SYSTEMS SYNTHESIZED FOR SAME EFFECTIVE CAPACITY FACTOR
- ECONOMIC ANALYSIS BASED ON LEVELIZED COSTS, 1990 START DATE
- COLLECTOR PERFORMANCE, HELIOSTAT COST AND RESERVE MARGIN ASSUMED SAME FOR ALL SYSTEMS

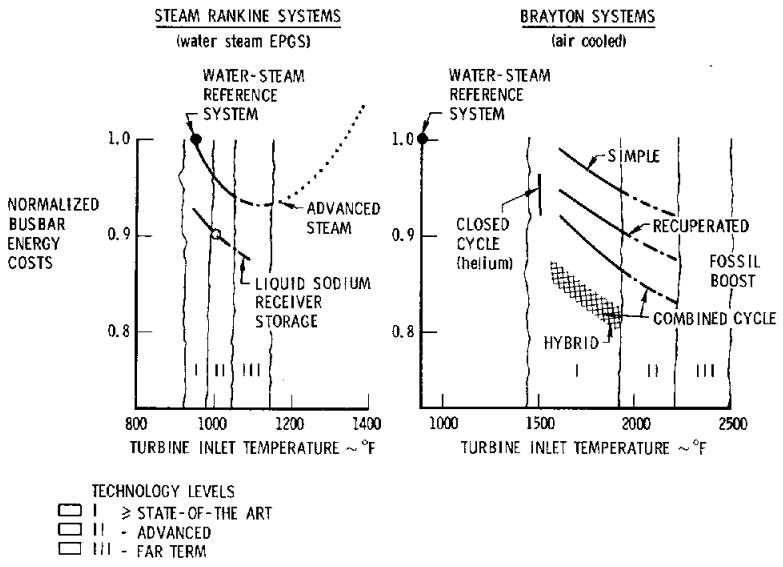

Figure 6. Comparative Systems Analysis (Preliminary Assessment)

Impact of Storage Performance Characteristics on System and Energy Cost

Figure 7 shows the effect of improvement in storage outlet steam design conditions on solar plant performance and its operating economics in a utility grid. The results are presented as a function of storage design temperature and equipment costs for the current technology water-steam system and for the sodium system discussed above. Figure 8 shows the results of a similar analysis conducted for a Brayton cycle solar plant utilizing checker stove type solid-gas storage subsystem designs.

Summary

The key findings of the comparative analysis are summarized in Table IV. The results are based upon nominal designs that take advantage of extensive performance, cost data available in the literature on various power conversion subsystems, heat exchangers, and the balance-of-plant designs. The solar receiver and storage subsystem designs for the advanced options have not yet been adequately defined and analyzed. The data used in this study for these subsystems is based on the analysis and broad extrapolation of available information from various EPRI and ERDA research contracts.

For the six-hour storage designs assumed in this analysis, a solar plant produces approximately one-third of its total electrical output energy while operating from storage or from combined storage and direct receiver thermal energy. For this case, the improvements in the storage design temperature show significant increases in the overall plant performance and energy production cost.

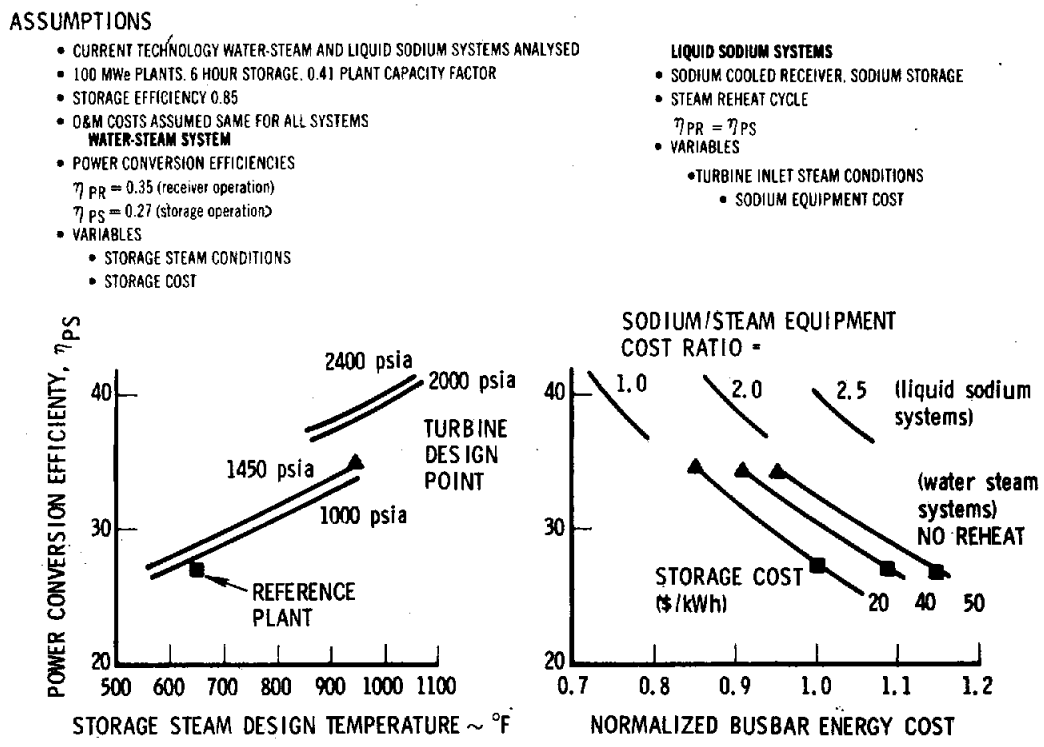

Figure 7. Impact of Storage Characteristics on Steam Rankine System Effectiveness

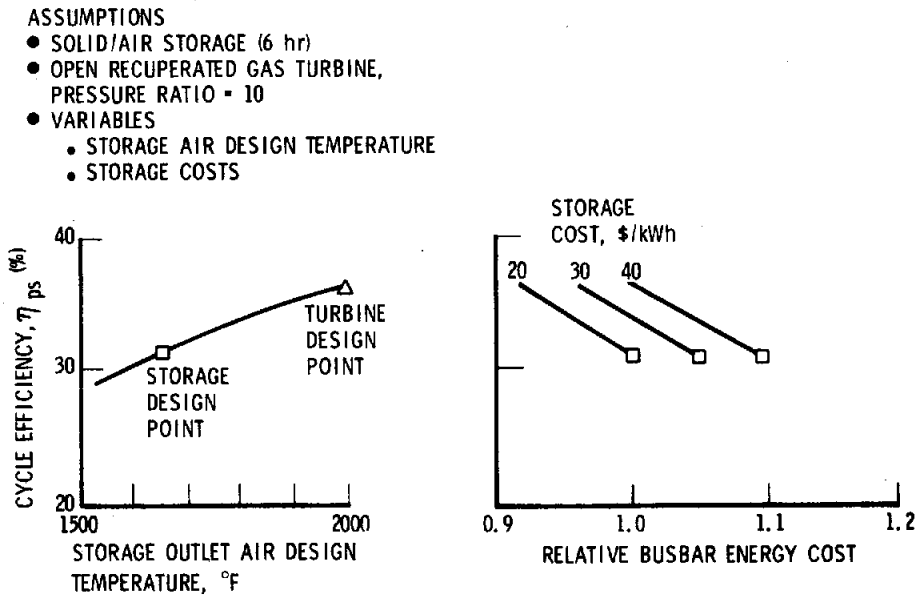

Figure 8. Brayton Systems

TABLE IV. SUMMARY

- ADVANCED WATER-STEAM SYSTEMS DO NOT OFFER SIGNIFICANT PERFORMANCE/COST IMPROVEMENTS
- SIGNIFICANT PERFORMANCE IMPROVEMENTS ARE POSSIBLE WITH LIQUID METAL AND MOLTEN SALT SYSTEMS. THESE ADVANTAGES COULD BE OFFSET BY INCREASED SYSTEM COSTS
- BRAYTON SYSTEMS ARE ALSO POTENTIAL OPTIONS. EMPHASIS ON RECEIVER AND STORAGE DEVELOPMENT REQUIRED
- HYBRID OPTIONS, PARTICULARLY THE FOSSIL BOOST, APPEAR ATTRACTIVE FOR INTERIM APPLICATION

CENTRAL RECEIVER PILOT PLANT DESIGN

Honeywell/Black and Veatch/Babcock and Wilcox/
Northern States Power/Research, Inc.

The Honeywell solar pilot plant preliminary design, shown in Figure 9, has been completed. Both the pilot plant and the commercial plant designs meet all of the ERDA derived requirements. Furthermore, careful attention to design scaling throughout the program ensures that success of the pilot plant will guarantee the success of the commercial plant. Both designs are based largely upon proven fossil fuel utility plant concepts and no new technology is required.

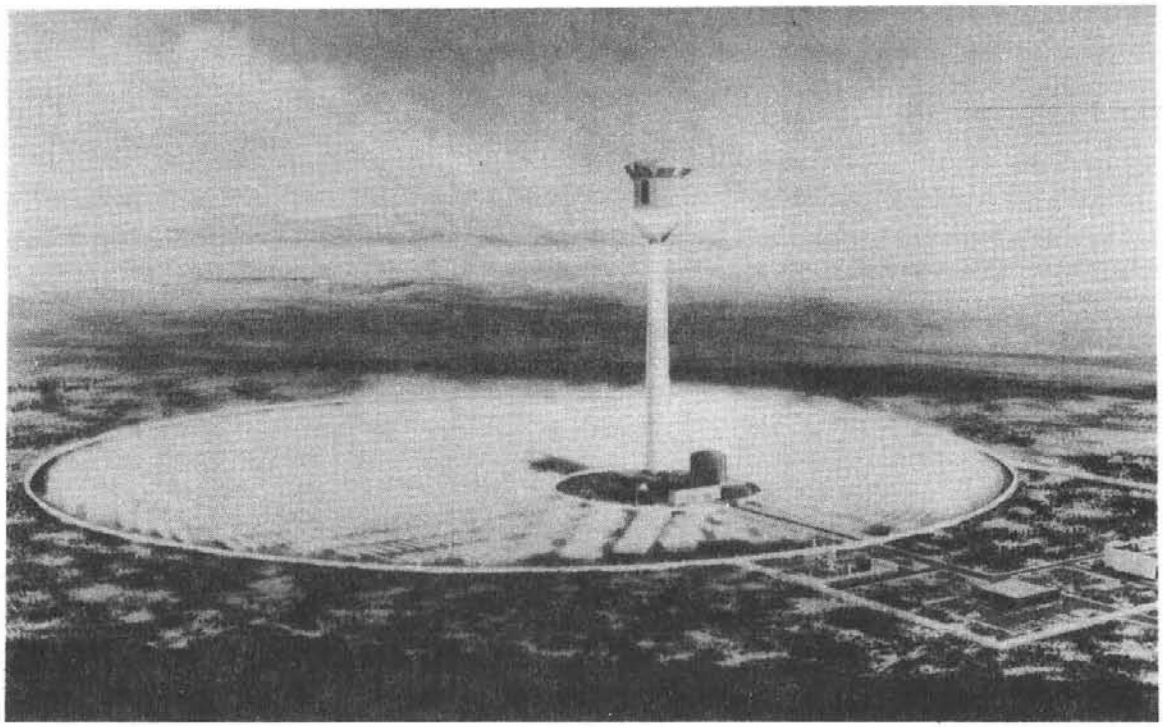

Figure 9. 10-MW_e Solar Pilot Plant

Figure 10 shows the plant elements and the conversion processes involved. Sunlight is redirected by the collector subsystem into the aperture of the receiver on top of a tower, where it heats water in a steam generator. The steam is either piped directly to a 15-MW_e turbine or, if it is not needed immediately, into storage. The storage subsystem normally supplies steam to the turbine when the receiver subsystem is inoperative. If the load demand requires it, steam can be drawn from both the receiver and storage. The pilot plant will generate 10-MW net busbar electricity at 2 PM on the winter solstice (21 December) using superheated steam from the receiver. It will generate 7 MW-net busbar electricity for three hours using superheated steam from thermal storage.

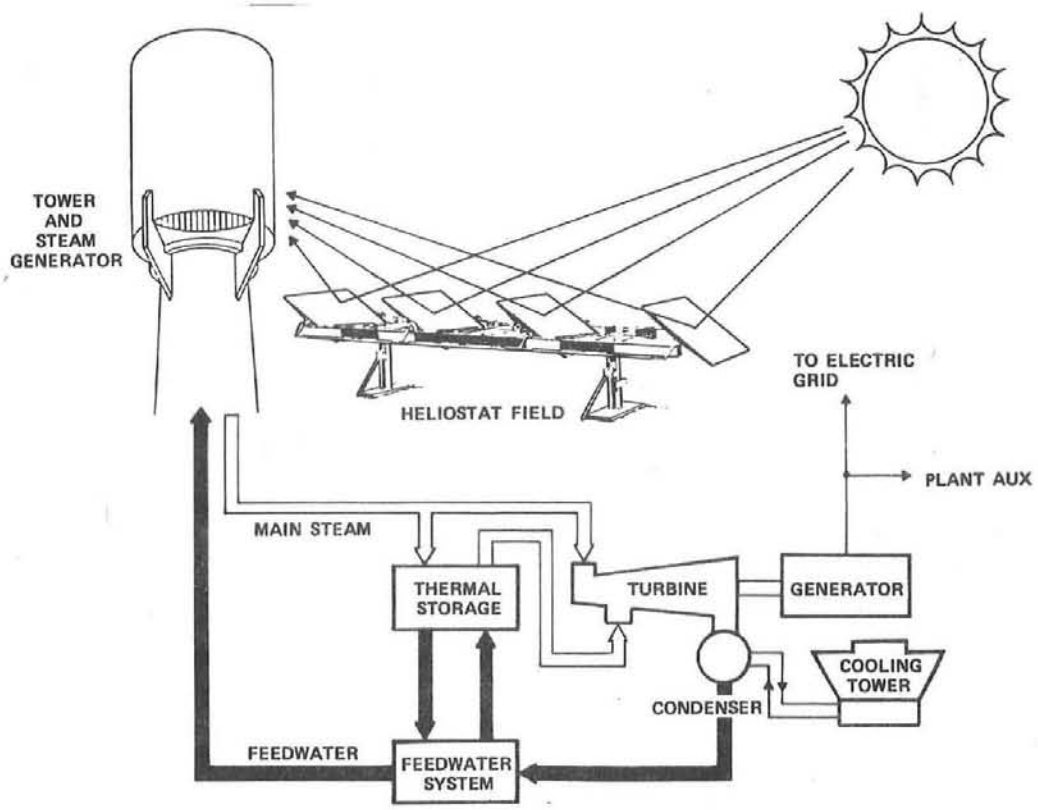

Figure 10. Central Receiver Concept

Pilot plant operation is controlled through a coordinated master control that regulates the subsystems to correlate load demand with the energy available. The control system features a manual override capability, and every design and procedural precaution is taken to ensure the safety of operating personnel and equipment.

The collector subsystem (heliostat field, controls, and calibration array) is shown in Figure 11. The field is circular, with the receiver tower one-half of the field radius south of center. The ratio of mirror surface to field area is 0.29. The field configuration was determined by computer analysis, the criterion being maximum redirected solar energy collected during the year.

The critical element in the collector subsystem is the heliostat because it is the single most important cost and performance factor in the plant system. Consequently, it was subjected to extensive analysis and design effort, and was the most tested item during the Phase I program. The heliostat was designed for quick, easy installation and maintenance and was provided with a high level of control to ensure reliability and safety. The computerized control system can address all (1598) heliostats simultaneously while performing calculations of sun position and pointing direction and compensating for known fixed errors. The Honeywell Level 6/45 computer permits cross-checking input, including weather conditions in the collector field.

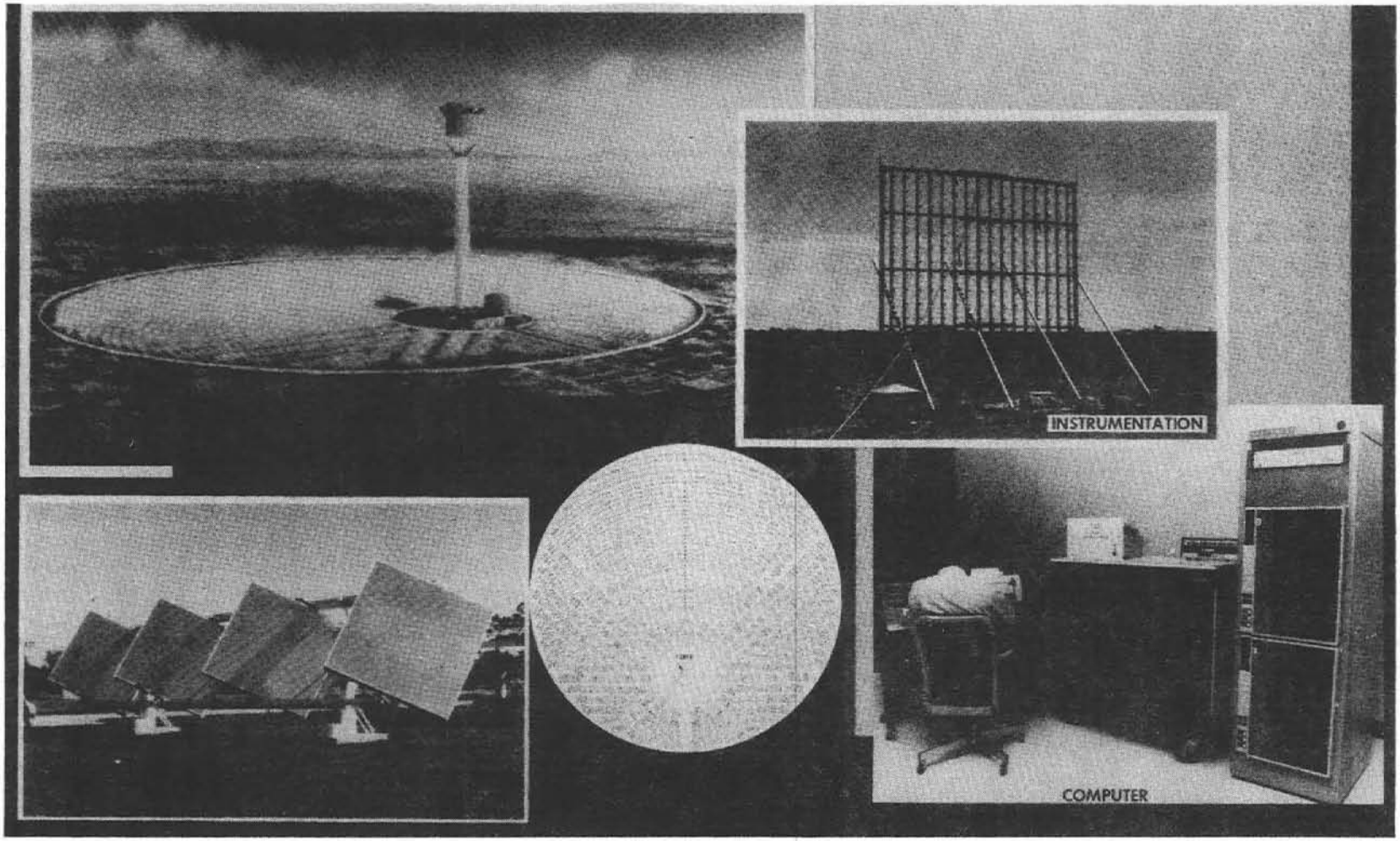

Figure 11. Composition of the Collector Subsystem

Calibration sensor arrays on top of the receiver tower provide the capability for measuring beam direction and energy. This information is used to correct minor pointing errors and determine when the mirrors need to be cleaned.

The subsystem tests, conducted at St. Petersburg, Florida, extended over a 9-month period and included both key components and the entire subsystem. The results were satisfactory, both for performance and for identifying potential cost savings through design improvements. Figures 12 and 13 are illustrative of the data obtained from the testing.

The function of the receiver subsystem (Figure 14) is to accept the redirected solar energy from the collector field and convert it to the steam-water working fluid that drives the turbine. The key element in this transformation is the steam generator. In addition to the steam generator, the subsystem consists of a receiver housing, cavity barrier (to conserve heat during overnight shutdown), piping, corbels, protective shielding, and access for maintenance and repair, all contained in the support tower. The tower structure is designed to withstand support reactions, its own dead and live loads, wind loads, and zone 3 seismic forces. The entire subsystem, receiver structure and steam generator, is based on state-of-the-art technologies, which make it low-risk.

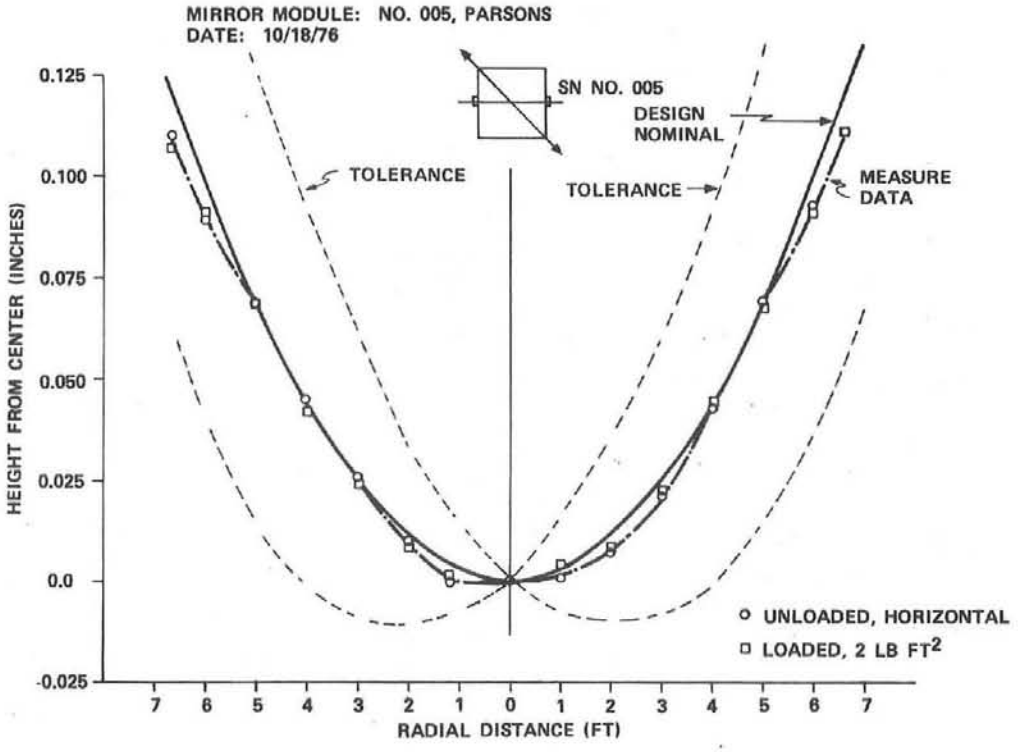

Figure 12. Typical Mirror Contour Data

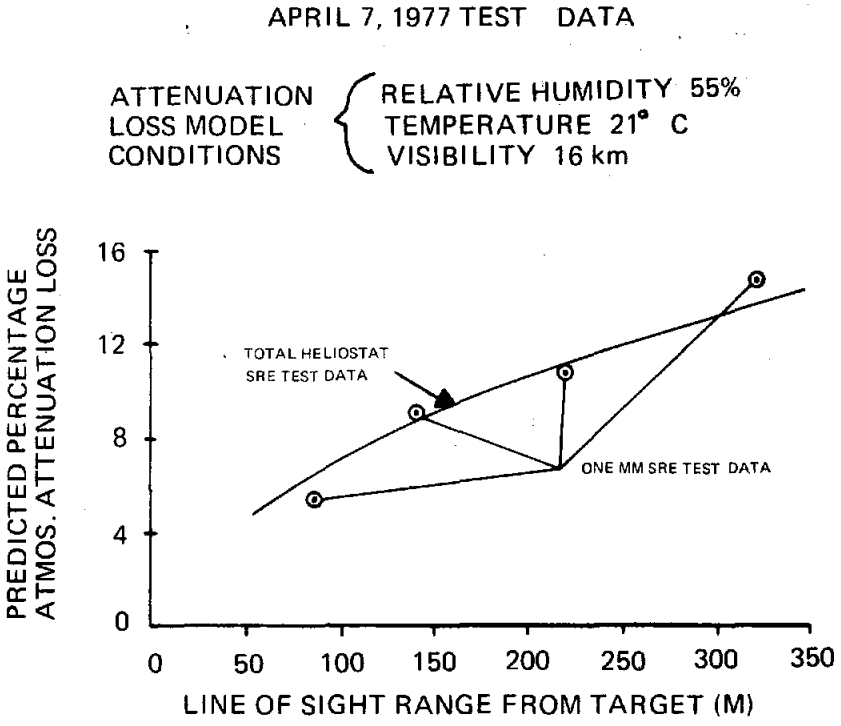

Figure 13. Predicted and Measured Losses as a Function of Range

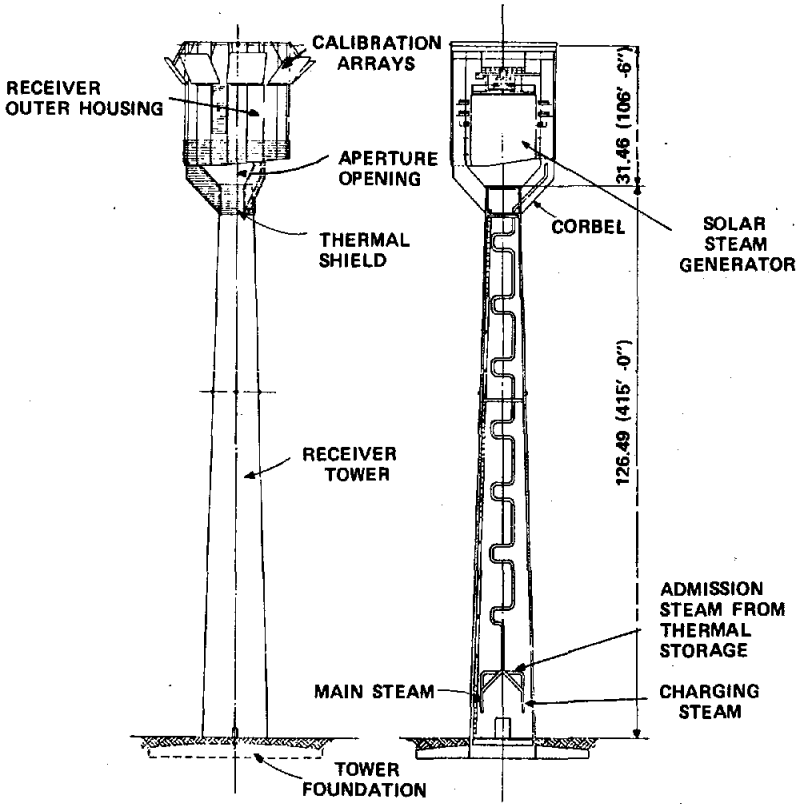

Figure 14. Receiver Tower Elevation and Structure

The arrangement of the steam generator (Figure 15) and the radiation properties of the heat transfer surfaces are such as to maximize absorptance (~0.9) and the efficiency of the receiver cavity. The steam generator heat transfer surface is an 18-sided polygon that forms the interior walls of the receiver cavity.

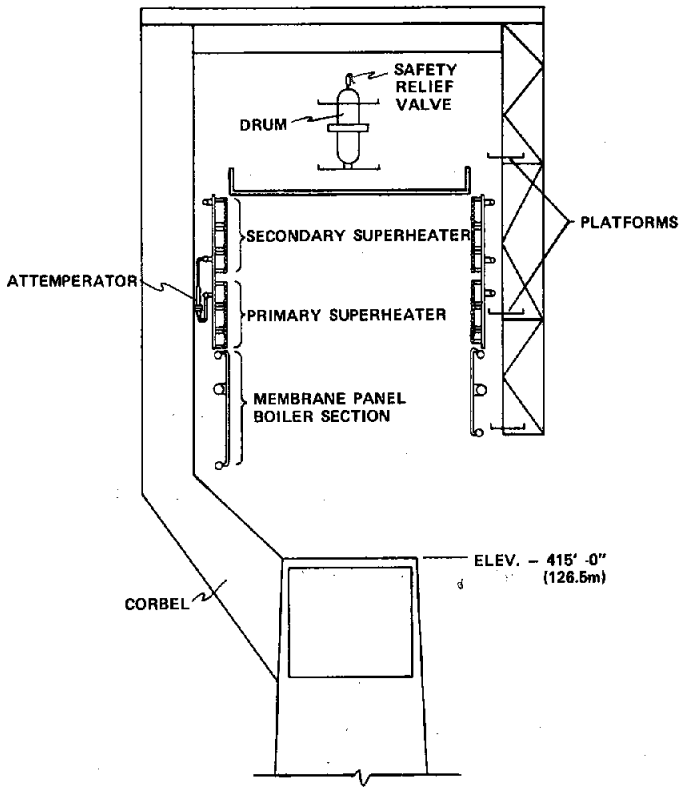

Figure 15. Pilot Plant Steam Generator Arrangement

The steam generator design is based on standard fossil fuel boiler technology. A model (Figure 16) with one-tenth the capacity of the pilot plant steam generator was built and tested in the Riverside plant of Northern States Power Company in Minneapolis, Minnesota. Care was taken to ensure that the test item related to the pilot plant item on either a one-to-one basis or other meaningful scale. Electrical power for a 9-megawatt radiant heat solar simulator was supplied directly from the power plant distribution system. Feedwater was supplied by a fossil boiler. Operating procedures were essentially those of a conventional power plant.

The measured performance corresponded closely with the predicted performance. The steam generator operated reliably and was responsive to control commands, as indicated by Figures 17 and 18, which show the responses of the main steam pressure and temperature to step changes of the steam control valve. Planning is now underway to dismantle the steam generator and ship it to the test facility at Albuquerque, New Mexico, for sunlight testing.

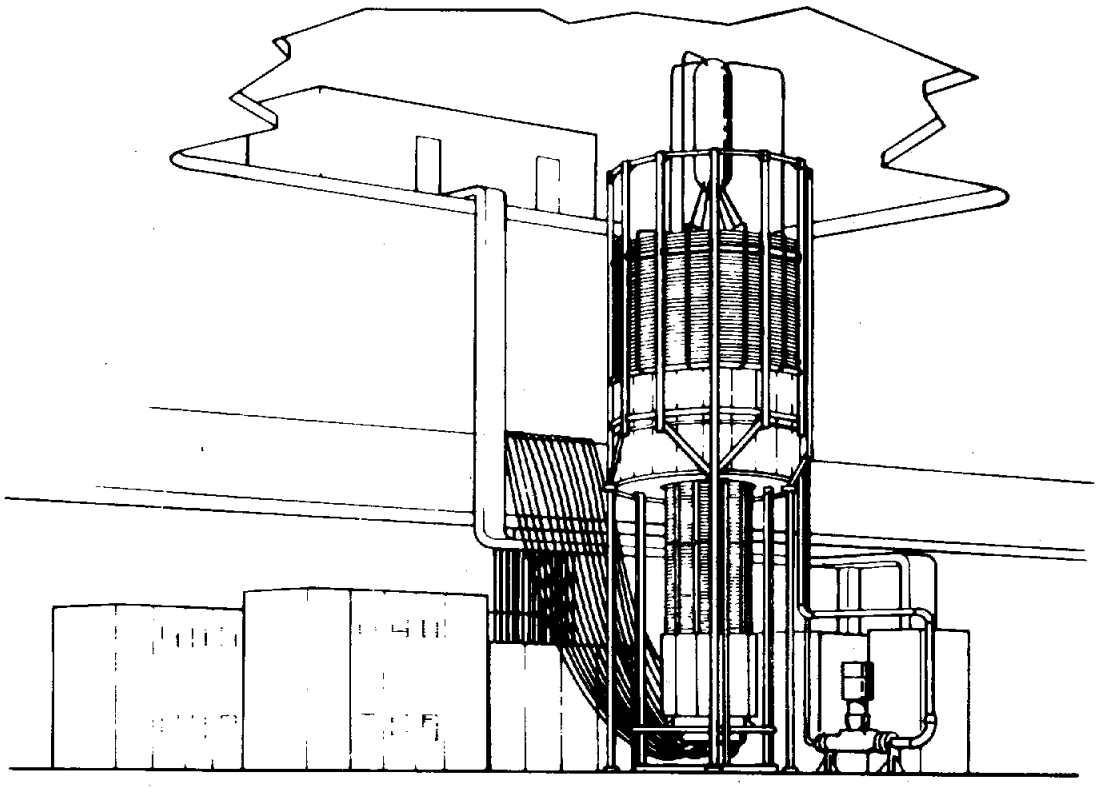

Figure 16. Steam Generator Test Arrangement

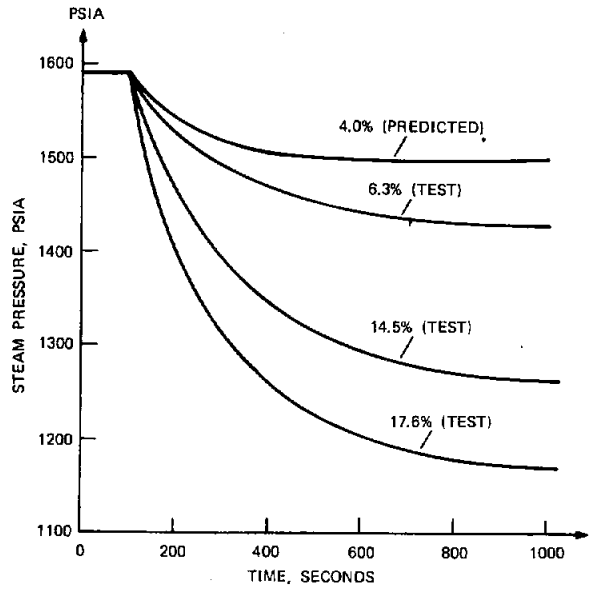

Figure 17. Steam Generator Main Steam Pressure Pressure (Steam Control Valve Step Change)

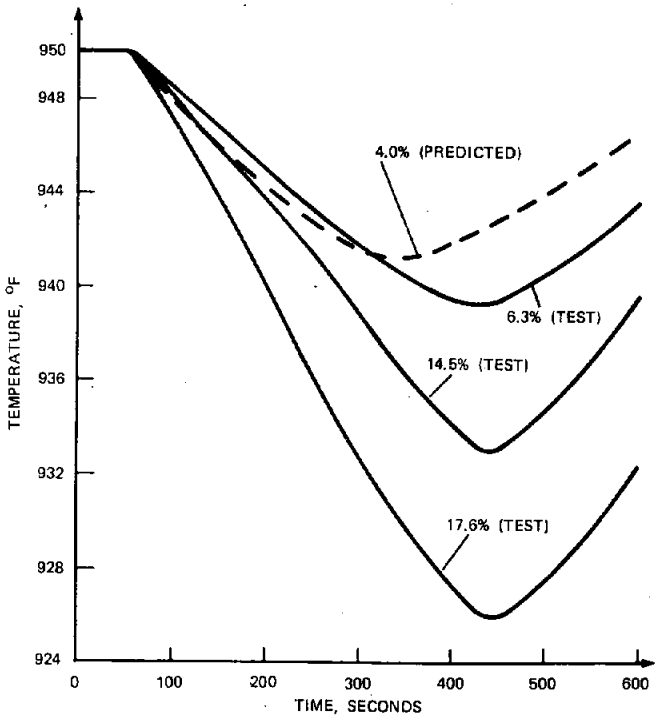

Figure 18. Steam Generator Main Steam Temperature (Steam Control Valve Step Change)

The thermal storage subsystem, shown conceptually in Figure 19, is a two-stage sensible heat storage arrangement that uses rock and oil in the first stage and an inorganic salt mixture in the second, or superheater stage. Guiding precepts in the design of the subsystem were modularity and the use of standard methods of construction and proven parts and components. This, and the fact that the storage technique itself is in common use, makes the subsystem design low-risk.

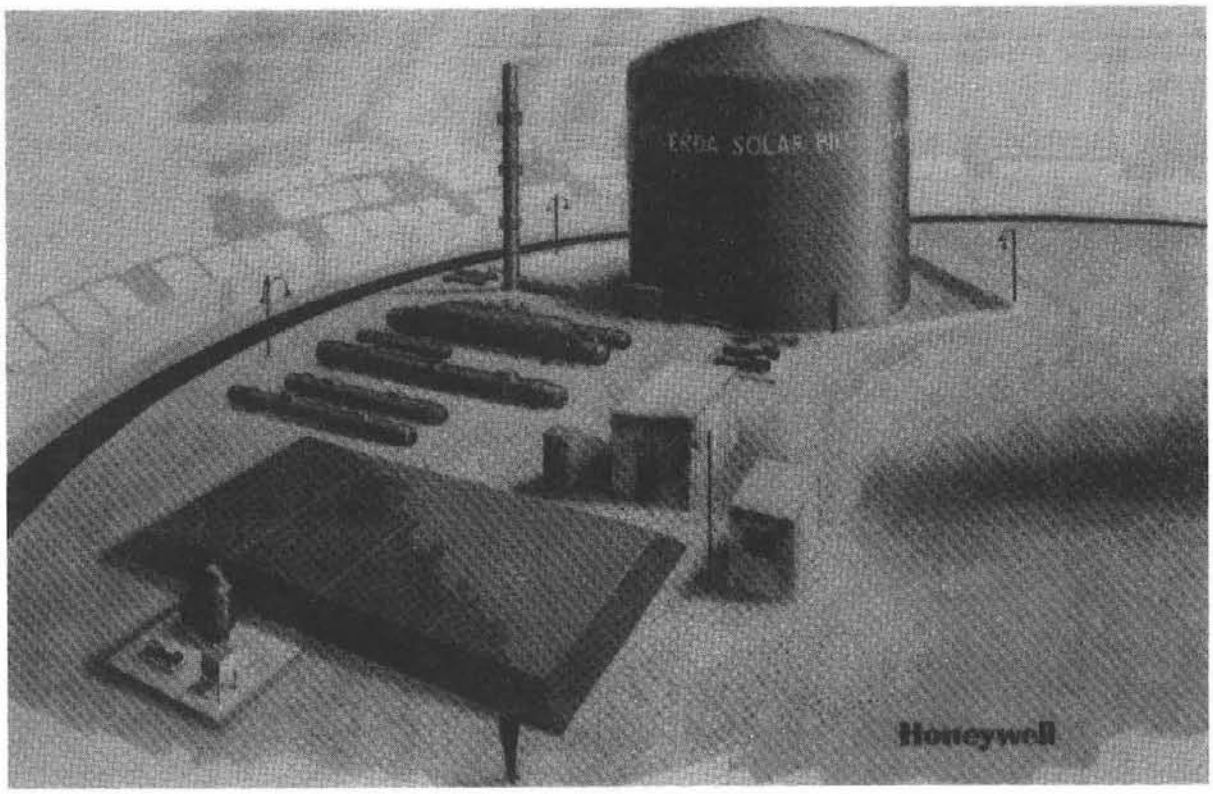

Figure 19. Thermal Storage Subsystem Preliminary Layout

The subsystem is shown schematically in Figure 20. In the main or first storage stage, which holds about 85 percent of the stored thermal energy, the latent heat in the receiver steam is transferred to Caloria HT-43 oil. The heat is discharged as saturated steam on demand. The steam is superheated to turbine admission requirements in the second stage, which stores receiver steam in an underground tank using Hitec salt as the storage medium. The salt is pumped into a second (cold) tank as it loses its heat. The subsystem includes an oil maintenance unit and a ullage maintenance unit.

The storage subsystem is designed to respond to a discharge demand instantaneously, limited only by valve and actuator response times. Thermal lags are minimized by periodically cycling the oil and Hitec discharge auxiliary pumps to maintain boiler pressure and line heat losses. To manage the necessary control functions, thirteen analog controllers are specified with set point controllers, which can be positioned manually or through a direct

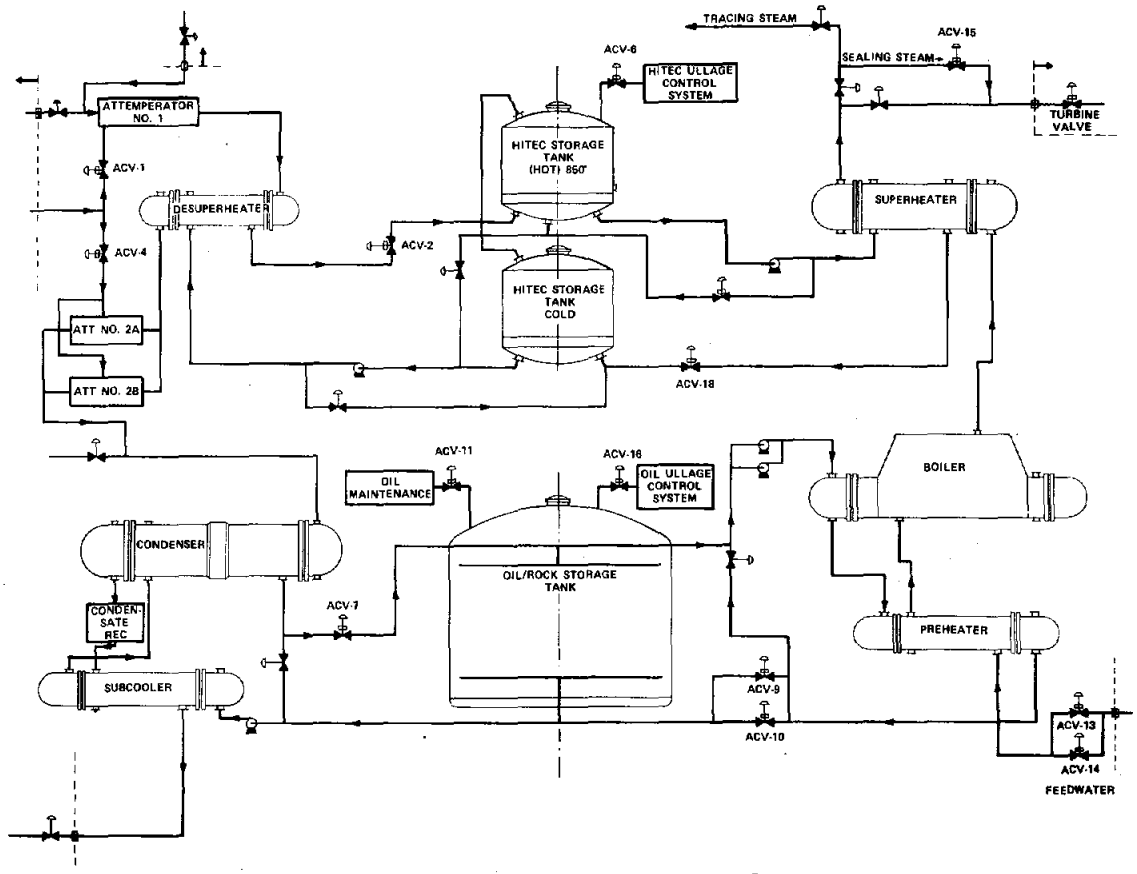

Figure 20. Thermal Storage Subsystem Schematic

digital control interface with the plant master control. On the charge side, controllers are used to maintain the steam at the proper temperature for heat transfer and for maintaining liquid inventory. On the discharge side, controllers are used to supply steam at the proper pressure and temperature, to maintain the proper energy balance, and to maintain liquid inventory.

The electrical power generation subsystem receives steam from the receiver subsystem and/or the thermal storage subsystem and converts it to electrical power. It also supplies feedwater to the receiver and storage subsystems and electrical power to the rest of the plant.

While the sybsystem design was based on analytical work (discussed later), it has a firm basis in state-of-the-art technology. The primary design problem (successfully solved) was matching turbine characteristics to the input cycles of the receiver and thermal storage subsystems to achieve maximal turbine efficiency.

The electrical power generation subsystem is designed around a General Electric automatic-admission, triple-extraction turbine generator sized to the output requirements of the pilot plant (Figure 21). The turbine offers high performance in a variety of operating modes.

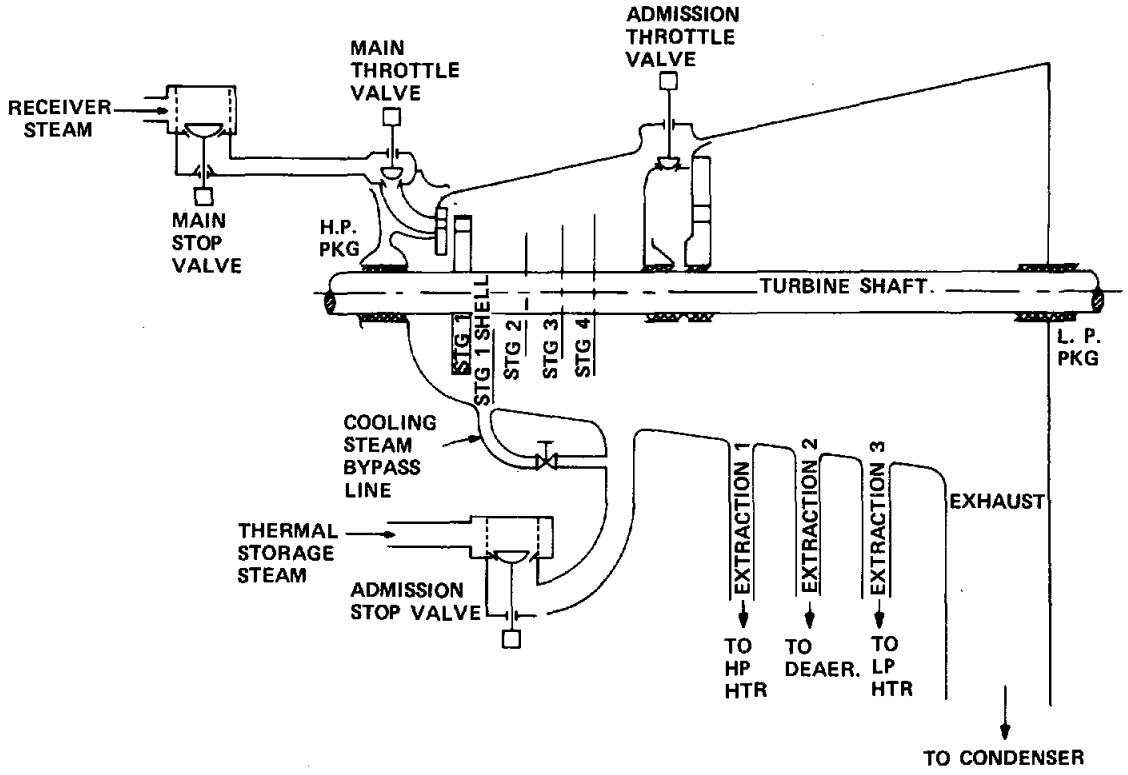

Figure 21. Turbine Generator

A number of ancillary chemical and mechanical support subsystems service the electrical generation. These include auxiliary water cooling, chemical cleaning and feeding, condensate handling, waste treatment, and water quality control.

Pilot plant control is exercised on three levels--system, subsystem, and minor loops. The system, or master, control coordinates demand signals to the collector/receiver subsystems, storage subsystem, and the turbine governor by sensing deviations in power generated from power required.

The receiver control regulates the receiver feedwater and superheater spray flows by focusing or defocusing heliostats as required to obtain the flow balance called for by the master control.

The storage subsystem has storage-in and storage-out controls. Storage-in control regulates and apportions surplus steam to charge main and superheater storage as dictated by the master control. Storage-out control regulates the generation of steam by the storage subsystem for the turbine as dictated by the master control.

In addition to the system and subsystem controls, there are local controls, e.g., for condensate flow control and turbine lubrication oil temperature control, and protection controls for the major subsystems.

A detailed mathematical model was developed to assess the effect of transient conditions, such as diurnal variation in insolation, cloud passage, load demand changes, and equipment failure on the plant system. The structure of the modeling is illustrated in Figure 22.

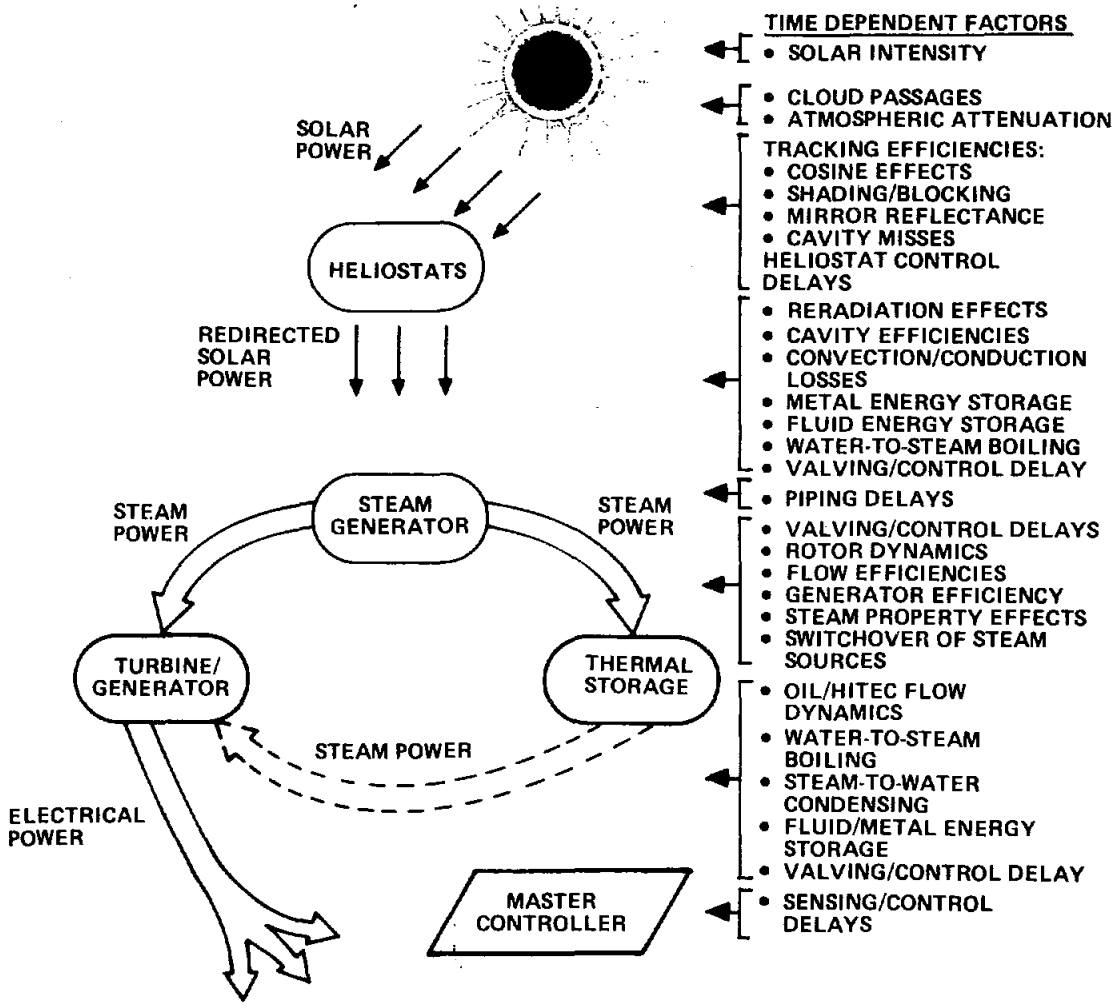

Figure 22. Time Dependent Performance Factors/Transient Analysis Studies

The model was exercised for several kinds of cloud passage that resulted in partial or total loss of insolation on the heliostat field. One such effect (on receiver fluid temperatures) is shown in Figure 23. The simulation showed that the response of the storage subsystem, which was critical to continued stable output, was capable of stabilizing the condition.

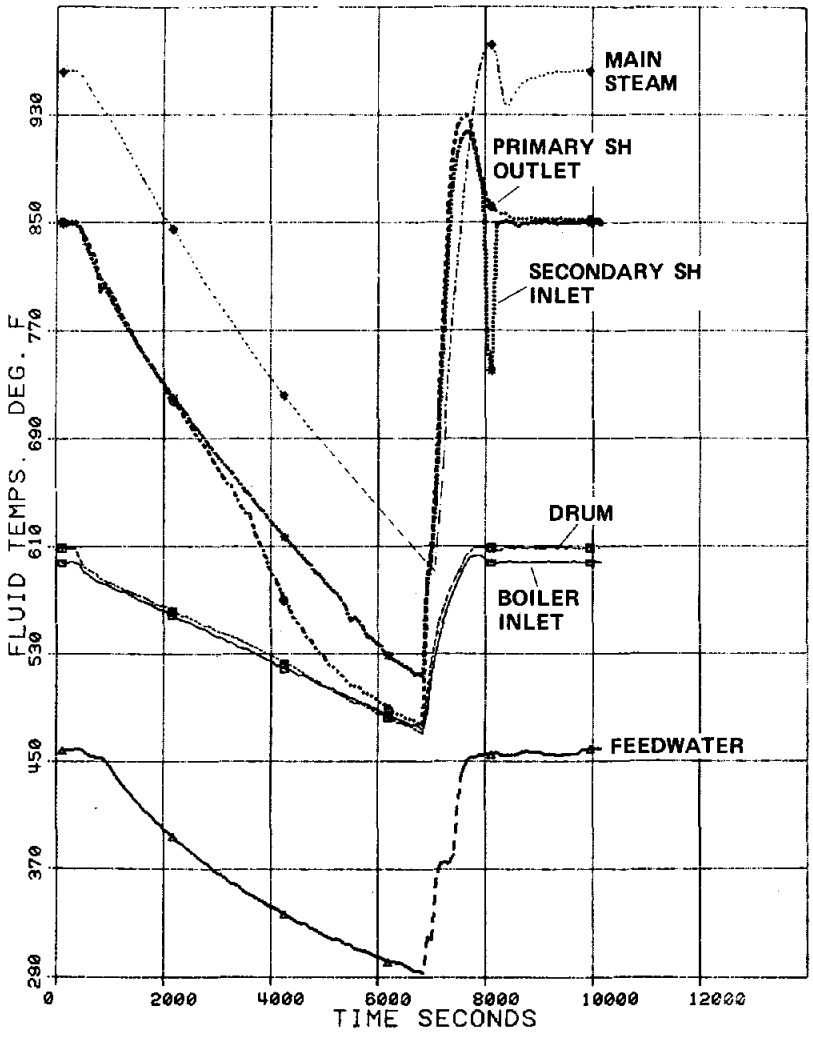

Figure 23. Cloud Transient Effect on Receiver Fluid Temperature

The effect of critical equipment failure (e.g., recirculating pumps) was also simulated. Again, the response of the storage subsystem stabilized conditions and prevented loss of output.

As stated earlier, the ultimate value of the pilot plant lies in how well it defines the requirements for and performance of a commercial plant. The Honeywell concept for the first commercial-scale plant is shown in Figure 24. It is comprised of four towers and fields, each producing the thermal equivalent of 25 MW_e, a central station complex located at the centroid of the four towers, an evaporation pond, and the requisite road accesses and fencing. The central station complex houses the 120 MW_e nameplate turbine, controls, thermal storage subsystem, and support equipment. The arrangement of the main steam lines, which minimizes piping requirements, is shown in Figure 25.

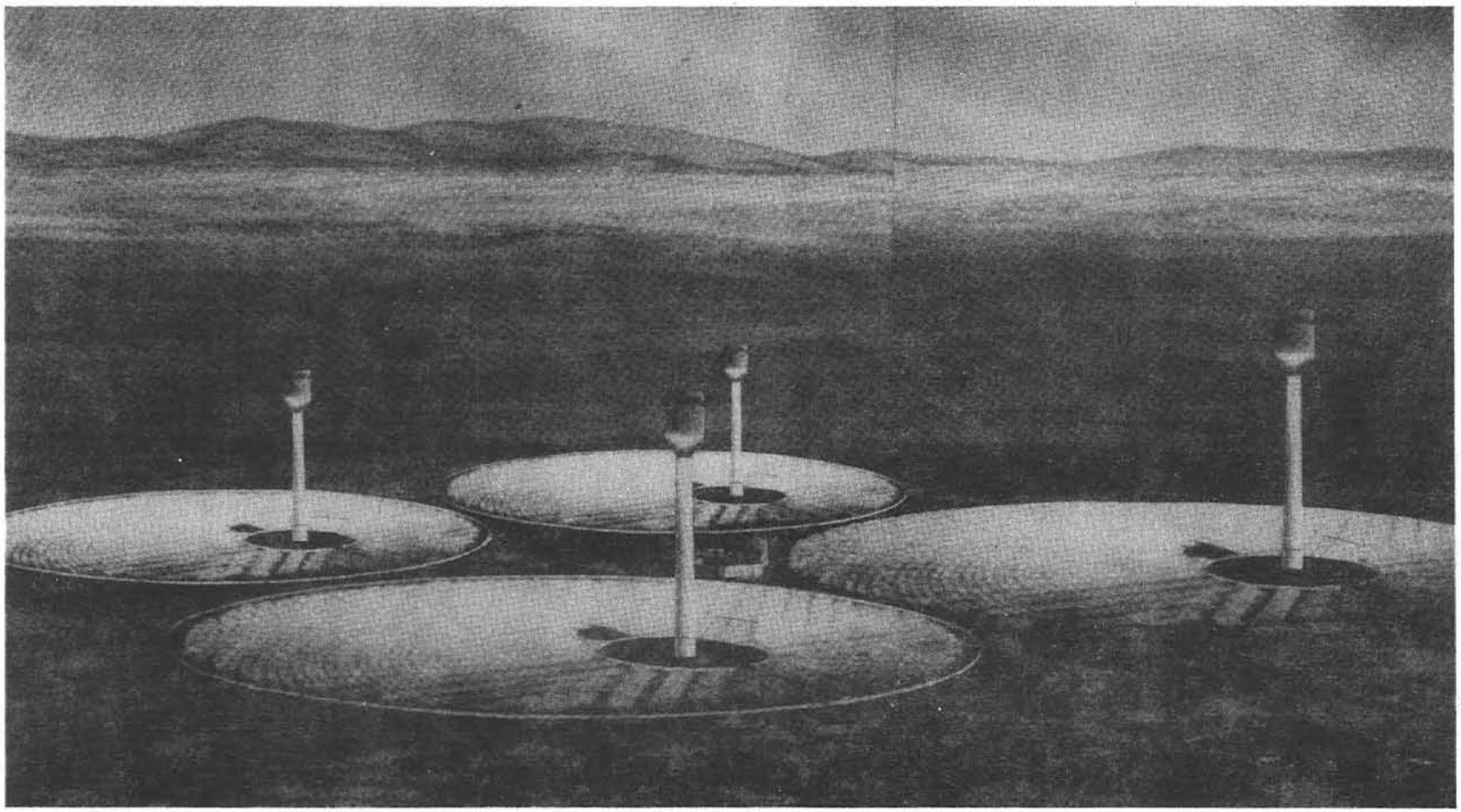

Figure 24. Commercial Plant Conceptual Layout

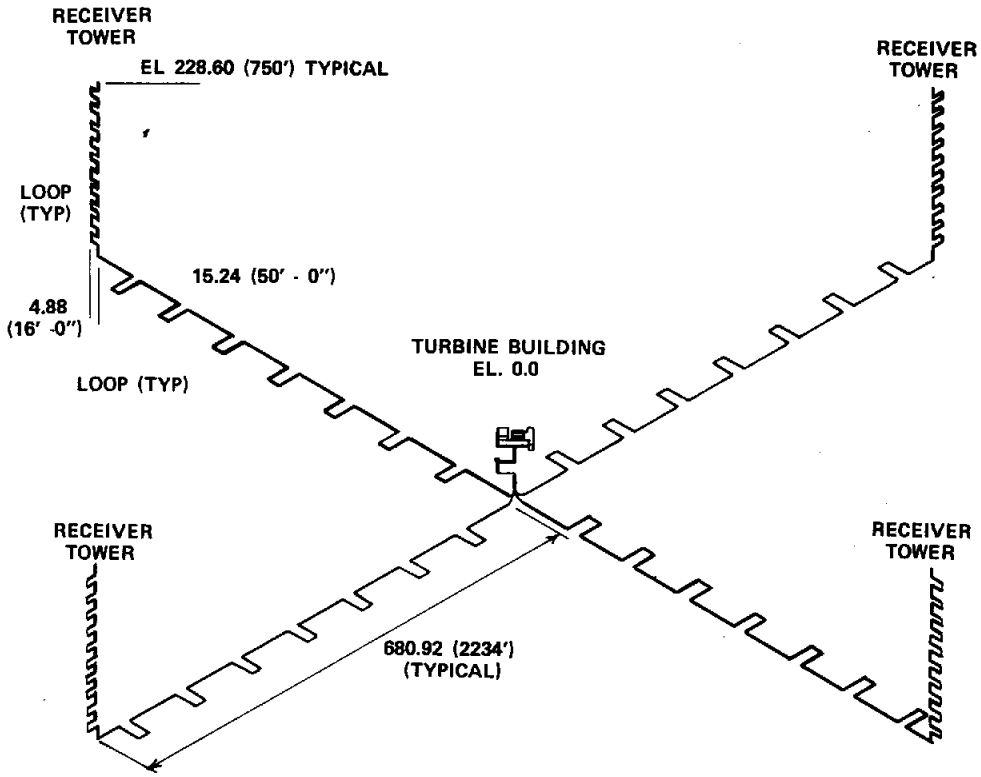

Figure 25. Arrangement of Main Steam Lines in Commercial Plant

The commercial plant layout (Figure 26) is the result of a study to determine a practical number of towers/fields to meet the performance specifications, which are compared with those for the pilot plant in Table V. Three configurations meeting all of the performance requirements were analyzed: one tower and one field, four towers and fourfields, and twelve towers and twelve fields. The four-tower configuration was selected because it was less expensive than the twelve-tower configuration and physically more practical than the one-tower configuration.

At the end of the first phase of the solar pilot plant program, which produced the pilot plant preliminary design and the commercial plant concept, Honeywell stated these conclusions:

- The feasibility of the preliminary design was established
- No unusual technology was required by the design
- The plant economics are highly dependent on ultimate costs of the heliostat and storage
- Phase II objectives can be achieved at low risk and moderate cost

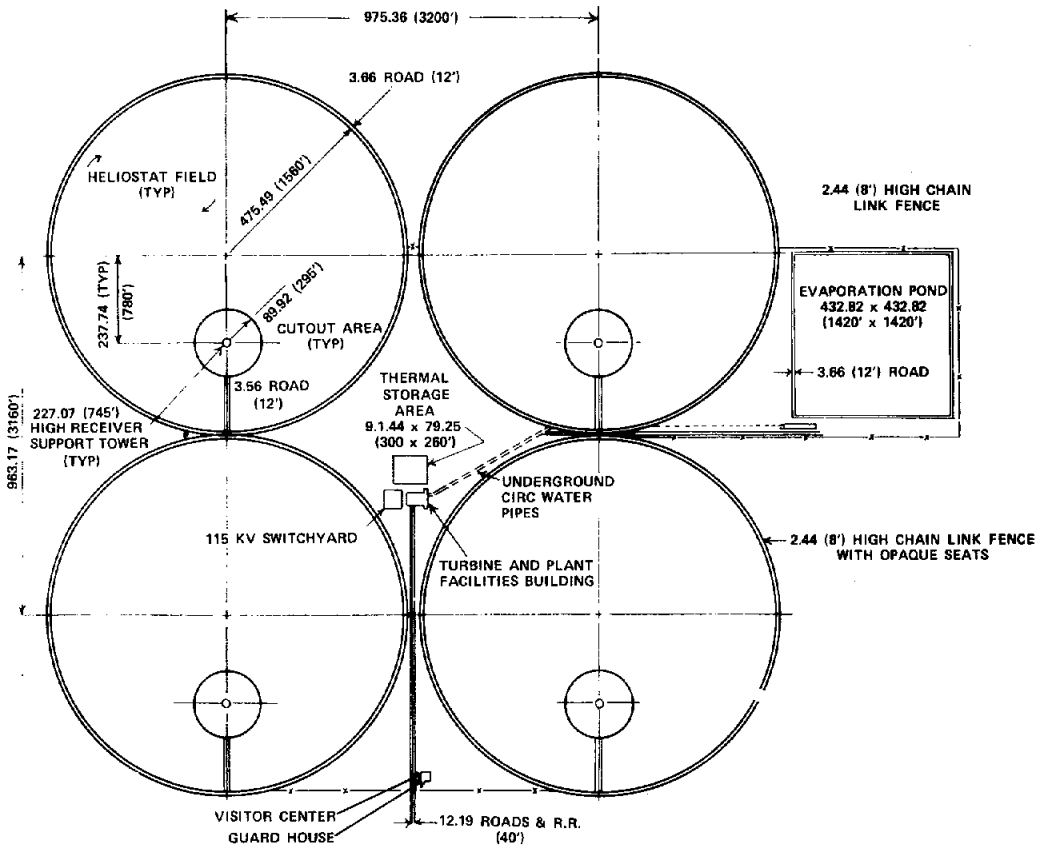

Figure 26. First Commercial Plant

TABLE V. PILOT/COMMERCIAL PLANT PRELIMINARY DESIGN SPECIFICATION

Parameter	Pilot Plant	Commercial
Location	Barstow	- - -
Name Plate Capacity	15 MW_e	120 MW_e
Design Point Net Power	10 MW_e - 12/21, 2 PM	100 MW_e - 3/21 Noon
Tower Height	126.5 M (415 Ft)	225.6 M (740 Ft), 4 Towers
Heliostat Size	40 M^2	Same
Solar Multiple	1.23	1.7
Number of Heliostats	1598	20,200
Total Mirror Area	63,920 M^2	808,800 M^2
Storage Type	Sensible	Same
Storage Capacity	7 MW_e for 3 Hours (115.2 MW HR(t))	70 MW_e for 3 Hours (908.6 MW HR(t))
Receiver Peak Flux	300 kW/M^2	Same
Aperture Area	218.3 M^2 (2350 Ft^2)	650.8 M^2 (7005 Ft^2)/Tower
Receiver Peak/Average EFF	87.2/84.1	Same
Turbine Cycle (from RCVR)	10.1 MPA/510°C (1450/950)	Same
Turbine Cycle (from Storage)	3.2 MPA/388°C (460 & 730)	Same
Design Point Net Efficiency (from Receiver)	25.9	29.3
Design Point Net Efficiency (from Storage)	22.1	26.3
Total Net Annual Energy (NAE)	2.22×10^4 MW HR(e)	2.89×10^5 MW HR(e)
NAE/Total Mirror Area	0.348 MW HR(e)/M^2	0.357 MW HR(e)/M^2

The following recommendations were made based on those conclusions:

- Proceed immediately to Phase II
- Establish a well-funded, flexible, on-going heliostat development program aimed at a low-cost heliostat
- Establish a well-funded, flexible, on-going thermal storage program aimed at low cost subsystem
- Proceed with sunlight receiver tests
- Proceed with latent heat storage tests
- Provide for additional subsystem research experiments as recommended by all contractors.

CENTRAL RECEIVER PILOT PLANT DESIGN

Martin Marietta/Foster Wheeler/Georgia Tech/Bechtel

	COMMERCIAL	PILOT PLANT
NAMEPLATE CAPACITY	150 MWe	10 MWe
TOWER HEIGHT	90 m	90 m
NUMBER OF HELIOSTATS	23,325	1555
HELIOSTAT SIZE	41.0 m^2	41.0 m^2
STORAGE TYPE	SENSIBLE HEAT	SENSIBLE HEAT
STORAGE CAPACITY	--	--
RECEIVER	CAVITY	CAVITY
COOLING	WATER	WATER

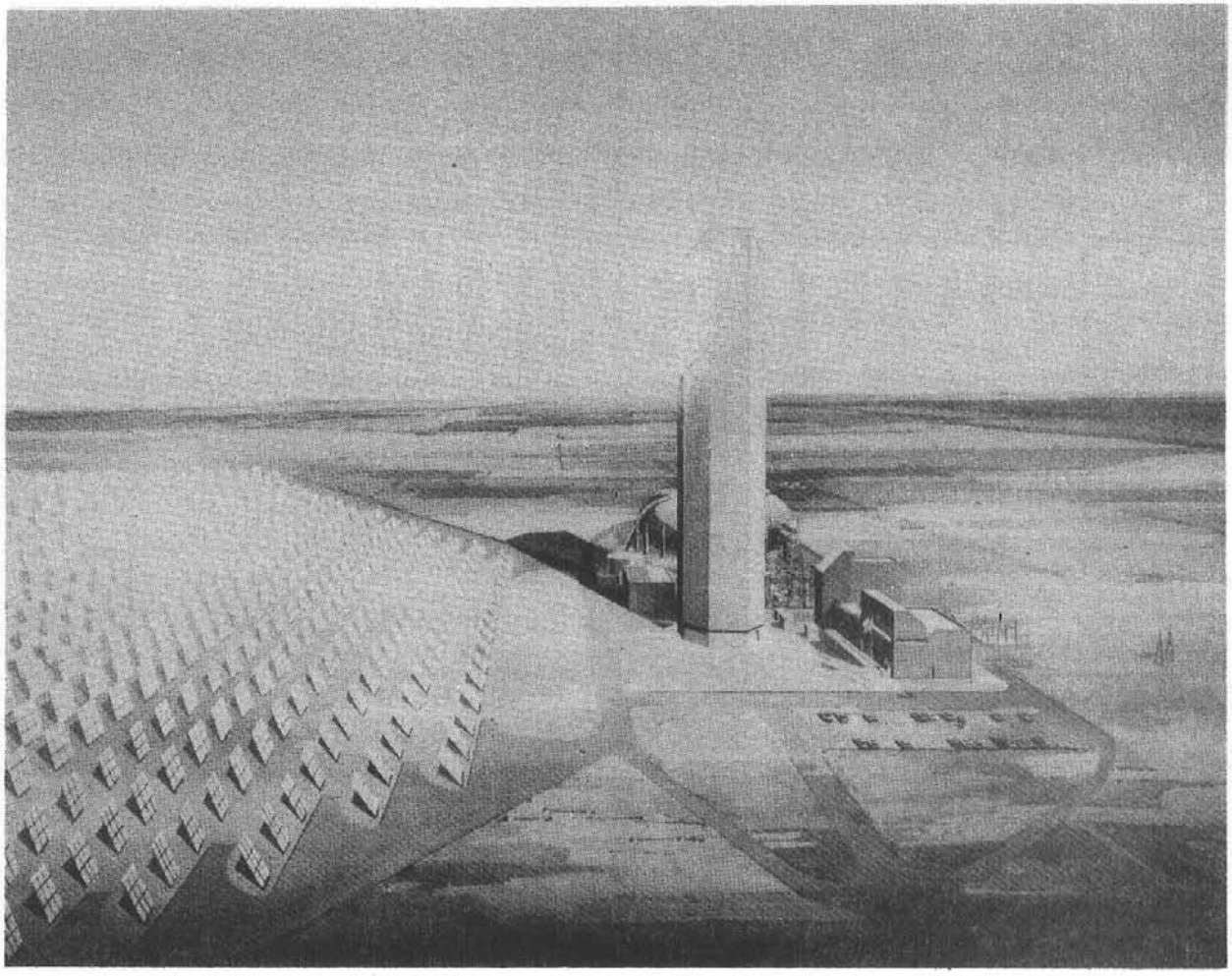

SYSTEM DESIGN

- o PILOT PLANT IS ONE MODULE OF MULTI-MODULE COMMERCIAL PLANT
- o COMMERCIAL PLANT RATED AT 150 MW

RECEIVER

- TILTED CAVITY HAS BEEN ELIMINATED
- RECEIVER IS NOW ENCLOSED IN CONCRETE TOWER

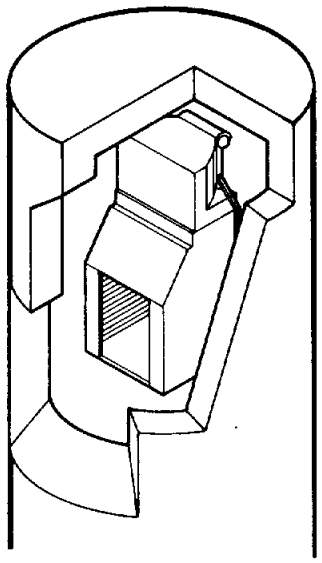

THERMAL STORAGE SUBSYSTEM

- STORAGE CONFIGURATION REDUCED FROM THREE TO TWO STAGES
- PARALLEL CHARGE AND DISCHARGE CAPABILITY INCORPORATED
- PILOT PLANT STORAGE SUBSYSTEM FUNCTIONALLY AND OPERATIONALLY IDENTICAL TO COMMERCIAL PLANT SUBSYSTEM

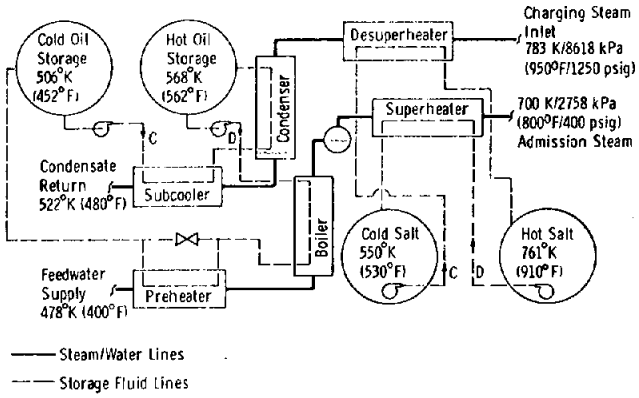

COLLECTOR SUBSYSTEM

- o PILOT PLANT HELIOSTAT WILL HAVE NINE FIXED-FOCUS MIRRORS, COMPUTER CONTROLLED TRACKING, AND FACE DOWN STOWAGE

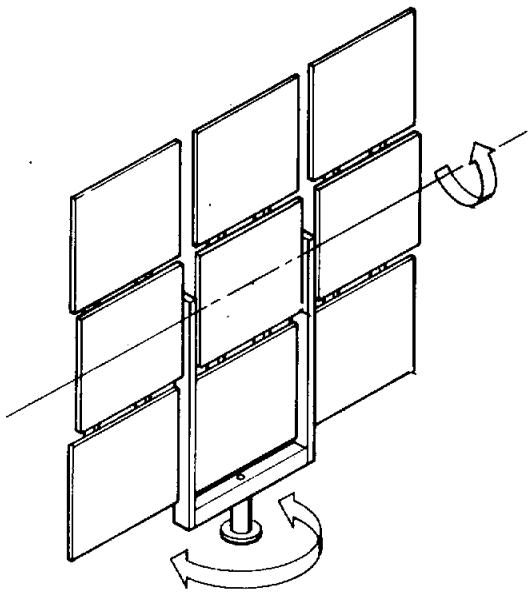

Preliminary Design

A team of organizations with complementary capabilities was formed to perform the central receiver solar thermal power system (CRSTPS) Phase I, Preliminary Design Phase. Martin Marietta Corporation was the team leader, responsible for program management, system integration of the CRSTPS commercial and pilot plant designs, the collector subsystem design, and the collector research experiment. Foster Wheeler Energy Corporation performed the design of the receiver steam generators for the full-scale solar plants, and the design, fabrication, and erection of the 5-MW_{th} receiver for the subsystem research experiment. Georgia Institute of Technology was responsible for the thermal storage subsystem designs and the thermal storage research experiment. Bechtel Corporation had design responsibility for the electric power generation subsystems and the architect and engineering features of the plants.

Basic features of the Martin Marietta solar power plant concept, shown in Figure 27, have been established to achieve a practical utility-scale solar plant with the highest performance consistent with the goals of (1) minimized capital and operating costs, (2) safe, flexible, reliable and long-life application features, and (3) timely development of solar power technology.

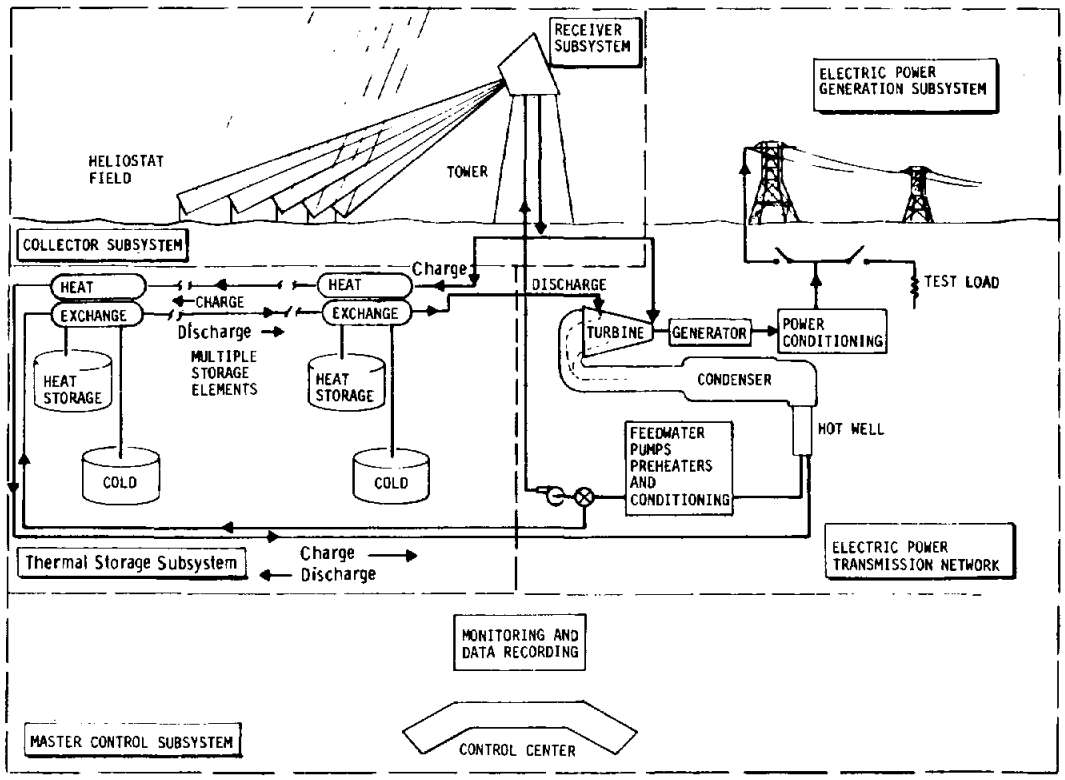

Figure 27. Overview Schematic of the Martin Marietta Team Central Receiver Solar Thermal Power System

The CRSTPS plant is made up of five major subsystems, the collector, receiver, and thermal storage, which are unique to the solar application, and the electric power generation and plant controls, which are currently commercial. Energy flow through the plant starts with the solar energy intercepted by the heliostats of the collector subsystem. The solar energy is reflected in concentrated beams to the receiver. Within the receiver subsystem the solar energy is converted to thermal energy in the form of superheated steam and is transmitted to the thermal storage and electrical power generation subsystems. Conversion of thermal energy from either the receiver or the storage system to electricity takes place in the turbine and generator of the electrical power generation subsystem. Energy flow in the thermal storage subsystem is from steam to sensible heat in the storage fluids during charging and from the sensible heat of the fluids to steam during discharge.

Finalization of the preliminary design occurred during the final six months of the basic program. Many evolutionary modifications to the design which occurred during the course of the program are visible in the rendering on page 41. These include (1) the shortened tower, (2) the enclosure of the receiver within the tower, (3) use of a sheathed steel rather than concrete tower, (4) relocation of the thermal storage subsystem, (5) reduced tankage of the thermal storage subsystem, (6) use of spherical tanks for the oil storage stage, (7) integration of the electric power generation and administration buildings, and (8) depiction of the plant at its selected site on the Southern California Edison site at Barstow, California. Many other important evolutionary modifications, not evident to the eye in a rendering, were also incorporated during the final period. Key among these were (1) collector layout optimization, (2) heliostat size increased to 41.0 m^2, (3) heliostat number decreased to 1555 per module, (4) use of open-loop computer controlled tracking for heliostats, (5) incorporation of dual mode (simultaneous charge discharge) operational capability for thermal storage, and (6) revision of the operating state points in the receiver, thermal storage, and turbine equipment.

General features of the CRSTPS commercial plant are shown in Figure 28. Dominating the layout and setting the land use requirement of 6.06×10^6 m^2 (6.52×10^7 ft^2 = 1498 acres = 2.34 sq. miles) are the fifteen solar collector subsystem modules with 1555 heliostats each. Two of the open triangular plots in the central zone of the layout are used for the thermal storage subsystem (TSS) and the electric power generation subsystem (EPGS). Insets in the figure show the layouts of the TSS and EPGS and an artist's rendering of the pilot plant module, which is typical of the commercial plant in the configuration of the collector and receiver subsystems. Table VI lists values for the major parameters of the commercial plant design. Modular design of the collector-receiver subsystems provides versatility of design and flexibility in operational deployment in that site variations and sizing variations over broad limits can be accommodated by this basic design. The modular design also provides the shortest development path to the commercial plant

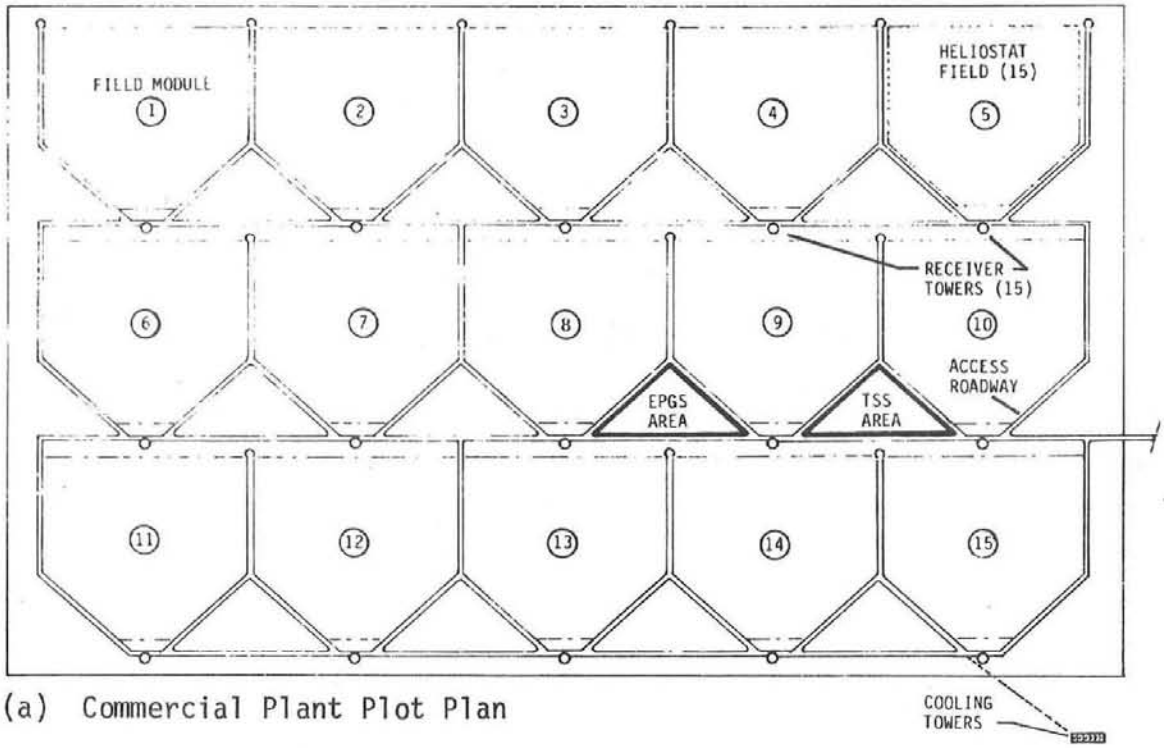

(a) Commercial Plant Plot Plan

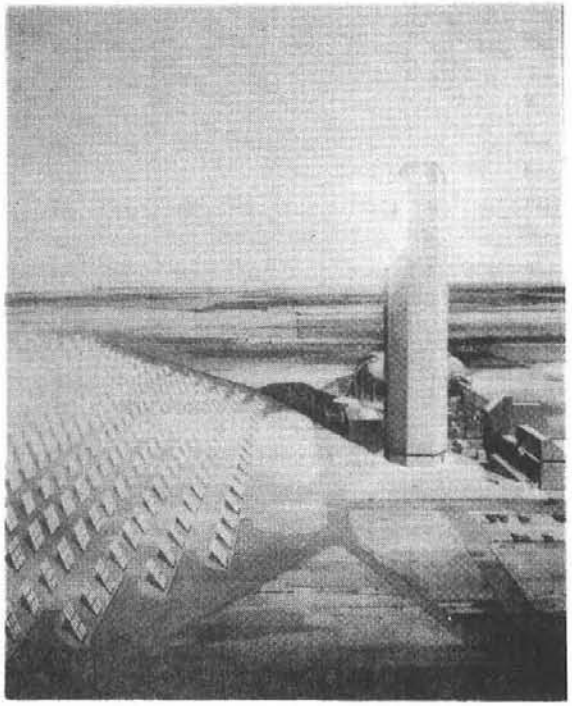

(b) Collector Module

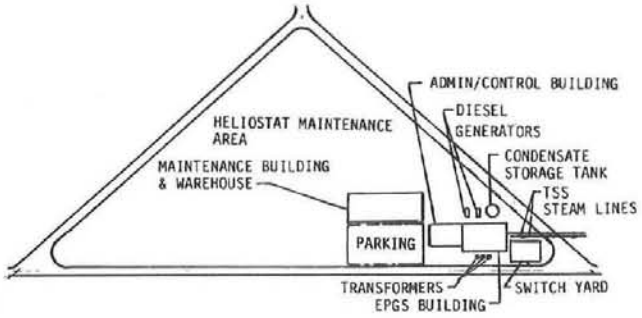

(c) Electric Power Generation Plant

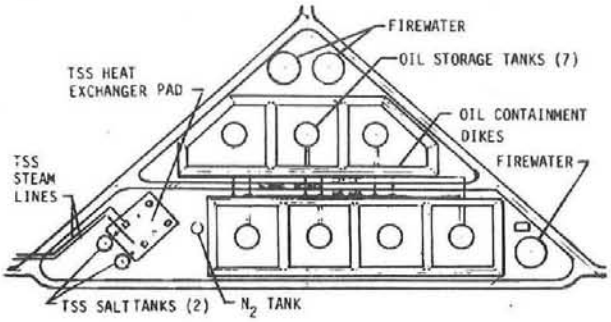

(d) Thermal Storage Subsystem

Figure 28. Martin Marietta Team Commercial Central Receiver Solar Thermal Power Plant Configuration

in that collector and receiver subsystems are full-scale in the pilot plant. Key also to attaining the rapid development, high reliability, moderate cost, and credible costing required for commercial acceptance are the low risk features of the design (notably the cavity receiver steam generator, the focused heliostats, sensible heat storage, and a non reheat dual admission turbine).

TABLE VI. MAJOR PARAMETERS OF COMMERCIAL CRSTPS PLANT

Rated Output, Receiver Steam	150 MW_e
Rated Output, Storage Steam	105 MW_e
No. of Collector Modules	15
No. Heliostats	23,325
Mirror Area	9.56×10^5 m^2 (10.29×10^6 ft^2)
Land Use	3,393 x 1.894 m (11,133 x 6,214 ft)
Receiver Type	North Facing, Horizontal Cavity
No. of Receivers	15
Maximum Receiver Input (ea.)	52.3 MW_t
Maximum Receiver Steam (ea.)	49.6 MW_t
Receiver Steam Conditions	10,783 kPa (1550 psig) 789 K (960°F)
Storage Type	Two-Stage Sensible Heat, Salt & Oil
No. of Tanks	7
Volume of Tankage	291,750 m^3 (10.07×10^6 ft^3)
Storage Steam Conditions	2,855 kPa (400 psig) 700 K (800°F)
Turbine Heat Rate - Receiver Steam (Gross)	9,655 kJ/kW-hr (9151 Btu/kW-hr)
Turbine Heat Rate - Storage Steam (Gross)	11,741 kJ/kW-hr (11,128 Btu/kW-hr)

The commercial plant design represents an optimization of performance within the frame work of optimum economics. These two goals have been consistent in power generation technology and have been generally consistent in this program. A specific exception occurred in the collector subsystem geometry where the optimum height tower for technical performance was 137.2 m (450 ft) and the optimum height for best economics was 90 m (295 ft). In this case, best economics was favored; the impact upon performance was

only 3 percent. The commercial plant has an end-to-end efficiency of 25.1 percent while operating on receiver steam, based on the 150 MW_e power delivered to the transmission line divided by the potential solar energy intercepted by the full area of the mirrors in the system (570 MW_t). This is a specific power generation of 238 W/m^2.

Each feature of the design was evaluated for the degree of its positive or negative implications over the broad range of selection considerations, as summarized in Table VII, and was incorporated only after being judged substantially beneficial. Table VII lists the key features of the system and subsystems and a brief summary comment for each of the evaluation criteria. While the primary design drivers are emphasized, it will be noted that strong support from the remaining categories is the rule for the design features finally selected.

The modular collector-receiver strongly contributes to the high performance goal of the commercial plant by providing maximized optical performance, thermal conversion efficiency, system reliability, and operational flexibility. Optical performance is maximized by using a north field collector of focused heliostats transmitting focused sunlight over moderate slant ranges. For the commercial plant module, 1555 concentrating heliostats, each having an area of 41 m^2 (441 ft^2), are computer controlled to reflect their energy to the focal zone of the receiver 90 m (295 ft) above the ground plane on which the heliostats are mounted. For the pilot plant, a collector field containing only 1325 heliostats will meet all of the specified requirements. However, this size field will provide only limited operational time at 10 MW_e and will provide no significant capability to charge the thermal storage while operating at 10 MW_e. The commercial size field of 1555 heliostats has two significant advantages for the pilot plant. First, it better simulates an operational plant (10 MW_e operation is raised from 4 to 7.5 hours on the design day, and the capability to charge storage while generating 10 MW_e is increased from 0.2 to 1.3 hours). Secondly, it will demonstrate the receiver performance and functional parameters at full scale for the commercial module.

The general configuration of the preliminary design heliostat is shown in Figure 29. Nine pre-focused facets, 2.13 x 2.13 m (84 x 84 in.), are mounted on a rack structure which is supported by and driven about its central horizontal shaft. A yoke structure supports the rack and is itself driven about its vertical centerline by a two-stage worm-spur gear drive. Gearing is identical in the elevation drive, mounted integrally with the mirror support rack. The azimuth drive interfaces with a caisson foundation. Honeycomb construction is used for the pre-focused facet back structure. A sandwich of steel face sheets and aluminum core is fabricated with the desired curvature, and the mirror is then bonded onto the concave side.

TABLE VII. SELECTION CONSIDERATIONS FOR MAJOR CRSTPS DESIGN FEATURES

KEY FEATURES OF CRSTPS PRELIMINARY DESIGN	TECHNICAL PERFORMANCE 1	TECHNICAL STATE-OF-ART 2	SAFETY 3	PRACTICAL UTILITY APPLICATION ASPECT 4	ECONOMIC OPTIMIZATION 5	TIMELY DEVELOPMENT, PILOT 1980, COMMERCIAL 1985 6	THIRTY-YEAR LIFE CAPABILITY 7	ENVIRONMENTAL IMPACT 8	PRIMARY SELECTION DRIVER(S)
1. SYSTEM									
Modularized Collector Near 50 MW_{th} Size	Near Optimum	Future Development	Not Impacted	Maximum Reliability, Versatility	Within 1% of Optimum	Vital to Commercial Plant 1985	Not Impacted	Minimizes Affected Air Space Envelope	1, 4, 6
150 MW_e Size Commercial Plant	High, Not Keyed to Plant Size	Turbo Machinery Available	Not Impacted	Common Utility Plant Size	Optimum	Compatible with Commercial Plant 1985	Not Impacted	Land Use Keyed to Plant Size	2, 5
1554-Heliostat Pilot Plant vs 1325-Heliostat Plant	High with Either Module	Not Impacted	Not Impacted	Simulates Operating Modes and Application	4-5% More Expensive Pilot Plant	More Fully Develops Receiver	Not Impacted	No Impact	4, 6
2. RECEIVER SUBSYSTEM									
Cavity Configuration, Aperture Diameter/Depth ≈1.5	Mandatory for Receiver, Effectivity = 0.92-0.94	Long History and Recent 1 MW_t Receiver Confirmation	Removes Major Optical Hazard from Reflection	Not Impacted	Optimum Due to System Size Minimization	Minimum Risk, 1 MW_t and 5 MW_t in Being	Not Impacted	Removes Major Optical Hazard	1, 2, 3, 8
Natural Circulation	Self-Compensating for Flux Variation	Widespread Use; Utility, Industrial, Naval Boilers	High, Function Not Keyed to Support Equipment	Well Understood and Accepted, Simple Controls	Optimum Due to Minimized Support Equipment and Controls	Minimum Risk, Current Practice	Demonstrated	No Effect	2, 3, 6
Conventional Boiler and Superheater Flux Levels	Attainable with Current Design Practice	Widespread Use	High, Readily Adaptable to ASME Code	Provides Highly Flexible Operation	Not Impacted	Minimum Risk, Current Practice	Demonstrated	No Effect	3, 4, 7
10687 kPa (1550 psig) Operating Pressure	Exceeds Minimum Requirement for EPGS and TSS	Well Within State of Art	Demonstrated Widely	Minimum Impact 5-10 minutes/Day Availability	Optimum, Higher Pressure Allowed, Smaller Piping	Current Practice	Demonstrated	No Effect	5
90 m (295 ft) Cladded Steel Tower	Net 3% Penalty	Well Within State of Art	Slight Reduction in Optical Hazard	Not Impacted	Optimum	Available Now	Not Impacted	Slightly Decreased Air Space Envelope	5
3. COLLECTOR SUBSYSTEM									
North Side Heliostat Field Feometry	Optimum Use of Reflector Area	SRE Confirmed Optics and Projected Performance	Confines Zone of Optical Hazard	Minimum Plant Capacity Variation during Year	Optimum, Keyed to Optimum Performance	Assured	Not Impacted	Confines Zone of Hazardous Air Space	1
Glass Mirrors	Highest Performance Now and Potentially	Only Consistently Successful Solar Reflectors	Not Impacted	Minimum Maintenance	Optimum, Highly Automated Industry in Being	Highest Performance with Process Modification	Only Type to Ever Be Used More Than 20 Years	No Effect	1, 5, 7

Steel Heliostat Structure	Readily Meets Requirements	Long History, SRE and STTF Confirmation	Readily Meets Requirements	Minimum Maintenance	Key Factor in Plant Capitalization	Assured	Demonstrated	No Effect	1, 3, 7
Focusing Heliostat	Vital to Minimum Cavity Size	New for CRSTPS, Demonstrated SRE and STTF	Confines Zone of Optical Hazard	Not Impacted	Optimum Due to Performance Benefit	Assured	Not Impacted	Confines Zone of Optical Hazard	1, 5
Open-Loop Computer-Controlled Tracking	Readily Meets Requirements	Demonstrated at STTF	Optimum, Enables Accurate Stow-to-Track Control	Maximum Flexibility of Control	Optimum	Assured	Periodic Maintenance Required	Not Impacted	4, 5
Face-Down Stowage	Reduces Structure for High Winds	Demonstrated SRE at STTF	Vital to Aerial Safety during Shutdown	Minimizes Cleaning Cycle	Optimum Due to Structure and Cleaning	Not Impacted	Not Impacted	Eliminates Hazard during Shutdown	1, 3, 4, 8
Gear Drives for Azimuth and Elevation	Achieve Drive Function with Minimum Power	Widespread Use	High	Highly Reliable, Minimum Maintenance	Key Factor in Plant Capital Cost	Assured	Demonstrated	No Effect	1, 4, 7
Caisson Foundation	Small Impact on Total Tracking Error	Widespread Use	Not Impacted	Simplifies Installation	Optimum	Available Now	Not Impacted	Minimizes Ground Disturbance	5, 8
Laser Focus and Alignment	Readily Meets Requirements	Demonstrated at STTF	Enhanced, Allows Night Focus/ Alignment	Benefits Installation and Maintenance	Optimum	Assured	Not Impacted	No Effect, Laser Power at Safe Level	1, 5
4. THERMAL STORAGE SUBSYSTEM									
Sensible Heat	Readily Meets Requirements	Only Option Ready for Application	Demonstrated Industrial Safety	Demonstrated Operational	Uses Low-Cost Commercial Materials	Assured	Periodic Makeup Required	Tankage Keeps Impact to Aesthetics	2, 4
2-Stage Oil, Salt Configuration	Highest Effective Utility Scale Storage	Commercial Materials, SRE Confirmed System Feasibility	Readily Meets ASME and Industry Codes	High Reliability, Broad Operational Flexibility	Optimum	Assured	On-Line (Oil) Maintenance Equipment Required	Requires Earthen Dike Spillage Control	1, 5
Dual-Mode Charging and Discharging Capability	Enables Optimized Charge and Discharge Exchangers	Expanded Version of SRE Reversible System	Slightly Enhanced by Independent Loops	Best Operational Flexibility, No Built-In Time Lapse	Optimum	Assured	Not Impacted	No Effect	4, 5
5. ELECTRIC POWER GENERATION SUBSYSTEM									
Dual Admission, 9308 kPa (1350 psi) 783K (950°F) Turbine	Highest Performance over Wide Range of Loads and Steam Conditions	Commercial Design	Demonstrated	Most Effective Equipment Meeting Broad Operating Requirements	Optimum at Commercial Size	Available Now	Attainable with Daily Cycling	No Effect	2, 4, 7

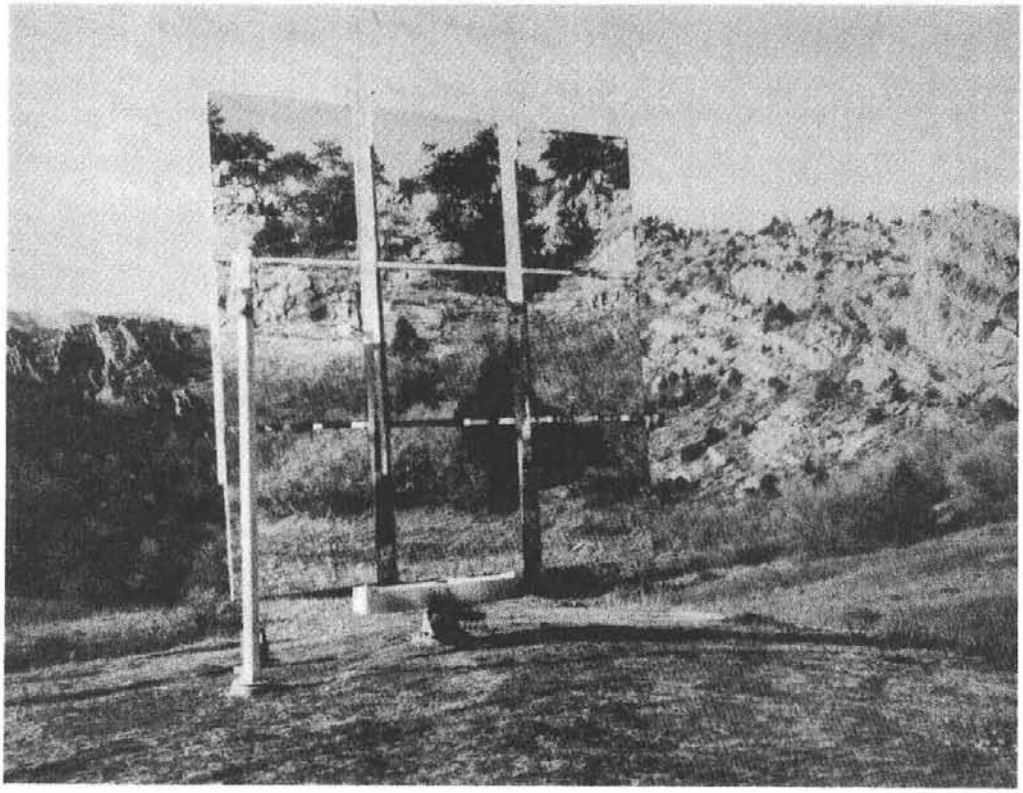

Figure 29. Nine Facet Pre-Focused Heliostat of Subsystem Research Experiment

Open-loop control has been selected for the heliostat rather than the closed-loop control used in the subsystem research experiment. The successful application of this technique for the 222 solar thermal test facility heliostats, being installed, enabled comparison of the two control techniques on similar heliostats at the hardware stage. Economic factors and design maturity favor the open-loop control.

In the receiver subsystem, maximized thermal energy conversion performance in the steam generator is keyed to the use of a cavity receiver with minimum aperture size. The cavity is designed for maximum performance with flux levels, materials, and natural circulation steam generation consistent with commercial powers, industrial, and naval boiler practices.

The MW_{th} receiver, built and tested in the subsystem research experiment phase of the current program, is shown in Figure 30. This unit was erected at Sandia Laboratories Radiant Heat Facility in Albuquerque by Foster Wheeler Energy Corporation. The support equipment module and the control console needed for the receiver operation were built by Martin Marietta. The infra-red lamp array, condenser, and water treatment equipment were supplied by Sandia. The SRE testing included (1) low-pressure cleaning and checkout runs, (2) high-pressure and high-temperature performance test runs, (3) hot start, cold start, and cloud interruption cycling

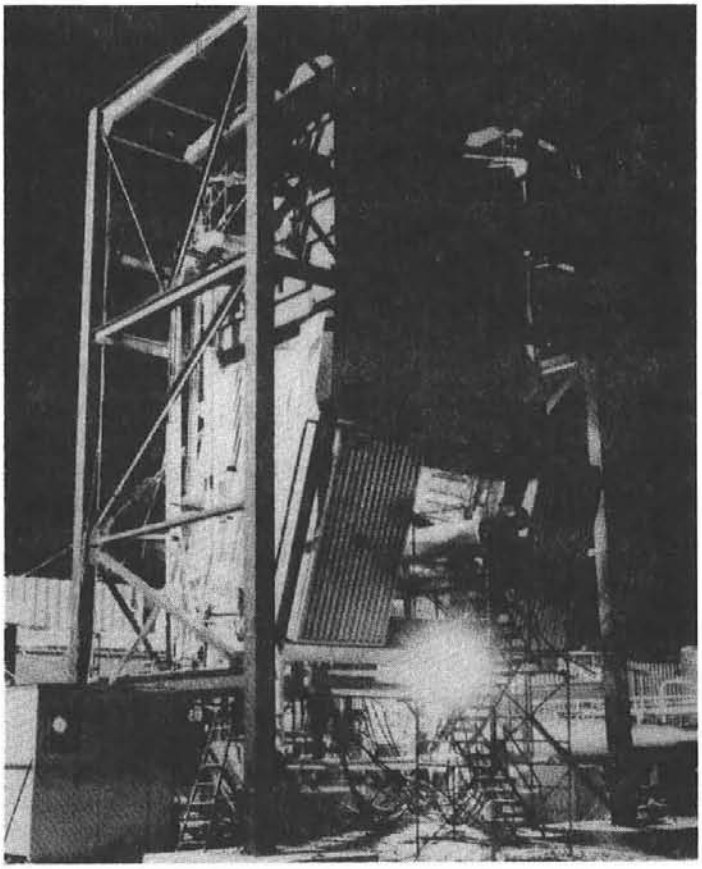

Figure 30. 5 MW_t SRE Receiver in Operation at Sandia Radiant Heat Facility

sequences, and (4) partial load performance runs. Total test time of 231.2 hours covered 53 operational cycles, of which 31 attained rated pressure, 9140 kPa (1325 psig), and rated temperature, 789 K (960°F).

Choice of sensible heat storage from the broad range of thermal storage technology options was based on its state-of-the-art readiness for incorporation into near-term plants. Use of two stages, molten salt and hydrocarbon oil, both of which are commercial heat transfer fluids, enables turbine performance to be maximized on steam generated from the stored energy at a superheat temperature of 700°K (800°F).

An overview of the thermal storage subsystem research experiment is shown in Figure 31. The subsystem research experiment, a complete subsystem scaled down to a 1.6 MW_{th}-hr capacity and 2 MW_{th} charge/discharge rate, was built by Georgia Institute of Technology on the Newnam, Georgia, power plant property of the Georgia Power Company. Testing of the thermal storage SRE included 15 complete charge/discharge cycles, 12 constant rate performance test runs, and 3 transient operation experiments.

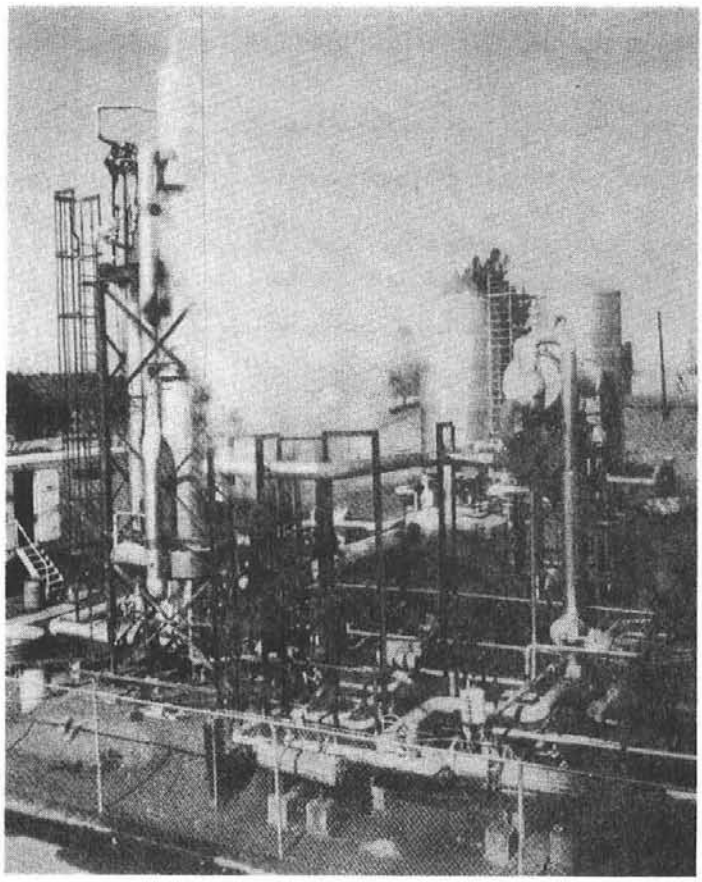

Figure 31. 2 MWh_t Thermal Storage Research Experiment in Operation at Georgia Power Company, Newnan, Georgia

Selection of a dual admission turbine in the moderate pressure range centered around the requirement for daily cyclic operation and utilizing a single machine to operate from either or both steam conditions present in the plant, receiver steam at 9308 kPa (1350 psig)/783°K (950°F) or storage steam at 2758 kPa (400 psig)/700°K (800°F). The superior partial load heat rate performance of the admission type turbine is of particular benefit to the solar plant operational flexibility.

Timely development is assured by the virtual elimination of a scaling difference between the commercial and pilot plants in the solar subsystems, thereby eliminating a development stage between the pilot and commercial size plants.

CENTRAL RECEIVER PILOT PLANT DESIGN

McDonnell Douglas/Rocketdyne/Sheldahl/Stearns-Roger
University of Houston/West Associates

Activities during this semi-annual period consisted of finalizing the conceptual design of a 100-MW_e commercial system, completing the preliminary design of the 10 MW_e pilot plant system, and finishing the SRE test programs for the collector, receiver, and thermal storage subsystems.

CHARACTERISTIC	COMMERCIAL (100 MW_e MODULE)	PILOT PLANT (10 MW_e)
FIELD DIMENSIONS	5704 FT X 6278 FT	1647 FT X 1811 FT
NUMBER OF HELIOSTATS	26,300	2200
HELIOSTAT SIZE	20 FT (6.1 m)	20 FT (6.1 m)
TOWER HEIGHT	735 FT (224 m)	197 FT (60 m)
RECEIVER TEMPERATURE (PEAK)	960 FT (516 C)	960 F (516 C)
THERMAL STORAGE TEMPERATURE	600 F (316 C)	575 F (302 C)
TURBINE INLET TEMPERATURE	950 F (510 C)	950 F (510 C)
TURBINE THROTTLE PRESSURE	1815 PSIA	1465 PSIA
NET PLANT EFFICIENCY		
DIRECT	33%	29.8%
FROM STORAGE	27%	23.6%

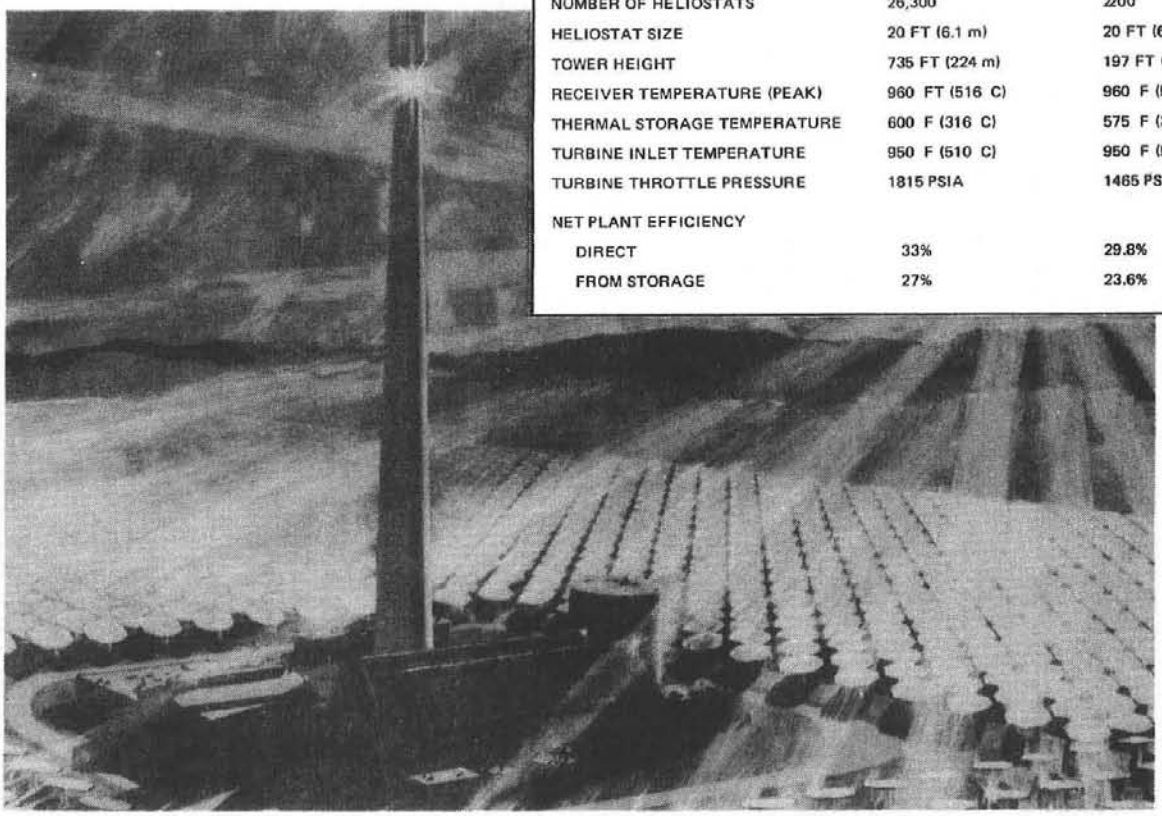

SYSTEM DESIGN

- EVALUATED THE IMPACT OF SOLAR MULTIPLE AND STORAGE CAPACITY ON COST OF ANNUAL ENERGY
- CONCEPTUALLY DEFINED 100-MWe COMMERCIAL PLANT-TECHNICAL FEASIBILITY AND ECONOMIC POTENTIAL INDICATED
- COMPLETED PRELIMINARY BASELINE DESIGN OF 10-MWe PILOT PLANT--

  COMMERCIAL/PILOT PLANTS SIMULATION VERIFIED
- PRELIMINARY DEFINITION OF TECHNICAL DATA APPLICABLE TO COMMERCIAL PLANT
- PRELIMINARY ESTABLISHMENT OF PILOT PLANT TECHNICAL RISK, SCHEDULE, AND PROGRAM COST

RECEIVER

- RADIENT HEAT FLUX TESTING OF SINGLE TUBE AND NARROW PANEL COMPLETED
- TESTING OF FULL-SIZE PILOT PLANT PANEL IN PROGRESS
- TESTING OF RECEIVER SURFACE COATINGS IN PROGRESS

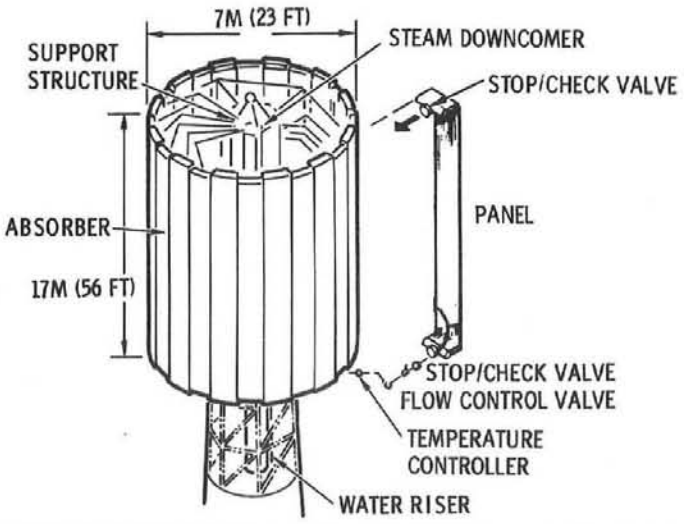

THERMAL STORAGE SUBSYSTEM

- TESTING INDICATES THERMAL STORAGE SUBSYSTEM MEETS PILOT PLANT PERFORMANCE REQUIREMENTS
- COMPARATIVE ANALYSIS CONFIRMS THAT PRESENT DESIGN PROVIDES BEST PERFORMANCE AT LOWEST COST AND LEAST TECHNICAL RISK

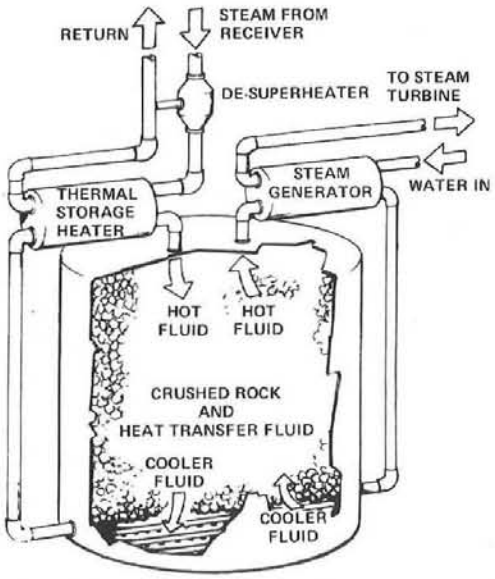

COLLECTOR SUBSYSTEM

- HELIOSTAT ARRAYS UNDERGOING SYSTEM TEST
- HELIOSTAT LABORATORY TESTING NEARING COMPLETION
- FIRST-SURFACE REFLECTORS PRODUCED USING COMMERCIAL PROCESSES

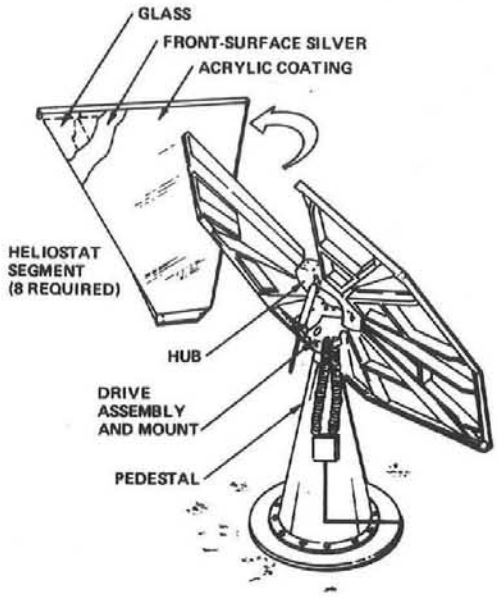

System Design and Integration

During this semiannual period, the SRE test results were used in combination with updated definitions of commercial and pilot plant requirements to expand the commercial system definition, generate commercial system cost estimates, update the pilot plant preliminary design, and refine the pilot plant cost estimates.

The commercial system design effort was performed to provide a design reference for the 10-MW_e pilot plant and to permit the early development of economic data. The basic ground rule used in developing the commercial design was to define a configuration that would minimize the cost of electrical energy on an annual basis while being compatible with ERDA-imposed guidelines and requirements. In addition, an effort was made at all times to use existing off-the-shelf equipment to minimize the need for additional hardware development and to minimize program risk.

A single module 100-MW_e commercial system was defined conceptually, based upon an electric power generation subsystem (EPGS) which utilizes an available dual-admission industrial turbine-generator sized to provide 100-MW net electrical power while operating on receiver steam and 70-MW net when using steam generated from thermal storage. The overall system was sized to have a solar multiple of 1.7 and 6 hours of operating capability from storage, based upon considerations of annual costs of generating electricity and operating flexibility to meet variations in utility requirements. The data used in making the sizing selection has been presented in past documentation. The overall field layout for the commercial system is shown in Figure 32, along with appropriate data on receiver height, tower height, and number and size of heliostats. The actual heliostat field outline will follow a smooth continuous curve as illustrated by the outer dashed line. The heliostats themselves would be arranged along circular arcs with heliostats in alternate arcs being staggered to increase the optical window to the receiver. The heliostat coverage fraction varies from ~43 percent near the central exclusion area to ~14 percent along the northern perimeter, with a field average coverage of 23 percent.

In the final version of the pilot plant system definition, those commercial system elements requiring verification were identified and ordered in terms of decreasing importance. The design and operational aspects associated with the water/steam loop were selected for preserving as much as possible, as well as the general geometric characteristics of the collector field and receiver. This latter objective ensured the verification of the collector/receiver interface from an operational standpoint. In addition, the decision was made to preserve the full-size commercial heliostats, since they comprise the most expensive subsystem. The final pilot plant collector

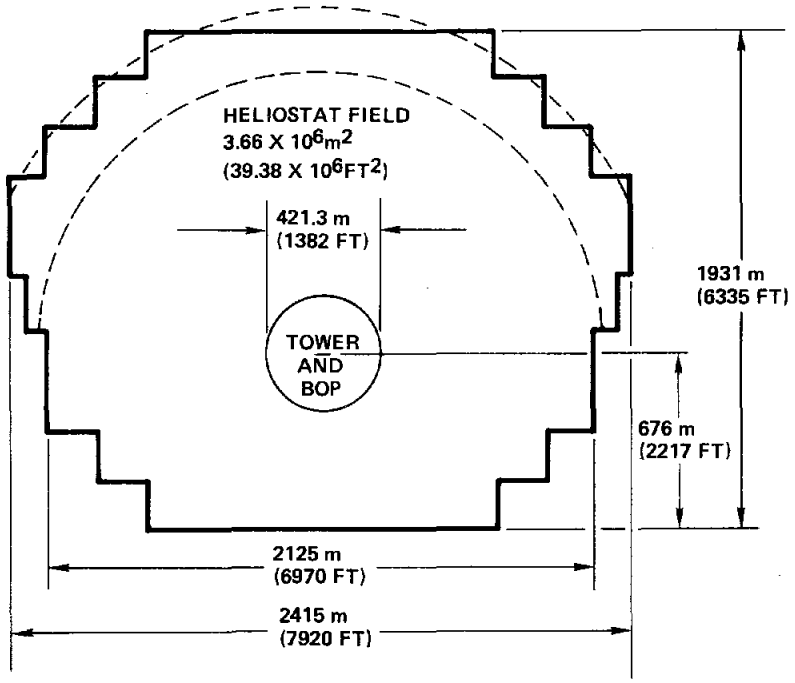

Figure 32. Commercial System Field Layout

field configuration, which represents a scaled-down version of the commercial system collector field, is shown to scale in Figure 33. The field is comprised of 1760 heliostats with each of the heliostat symbols shown corresponding to the exclusion area required for the heliostat. Also shown is the arrangement of the power house, auxiliaries, receiver/tower, and thermal storage in the central exclusion area. The radial stagger nature of the pilot plant collector field preserved the nature of the commercial field shown in Figure 32. The collector field requires 75 acres of land, with an additional 2.6 acres being used for the central exclusion area. Field coverage fractions are the same as the commercial system.

Collector Subsystem

The primary activities during the past semiannual period on the collector subsystem consisted of finalizing the pilot plant preliminary design completing the subsystem research experiment (SRE). Preliminary designs were developed and SRE tests were conducted on two heliostat configurations. One heliostat design features an octagonal shape and is noninverting, while the other is an orthogonal shape and can be inverted for stowage. The inverted stowage heliostat was selected as the pilot plant configuration.

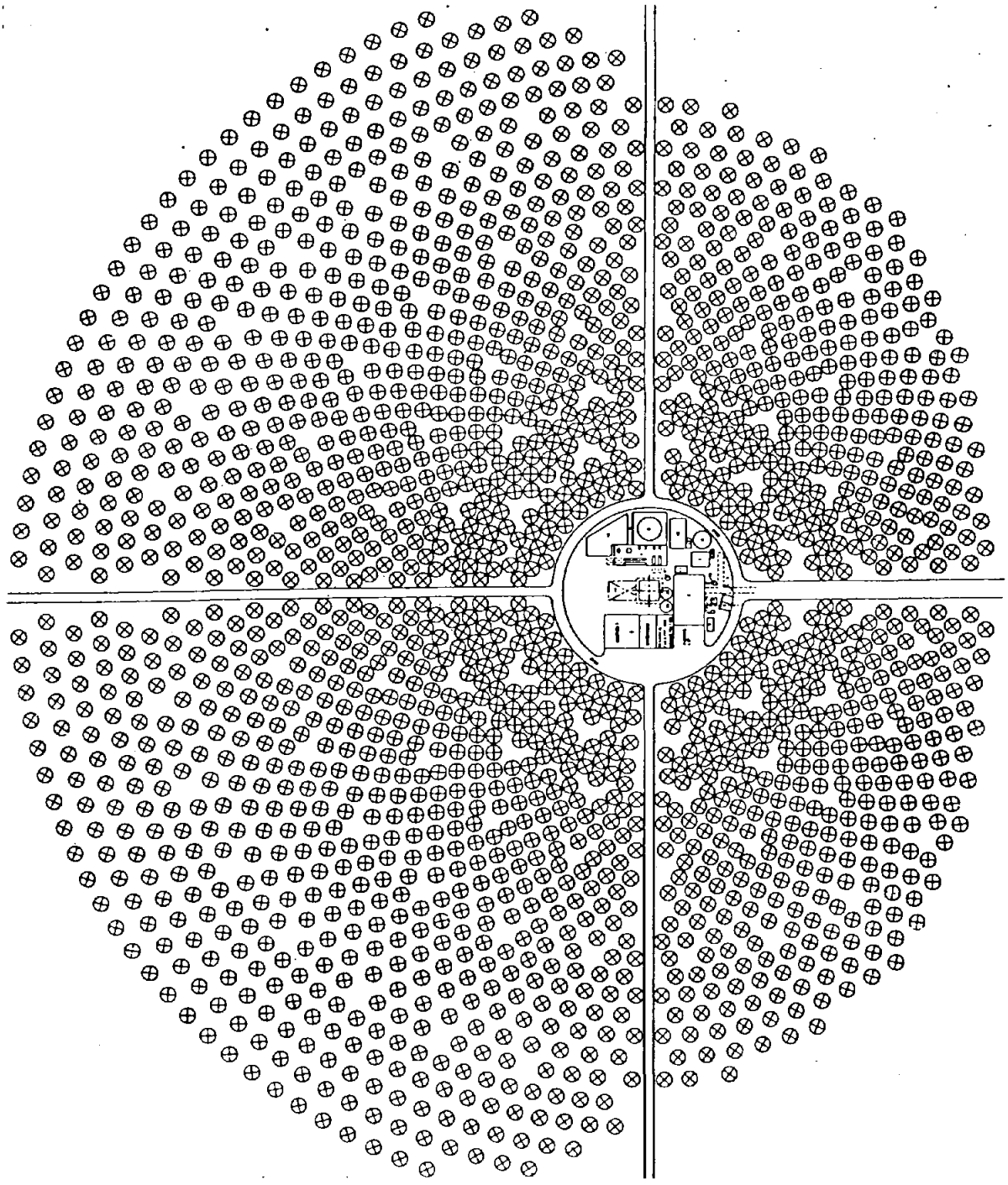

Figure 33. 10-MW Central Receiver Collector Field Layout

An array of heliostats was installed and operated at the Naval Weapons Center, China Lake, California. As shown in Figure 34, five heliostats were installed on foundations north of the two towers supporting the target. Heliostat array tests using both of the aforementioned configurations are depicted in Figure 35. The two types of test data derived from the subsystem-level test program conducted at NWC were engineering performance data and significant information on installation, operation, and maintenance.

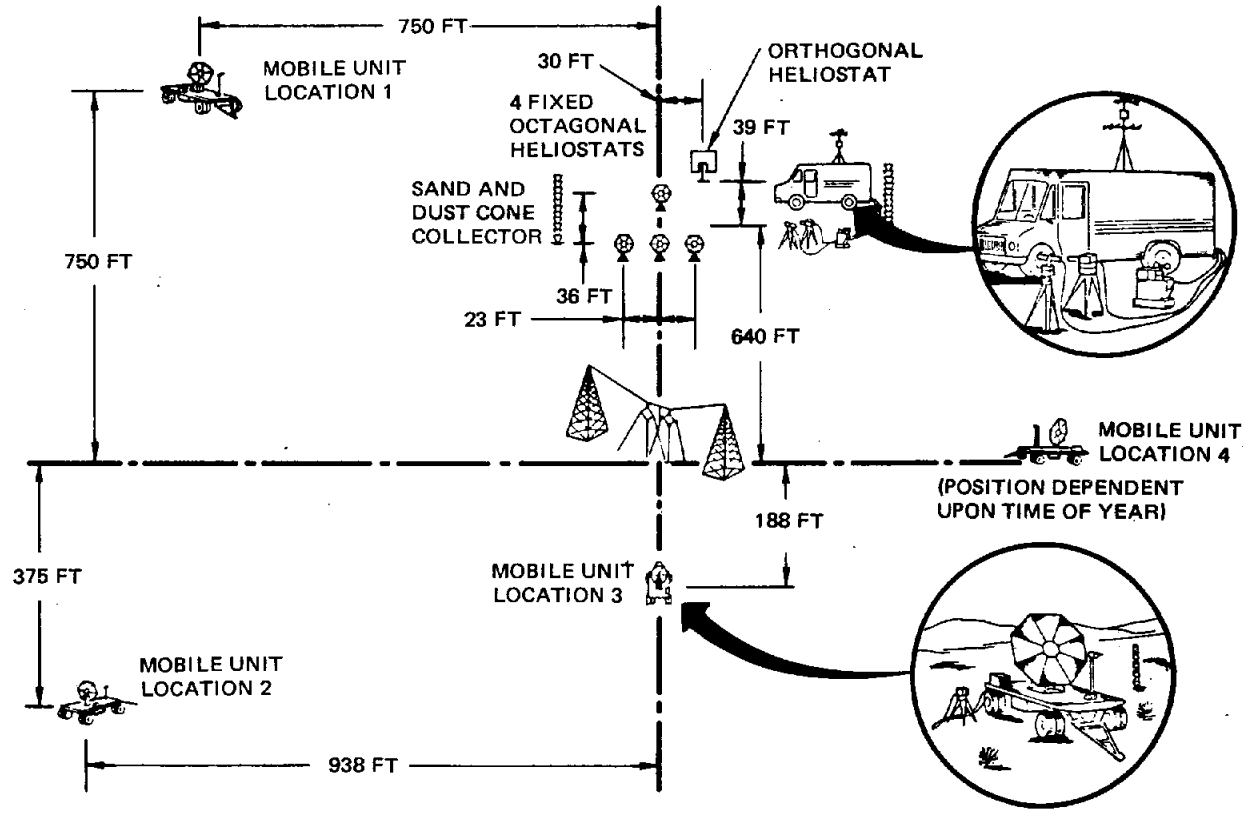

Figure 34. Heliostat Array Test Locations

The results of the collector SRE testing indicate:

- The control system that has been defined using a closed-loop beam sensor is capable of orienting the reflector surface to within 1 milliradian of the desired direction throughout the range of operating wind speeds.
- Reflectors incorporating sufficient surface contour accuracy for both pilot plant and commercial plant operation can be produced.
- The proposed configurations of the reflector, drive unit, and support structure are able to withstand the anticipated

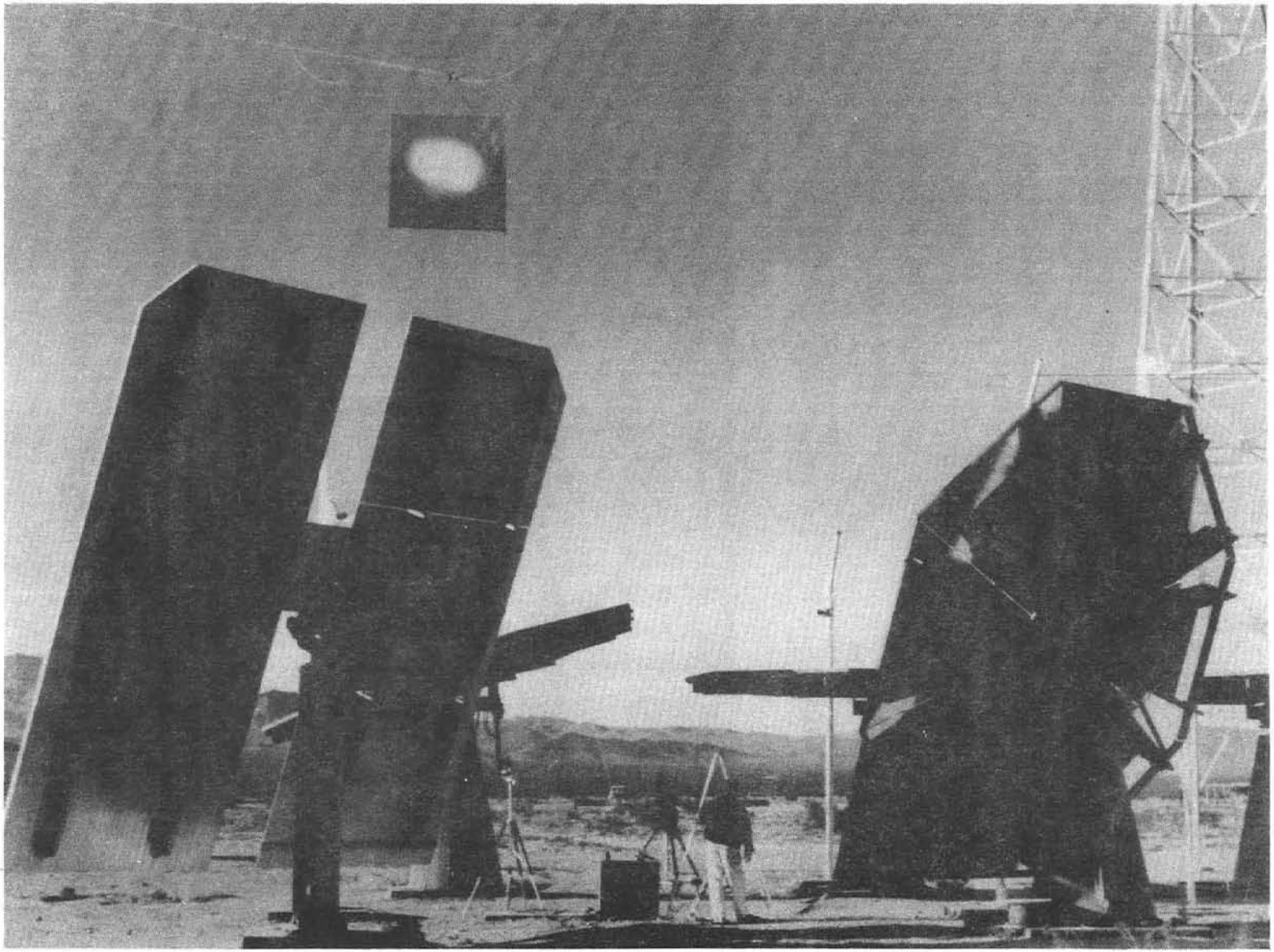

Figure 35. Heliostat Array Tests

environment, including winds up to 100 MPH, blowing dust, rain, hail, icing, and wide ranges in temperature.

- Multiple heliostat control by a field controller presents no significant problems.
- Heliostat power consumption is very low (12 watts average).
- Excellent reflector cleaning techniques have been identified which require minimal time and materials.
- Installation, operation, and maintenance data for the collector were obtained and documented for a site which is close to the pilot plant site and has similar weather and soils.
- Pedestals and foundations were quite stable.

Receiver Subsystem

Receiver activities during the first half of 1977 consisted of conceptually defining a commercial receiver, completing the preliminary design of a pilot plant receiver, and completing the SRE test program.

Both commercial and pilot plant receivers are of external, single-pass-to-superheat design and feature 24 panels of Incoloy 800 tubing which are attached to the inner receiver support structure. The commercial receiver and tower are shown in Figure 36. This configuration has 20 boiler panels and 4 preheat panels, with the preheaters located on the south side. All tubes are 27 m (89 ft) long, with an exposed length of 25.5 m (83.6 ft). The additional length provides for folding over at the top and bottom of the panels to protect the Incoloy 800 inlet and outlet manifolds and support structure from radiation. The surfaces of the tubes exposed to solar radiation are coated with Pyromark paint which has demonstrated an absorptivity of 95 percent over a wide range of wavelengths. The coating is resistant to weathering and was tested for long-term compatibility with high-intensity solar radiation during the SRE tests.

The receiver tower is of jump-formed concrete construction and extends 242 m (794 ft) above grade to the interface with the receiver unit steel support structure, which continues up through the receiver unit to an elevation of 281 m (921 ft) where it is crowned with a 20-ton capacity service crane (not shown). The top of the concrete has an outside diameter of 15.3 m (50.25 ft) with a nominal 0.305 m (12 in.) wall thickness. The base of the tower has an outside diameter of 45.7 m (150 ft) with a 0.46 m (18 in.) wall thickness.

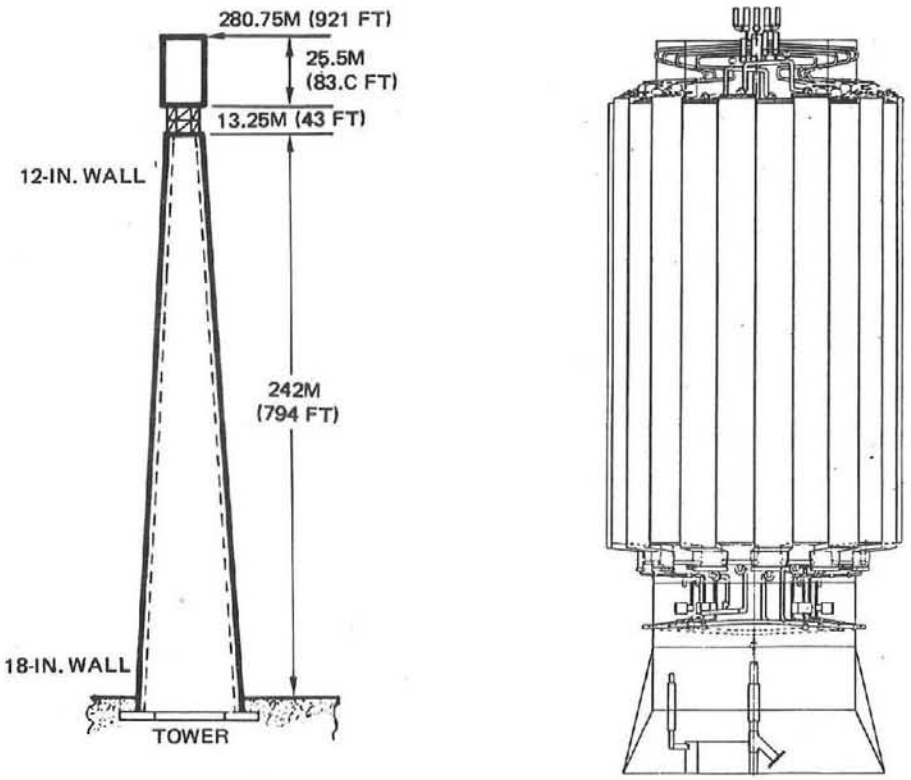

Figure 36. Commercial Plant Receiver and Tower

The pilot plant receiver and tower are shown in Figure 37. This configuration has an external receiver assembly comprised of 18 boiler panels and 6 preheat panels, all of Inconel 800, attached to the inner structure and mounted above a 65 m (213 ft) free-standing steel tower. The principal development in receiver design for the pilot plant during the last semiannual review period was the reduction in panel length from 17 m (56 ft) to 12.5 m (41 ft), with a resulting increase in performance due to a reduction in thermal losses. The reduction in receiver weight also was beneficial in designing the receiver and tower structures to withstand the postulated 0.25-g (horizontal) seismic environment.

The principal SRE activities centered around the testing of a full-size pilot plant receiver panel (Figure 38) in the Rockwell B-1 radiant heat flux test facility in El Segundo. The objectives of the full-scale receiver panel tests were to (1) demonstrate that pilot plant panel could be fabricated and transported, (2) verify pilot plant receiver performance and operation at safe wall temperature with design pressure drop, (3) verify control and stability of the panel during steady-stage and transient operations, and (4) verify thermal stress and expansion provisions.

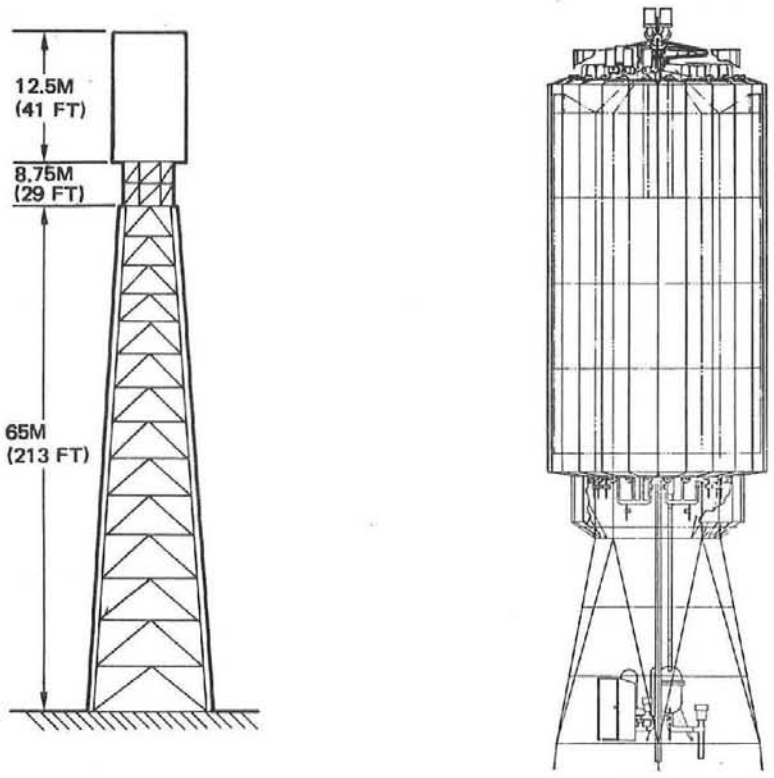

Figure 37. Pilot Plant Receiver

Upon completion and erection of the test tower, the full-scale panel was installed vertically into the test tower and testing was conducted, as indicated in Figure 39. Solar flux on the panel was simulated using a stack of 165 resistance heaters in front of and across the panel absorptive surface. Flow stability and uniformity testing of the 70-tube panel was initiated using Inconel heater elements to obtain long heater life during the low flux phase of the test program. Test results fully confirmed the expectations created by the single and five tube testing. No indications of flow instability were detected even at low flow rates. Flow uniformity was also excellent across the panel as indicated by uniform steam discharge temperatures. Flow stability and uniformity were maintained during simulated pilot plant starts in which temperature and pressure were manually stepped from 275°C (530°F) to 325°C (620°F) at 2.76 MN/m^2 (400 psi) and then to 450°C (840°F) and 10.4 MN/m^2 (1500 psi).

The fatigue life capability of the basic panel design had been demonstrated during the five-tube panel test program under high flux levels up to 90 percent of the maximum flux anticipated for the pilot plant. Maximum hot wall tube temperatures during those tests were 103°C (185°F) below the predicted values indicating a wide margin on panel fatigue life. Full panel test results confirmed the earlier margin in heat transfer characteristics and fatigue life shown by the earlier five-tube panel tests. Tube wall differential temperatures were well below the predicted values, which indicates a comfortable margin in the fatigue life of the pilot plant panel.

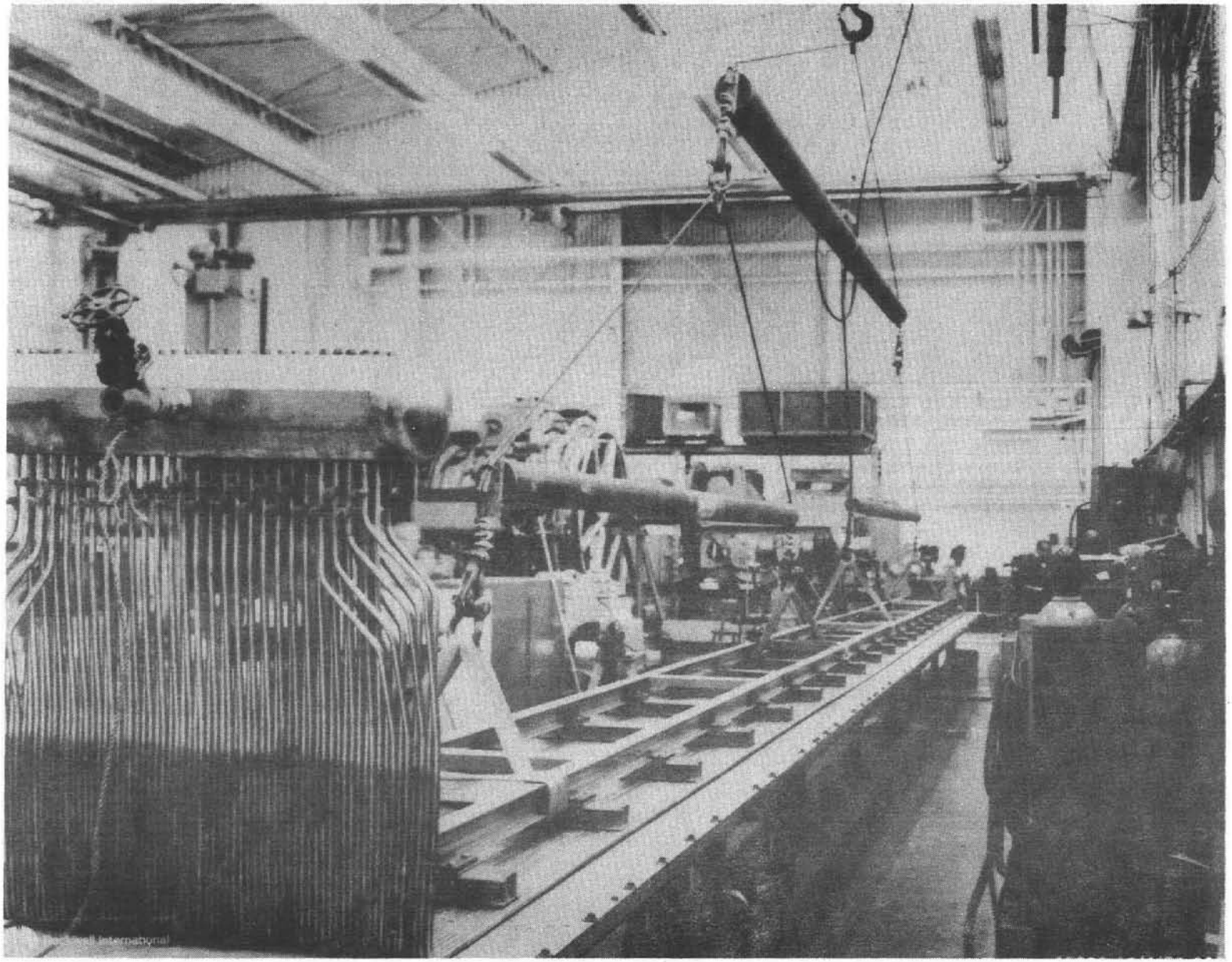

Figure 38. Completed Pilot Plant Panel

Figure 39. Pilot Plant Panel in Test

Thermal Storage Subsystem

The thermal storage activities during the first half of 1977 consisted of defining a conceptual design of a commercial configuration for a 100-MW_e power plant, finalizing the pilot plant preliminary design, and completing the SRE test program.

Both commercial and pilot plant configurations use a single-stage sensible heat concept with a dual-medium rock and oil approach to storage. The thermal storage units defined for the commercial system are 18.3 m (60 ft) tall and 27.6 m (90.5 ft) in diameter, and four of these units are used in parallel to accommodate the storage of 1857 MWh_t extractable energy. The storage capacity can provide sufficient thermal energy to operate the turbine-generator at 70 MW_e net power output for six hours. Parallel trains of five charging heat exchangers and five steam generators provide charging rates between 12.5 and 255 MW_t and discharge rates between 31.1 and 285 MW_t.

The pilot plant thermal storage subsystem configuration was not changed in concept during this semiannual period. However, in response to a change in program requirements by ERDA, the capacity was reduced to provide 7 MW_e net power for three hours instead of the previous six hours. The pilot plant thermal storage unit is a single tank, 15.2 m (50 ft) in diameter and 13.4 m (44 ft) high, and will accommodate 103.8 MWh_t of extractable energy. A parallel train of two charging heat exchangers provides a range of charging rates from 1 to 30 MW_t, while two parallel steam generator modules provide discharge rate capability between 3.1 and 32.1 MW_t.

The thermal storage SRE program consisted of two series of tests: (1) prequalification tests and (2) model subsystem tests. All tests were completed successfully, and all test objectives were met.

Thermal stability and compatibility tests were designed on a laboratory scale to determine the characteristics of candidate heat transfer fluids during long-term contact with rock and construction materials at operating temperature. The tests were conducted on Caloria HT-43, Therminol 55, and Therminol 66. In summary, the SRE prequalification testing has fully confirmed the choice of Caloria HT-43 as the baseline heat transfer fluid, and demonstrated that it can fulfill the requirements of this solar power application. This fluid was found to have excellent stability and compatibility with rocks and construction materials in tests up to 316°C (600°F) and for extended test durations. In addition, Caloria HT-43 did not foul the heat transfer surfaces. The prequalification testing has now been expanded to include Mobiltherm 123 and extended into 1978.

The SRE model subsystem tests were conducted at the Rocketdyne Santa Susana test facility, as indicated by Figure 40. The thermal storage unit (TSU) is shown in the left foreground. The basic objectives of the thermal storage SRE tests included the evaluation of charging and extraction capabilities of a scalable TSU, obtaining performance of the TSU over all ranges of equivalent operating conditions in the pilot plant, and demonstration of stable operation over a wide range of operating conditions. All test objectives were met or exceeded in the test program conducted on the model subsystem. A large variety of tests were conducted with thermal charging and discharging rates from 0.1 to 2 MW_t and with hold periods up to 144 hours. The performance of the subsystem was excellent. Sharp, stable thermoclines were present, even during partial charging and discharging, with variable rates, and under repeated cycling. Figure 41 compares actual thermocline shape and travel during a 100 percent extraction with pretest predictions. Figure 42 shows the heat transfer fluid temperature leaving the top and entering the bottom of the TSU. The extraction fluid was maintained within 2°C (3.6°F) of the target temperature of 302°C (575°F) for more than three hours and within the minimum desired temperature of 293°C (560°F) for almost four hours at an extraction rate of 1.34 MW_t. The performance of the TSU was even better than expected for a unit of this size. The unit delivered over 5.1 MWH_t of energy, which exceeded the design goal of a minimum of 4 MWH_t.

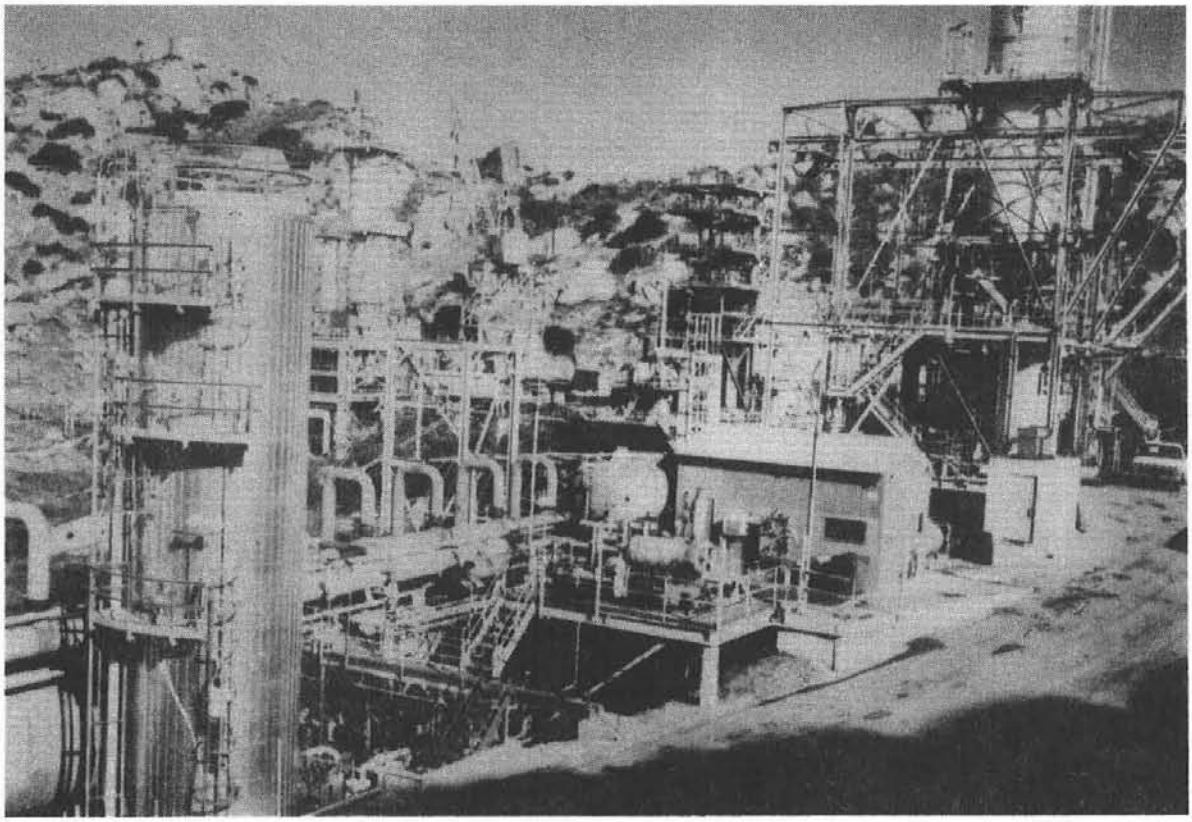

Figure 40. Thermal Storage SRE Test Site

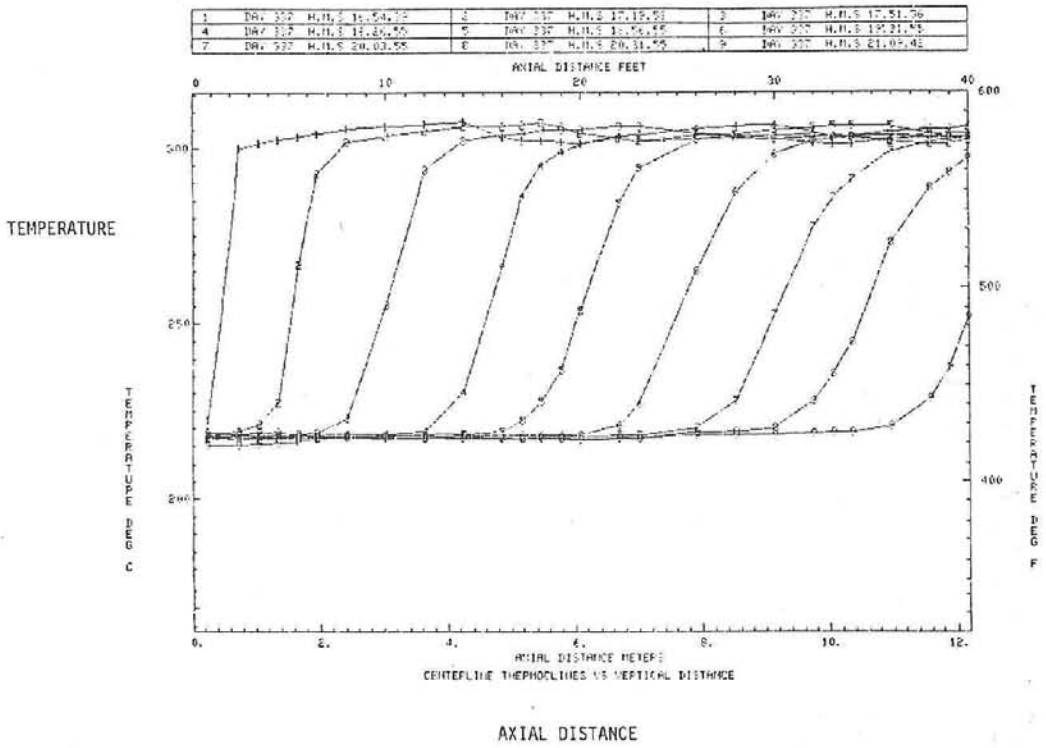

Figure 41. Typical Extraction Thermoclines, SRE Subsystem Tests and Design Predictions

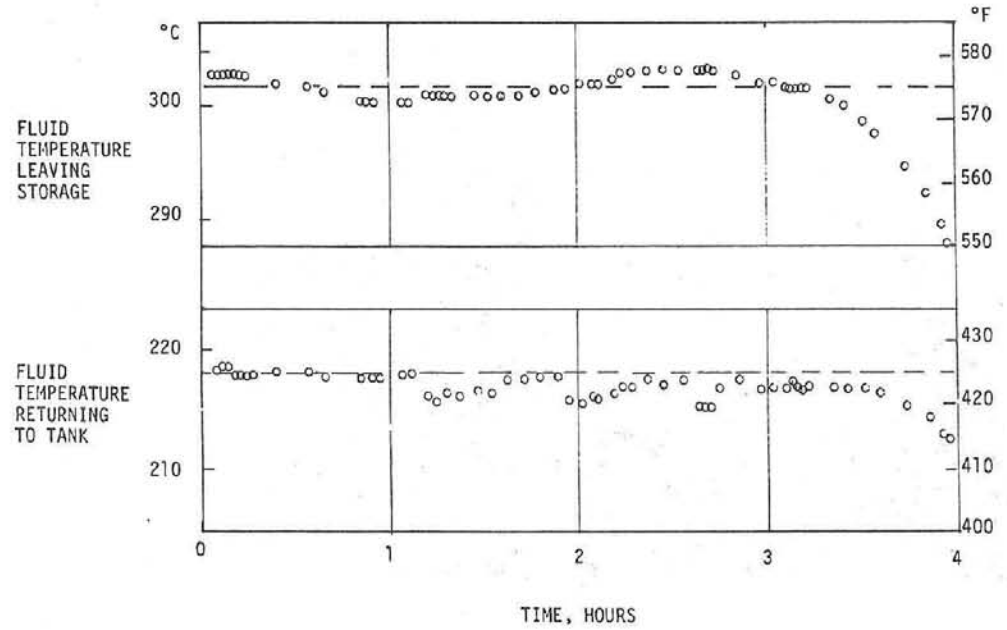

Figure 42. Typical SRE Performance Data During Extraction

CENTRAL RECEIVER-SOLAR THERMAL POWER SYSTEM COLLECTOR SUBSYSTEM

Boeing Engineering and Construction

In conjunction with the overall national effort to develop solar thermal electrical power as an alternate energy source, Boeing Engineering and Construction, Seattle, Washington, under contract with ERDA, developed a preliminary design of the collector (heliostat) subsystem for a 10-MW_e solar pilot plant. Technical monitoring of contract progress is being performed for ERDA by Sandia Laboratories. Although Boeing designed only the collector subsystem, interface requirements with other portions of the pilot plant were satisfied through coordination with Sandia Laboratories.

The Boeing collector subsystem is shown operating with a central receiver installation in Figure 43. In this concept, circular membrane reflectors formed with aluminized polyester film direct sunlight to the central receiver. The reflectors are 7.85 m (25.75 ft) in diameter, and are "gravity focused" by establishing proper tension in the reflective membrane. Transparent air-supported plastic enclosures protect the lightweight reflectors

Figure 43. Boeing Collector Subsystem

from the environment. These enclosures are 8.54 m (28 ft) in diameter, and are fabricated from gores of 0.02 cm (0.008 in.) thick polished Tedlar. The reflectors are individually aimed with a 2-axis gimbal, driven by digital-controlled stepper motors. Minicomputers, located in a central control facility, provide signals to the stepper motors.

Several heliostat field geometries have been investigated with the aid of a Heliostat Array Simulation Computer Model. The model takes into account mirror reflectance, dome transmittance, mirror aspect angle, receiver capture geometry, shadowing-blocking, and pointing accuracy in computing field performance. Figure 44 shows the heliostat field geometry developed for the preliminary design heliostat when the heliostats are operating in conjunction with a vertical-cylinder surface receiver. The field of heliostats, arranged in a nonuniform EW/NS rectangular grid of about 600 by 600 meters, will provide approximately 42 MW_{th} to the receiver at noon equinox. The irregular field boundary is primarily the result of satisfying thermal flux uniformity requirements on the vertical-cylinder surface receiver at the highest heliostat efficiency.

The receiver used in the preliminary design analysis is the McDonnell-Douglas Corporation cylindrical surface receiver. It is 12.5 m high, 7 m in diameter, and mounted atop a 80 m tower. For the present analysis, it was assumed that the heliostats are aimed at the middle of the cylindrical surface. Based on receiver thermal requirements of 42 MW_t at noon equinox, about 1650 heliostats with 7.85 m (25.75 ft) diameter reflectors are required. This results in a total reflector area of 79,721 m^2 (857,670 ft^2).

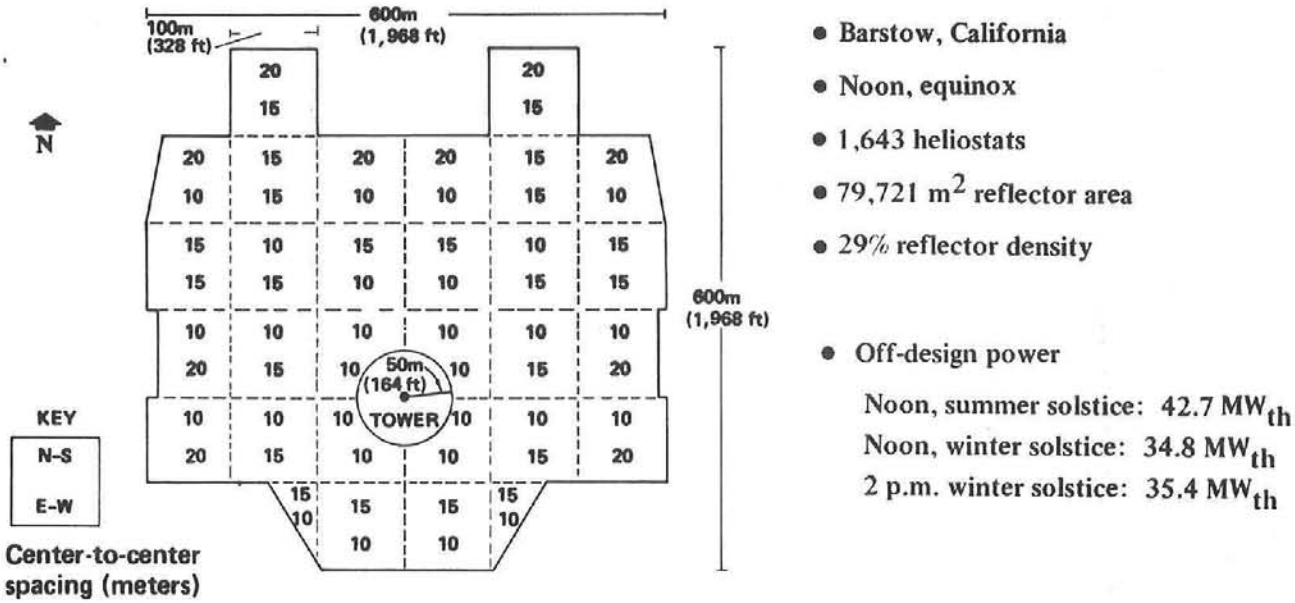

Figure 44. Surface Receiver Heliostat Field

As part of this effort, three heliostats and a drive and control assembly were fabricated and tested to provide design data and verification of the heliostat. In addition, an extensive evaluation program was conducted on the key plastic materials used in the protective enclosure and reflector. Performance tests on large-scale heliostats were conducted at a Boeing desert test site in northeast Oregon. The test, shown schematically in Figure 45, was to determine optical performance, demonstrate operation of the drive and control assembly in the various operational modes, and verify survivability of hardware in the environment. Plastic materials evaluation tests included measurement of mechanical and optical properties, creep, chemical exposure, cleanability, accelerated simulated sunlight, and actual desert sunshine exposure tests. The latter test was conducted at two different locations in the southwest (Albuquerque, NM, and China Lake, CA).

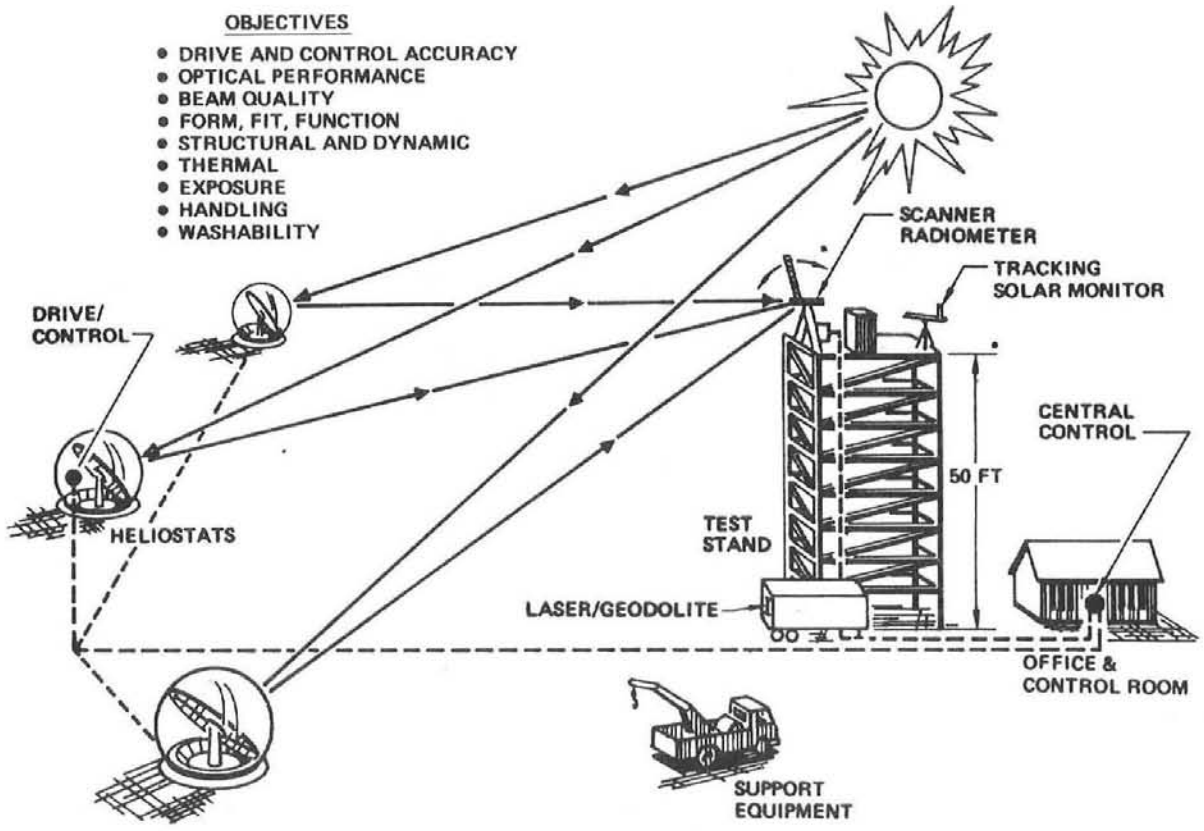

Figure 45. Research Experiments - Array Test (Boardman, Oregon)

Three of the heliostats at the desert test site are shown in Figure 46. The principal features of this research experiment heliostat include: a 5.18 m (17 ft) diameter Tedlar enclosure; a 4.57 m (15 ft) diameter aluminized Mylar reflector; an azimuth/elevation gimbal assembly; a cylindrical, steel base ring for enclosure support; and a concrete-slab foundation.

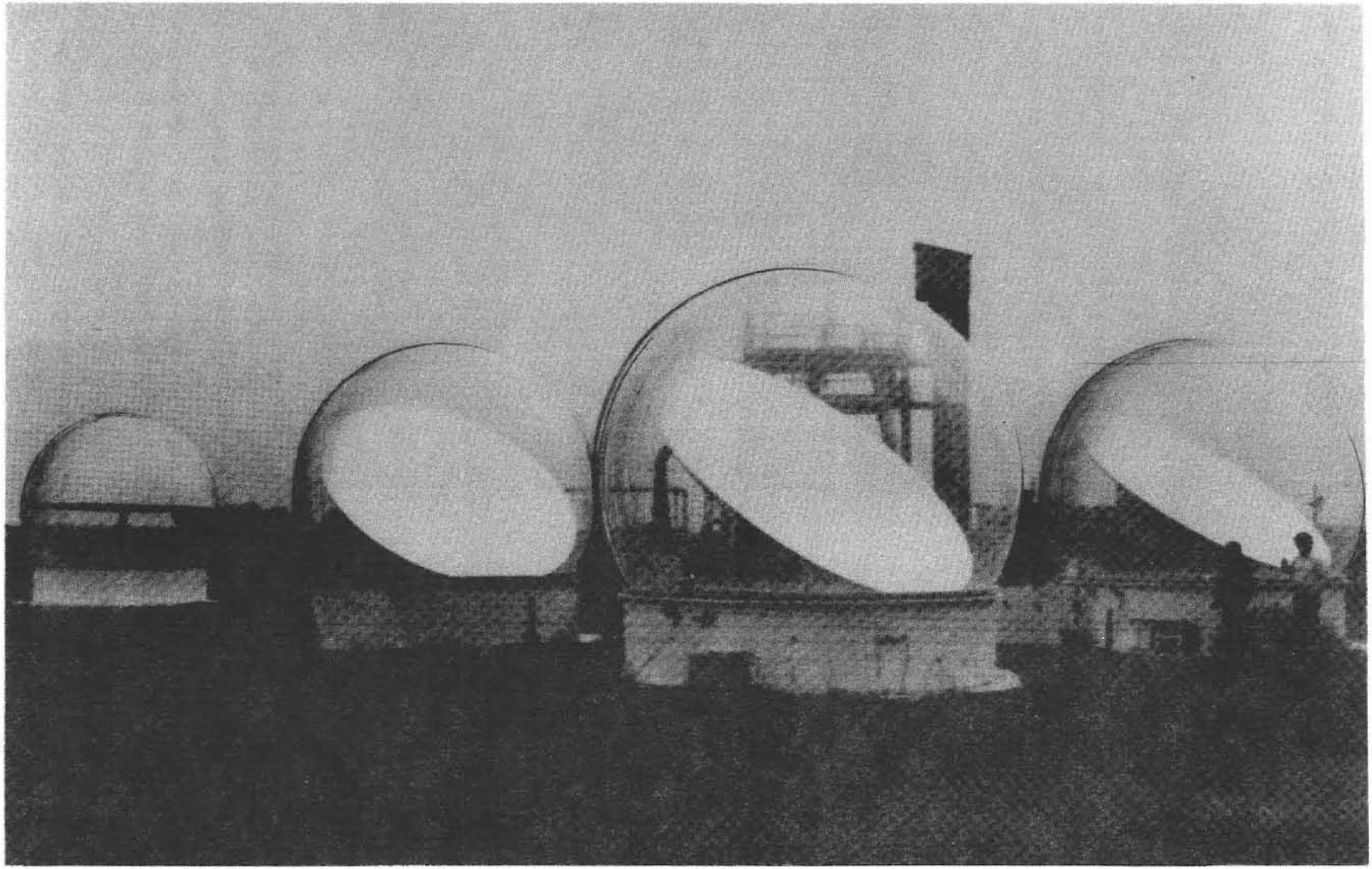

Figure 46. Heliostat Array at Boardman

A rocket test stand was used to support an optical scanner for heliostat performance tests. In operation, the scanner arm swept out a 7.32 m (24 ft) diameter circule with calibrated photovoltaic cells located at 15.24 cm (6 in.) spacings on the arm. A computerized data retrieval system plotted the heliostat image intensity distribution, calculated total image power, and calculated the aiming accuracy of reflectors. Figure 47 shows a typical optical image from one of the heliostats, measured at 10:46 a.m. on April 4, 1977. The elliptically shaped image is expected, based on the field location of the heliostat and time of day.

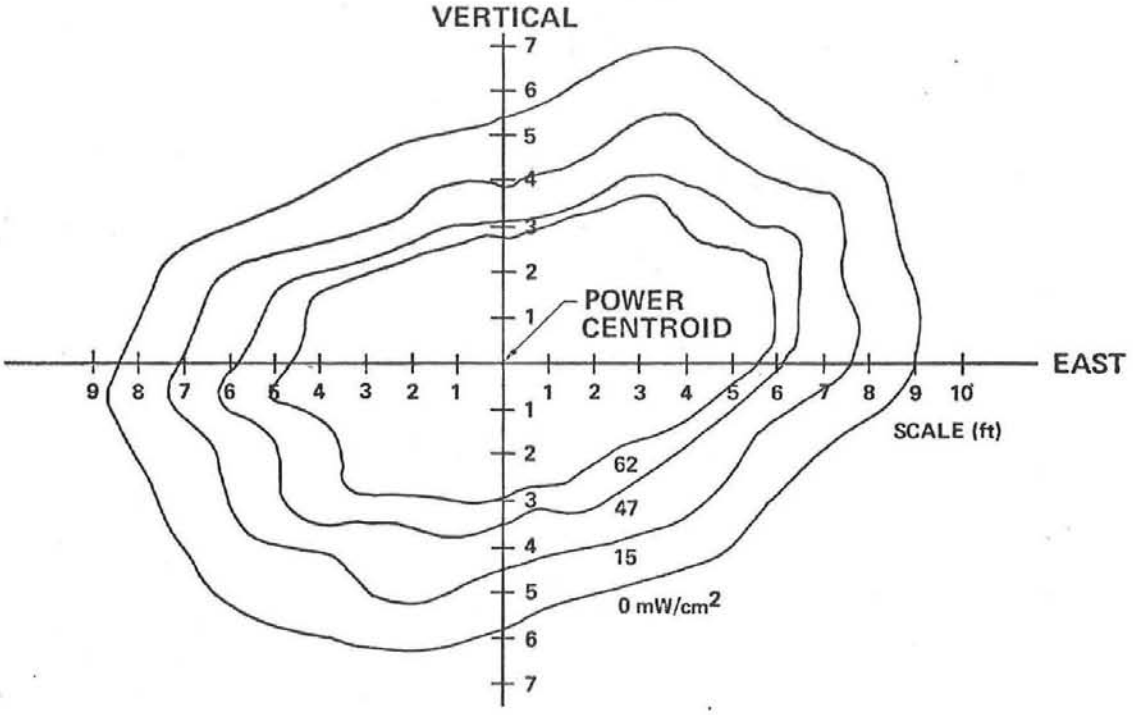

Figure 47. Single-Heliostat Optical Image

A summary of heliostat efficiency data is given in Table VIII. Measurements were made on both individual heliostats and on the group of three heliostats under various conditions over a 4 1/2-month time period. Results showed a nominal average efficiency of 69 to 72 percent for heliostats with cleaned domes, with some data scatter as indicated in the Table. Heliostat No. 1 was measured in an uncleaned condition after 5 months, and found to have a nominal average efficiency of 65 percent. In general, the results show no degradation in efficiency throughout the test, and are in good agreement with the efficiency that was predicted from the material's optical properties.

TABLE VIII. HELIOSTAT EFFICIENCY DATA

Test Condition	Heliostat No.	Date	Time	Efficiency (%)	Average Efficiency
Dome Clean	H0	11/19/76	1430	70	72 +1
		3/30/77	1605	73	-2
		4/04/77	1009	72	
	H2	4/02/77	1309	64	69 ±5
		4/02/77	1359	65	
		4/03/77	1655	71	
		4/03/77	1552	73	
		4/03/77	1558	74*	
Uncleaned for 3 Months	H0	2/11/77	1235	66	70 ±4
	H2	2/11/77	1100	70	
		2/10/77	1150	74	
Uncleaned for 5 Months	H1	3/30/77	1240	62	65 +7
		3/30/77	1514	63	-3
		4/02/77	1117	63	
		4/03/77	1503	72	

*Manual induced vibration of reflector membrane

A wind tunnel test was performed in the University of Washington Aeronautical Laboratory (UWAL) low-speed wind tunnel to determine wind loads acting on the pressurized enclosures in a heliostat array (Figure 48). The tunnel accommodated a 3.7 x 3.7 m (12 x 12 ft) ground plane and up to 60 enclosure models 19.1 cm (7.5 in.) in diameter (D). Testing was performed with single enclosure and with square and diagonal arrays at three spacing densities. Tests were performed with fences of two heights (D/2 and D/4) and without a fence. The models on one side of the ground plane were tested with a cylindrical skirt (as shown in the current design) and the other side without a skirt. One instrumented model was placed at various locations in the array to determine pressure coefficients, and a movable Pitot probe was used to determine wind velocity profiles. The test program consisted of 140 runs over a 45-hour period.

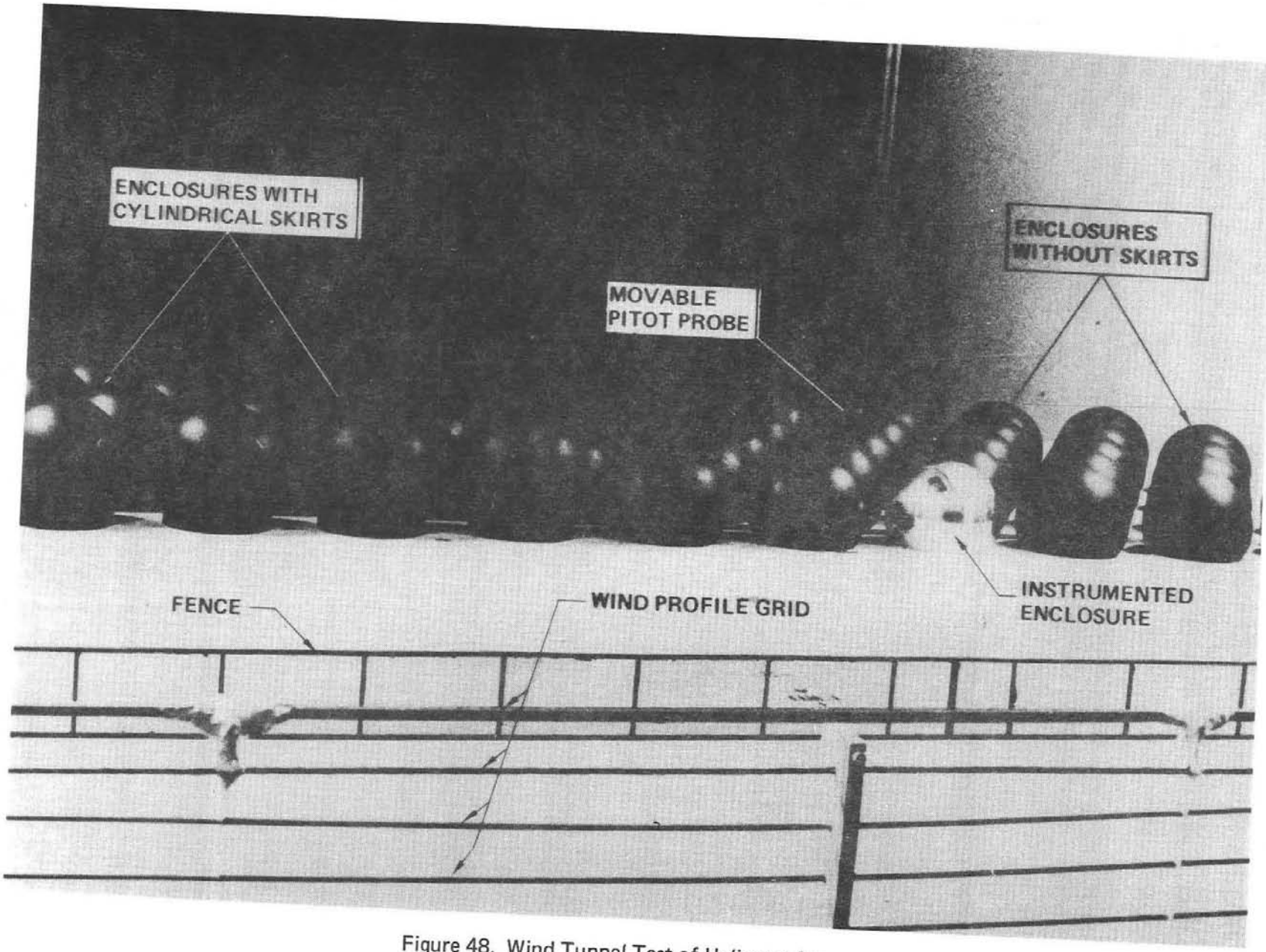

Figure 48. Wind Tunnel Test of Heliostat Array

Central Receiver Research Study

FMC

General

The objectives of this research study are to estimate and optimize the performance of a solar thermal electric power plant using an array of novel single-axis focusing heliostats and a cavity-type line central receiver. Another objective is to build a heliostat module and measure its performance. The specific efforts include calculation of steam temperature, heat flux distributions, and steam generation capacity for various receiver configurations and operating conditions of the heliostat field size to minimize electrical power costs. An 18.3-meter heliostat module will be built, based on the results of the system performance and tradeoff analysis, and the reflected solar flux density will be measured over the focal plane of a simulated receiver. The automatic heliostat controls will be tested to measure their ability to aim and focus a heliostat automatically during a solar day.

Tradeoff Analysis

Collector Subsystem

A good prediction of the performance capabilities of candidate collector field configurations is a prerequisite to concept selection and design of the rest of the system. Accordingly, a computer program was written to calculate the hourly predicated performance of collector fields of varying layouts. Collector field parameters were systematically varied to achieve the most favorable ratio between the receiver aperture flux intensity and the mirror-row. The configuration so obtained was useful for establishing realistic input levels and distributions for receiver, control, and storage design.

The optical analysis included but was not limited to the following: collector focusing, effect of curvature irregularities on focal size, effects of aperture plane angle, direct intensity distribution on inner receiver cavity walls, and field performance.

During the investigation of collector field designs, several sloped field configurations were examined. Slope angles and mirror spacings were varied to maximum output and peak concentration per row. Noon winter solstice was chosen for these calculations. Peak performance from a north field was obtained from a 30 percent (16.7 degree) slope, containing 30 heliostat rows

spaced in parabolically varying intervals from 12 feet at the inside to 20 feet at the outside of the field. Comparison between an optimized sloped north field and an optimized flat north field is shown in Table IX. As a result of data obtained and other factors, an economic analysis for a central receiver using a north-field only was initiated after system performance and economic analysis were completed.

TABLE IX. COMPARISON OF OPTIMIZED COLLECTOR FIELDS

Parameter	Sloped North Field	Flat North Field
Horizontal width, meters	130	130
Slope, degrees	16.7	0
Number of rows	30	21
Aperture angle, degrees	45	45
Tower height, meters	61	61
Peak concentration, suns	99.5	64
Concentration, suns per row	3.32	3.05

Receiver Subsystem

Two concepts for the receiver design were considered:

- Natural Convection Receiver with Vertical, Double-Row Tube Array
  This design concept consists of an open cylindrical cavity fitted with a double screen of heat-absorbing vertical boiler tubes and appropriate shell insulation (natural convection design). Saturation boiling occurs in the front tube bank. Saturated steam is separated by natural convection and passed to the rear tube bank for superheating.

- Forced Convection Receiver with Horizontal Tube Banks
  Two basic concepts were considered: A flatplate design consisting of a plane of tubes mounted in the receiver focal plane and backed by a refractory material, and a circumferential design in which the tubes are mounted on the inside circumference of the cavity. In both concepts boiling occurs in the outer tube rows and superheating in the inside rows (about the receiver symmetry axis).

Parametric simulation models of the receiver concepts were developed. The models encompassed all major energy loss mechanisms including reflection, radiation, convection, and conduction. Thermal performances at the design point of 2:00 p.m. on winter solstice were simulated for various design parameters to optimize the design of each concept. Detailed cost

analyses of each concept were also made concurrent with the performance analyses. The results of the performance and cost analyses led to the selection of the circumferential, once-through horizontal tube receiver as the baseline for the line central system.

Controls Subsystem

Since sunlight is collected by the heliostat field to supply energy to the receiver boilers, the sun/heliostat/receiver relationship is the key to the control of plant output. Additional environmental factors--wind, clouds, etc.--also influence performance. Despite the complex parametric interrelationship, the only controllable factor of plant output is mirror-field elevation angle and focusing. Because the receiver cavity aperture of 4 feet is considered near optimum, the accuracy of the elevation and focus control systems were a major factor. It is believed that a 2-milliradian accuracy figure for both elevation and focus control can be realized from control components commercially available.

Economic Analysis

The economic analysis was based on a system which produces 10-MW_e net power at 2:00 p.m. winter solstice using a turbine which receives superheated steam at 477°C (890°F) and 10 MN/m^2 (1,450 psia) and discharges saturated steam at 57°C (135°F), 0.017 MN/m^2 (2.5 psia). These conditions correspond to the General Electric turbine selected as the baseline for the system.

A thermal storage subsystem similar to that of the McDonnell Douglas Aerospace Corporation (MDAC) design (organic liquid and rock) appeared to be the least expensive for the expected storage temperature (<600°F). The sizing, performance, and costs estimated by MDAC were used for the FMC subsystem. The designs of the other solar thermal contractors were reviewed so that our costing and design efforts have concentrated on areas unique to the cavity-type line central receiver system concept.

Two system configurations were analyzed. One configuration employed both north- and south-facing receiver/collector subsystems (north/south system). The other configuration employed only south-facing collectors and north-facing receivers (north-only system). The receiver subsystem for the north/south system consists of ten sections, each 61 meters (200 feet) in length, containing two boiler/superheat cavities. The north-only subsystem contains 20 sections of the same length, but with a single cavity in each section. In both subsystems, each section produces steam at turbine operating requirements. Table X summarizes the characteristics of each system.

TABLE X. CHARACTERISTICS OF 10-MW_e BASELINE SYSTEMS

Subsystem Characteristic	North/South System	North-Only System
Number of heliostats	2,020	1,563
Number of 61-m receivers	10(double)	20(single)
Number of 61-m towers	11	21
Collector area (km^2)	0.121	0.094

Annual Generating Capacity

Annual generating capacity for each system was estimated from the daily outputs computed for 3 solar days, as shown in Table XI. The annual capacities, shown in Table XII, were computed by linear interpolation between the solar days to estimate monthly capacity for January-June, and then assuming symmetry about summer solstice to estimate capacities for July-December.

TABLE XI. DAILY PERFORMANCE FOR DESIGN POINT SIZING

Solar day		Winter Solstice		Equinox		Summer solstice	
System		North/ South	North Only	North/ South	North Only	North/ South	North Only
Direct operation of turbine	Net power (MW_e)	10.0	10.0	10.3	10.2	10.2	10.2
	Net energy (MWh_e)	40.0	49.6	62.0	61.2	61.0	60.8
	Hours of operation/day	4.0	5.0	6.0	6.0	6.0	5.2
Operation from thermal storage	Gross energy input (MWh_t)	123.0	106.6	114.0	109.4	147.0	114.0
	Maximum charging rate (MWh_t)	27.0	33.4	29.0	25.4	21.0	19.5
	Net energy (MW_e)	28.0	24.0	26.0	24.6	33.0	25.7
	Hours of operation @ 7 MW_e/day	3.9	3.4	3.7	3.5	4.7	3.7
Daily summary	Net energy (MWh_e)	68.0	74.0	88.0	85.8	94.0	85.5
	Hours of operation/day	7.9	8.4	9.7	9.5	10.7	9.7
	Load factor[1]	0.28	0.31	0.37	0.36	0.39	0.36
	Mean power output[2] (MW_e)	8.6	8.4	9.0	9.1	8.8	8.9

1. Load factor = net energy/24 hours x 10 MW_e net capacity.
2. Mean power output = net energy/hours of operation/day.

TABLE XII. COMPARISON OF ANNUAL GENERATING CAPACITY FOR BASELINE SIZING

Turbine operating temperature °C (°F)		Electric energy output, 10^6 kWh		Mean daily power, MW_e		Mean annual load factor	
		North/ South	North Only	North/ South	North Only	North/ South	North Only
371	(700)	29.8	27.2	8.9	8.4	0.34	0.31
427	(800)	30.4	30.1	9.0	8.9	0.35	0.34
482	(900)	31.1	30.5	8.9	9.3	0.36	0.35
538	(1,000)	30.9	31.0	8.8	8.9	0.35	

System Investment Costs

Subsystem investment costs were estimated to compute the total plant investment cost (TIC) in 1976 dollars. Subsystem costs for the receiver, collector, and control subsystems were based on automated production of 2,000 heliostats, with tooling costs amortized over the initial 1,000 units. Costs of the thermal storage and electric generation subsystem were based on those estimated by McDonnell Douglas for their 10-MW_e power central receiver system.

Table XIII summarizes the subsystem costs and TIC for each system. The lower TIC of the north-only system is due to the requirement of fewer heliostats to achieve equivalent annual generating capacity of the north/south system. The numbers in parentheses are the cost per unit area (m^2) of collector surface.

TABLE XIII. INVESTMENT COSTS FOR BASELINE SYSTEMS

Subsystem	Investment Cost, Millions of 1976 Dollars			
	North/South System		North-Only System	
Collector	6.4	($52/m^2$)	4.9	($53/m^2$)
Receiver	1.8	(15)	2.3	(25)
Control	4.5	(37)	4.3	(46)
Storage	1.3		1.2	
Generating	6.9		6.9	
Other	5.2		4.3	
System Cost	26.1	(216)	23.9	(254)

Table XIV contains a summary of TIC and annual cost performance for baseline systems at varying turbine operating temperatures.

TABLE XIV. COST/PERFORMANCE FOR BASELINE PLANT SIZINGS

Turbine Operating Temperature °C (°F)	Investment Cost ($10^6$$)	Annual Output (10^6 kWh)	Base Year Cost/Performance[1]	
			¢/kWh$_e$	$/kW$_e$[2]
	North/South	North/South	North/South	North/South
371 (700)	26.0	29.8	87	2,890
427 (800)	26.0	30.4	86	2,600
482 (900) - Design point	26.1	31.1	84	2,610
538 (1,000)	26.2	30.9	85	2,620

1. Not discounted or amortized over the life of the plant, and not including annual operating costs.
2. Based on 9-MW$_e$ design capacity for 371°C operation, 10-MW$_e$ for other operating temperatures.

Busbar energy costs were computed for plant sizes of 10-MW$_e$ and 100-MW$_e$ peak generating capacity for each baseline system. The Aerospace Corporation Power Plant Economic Model (PPEM) was used to make the computations. Subsystem investment costs (1976 dollars) for the 10-MW$_e$ plant using a 482°C (900°F) turbine were used to compute investment costs per kW$_e$. The default values in the PPEM program were used for the input data parameters, with the exception of the following:

- Investment Cost Year (YRD): 1976
- Year of Constant Dollars (YRO): 1976
- Plant Capacity Factor (PCF): (north-field only) 0.36 for 10 MW$_e$; 0.46 for 100 MW$_e$ (0.35 for 10 MW$_e$; 0.45 for 100 MW$_e$)
- Annual Operating Expenses (OPEX): $100/kW$_e$ for 10 MW$_e$; $10/kW$_e$ for 100 MW$_e$
- Annual Inflation Rate (XINF): 0.05 (5 percent per year)

Table XV contains the results.

TABLE XV. SUMMARY OF PPEM OUTPUTS

Plant Size	10 MW_e		100 MW_e	
System	North/South	North Only	North/South	North Only
Total capital investment to year 1 of commercial operation (dollars/kW)	5,648	5,295	1,908	1,615
Busbar costs in 1976 dollars (mils/kWh)				
Year 2 of commercial operation (1991)	139	136	30	27
Year 20 of commercial operation (2010)	80	78	17	15
Net cash flow in 1976 dollars (mils/kWh)				
Year 2 of commercial operation	63	61	16	13
Year 20 of commercial operation	33	31	9	8

The data in Table XV shows that the North-system only 100-MW_e baseline design reduces total capital investment by 15 percent (from \$1,908/kW_e to \$1,615/kW_e) and net busbar costs by 10 percent. The principal reason for the decreases is the reduction in the size of the collector field required to achieve baseline performance.

Table XVI summarizes net busbar costs (1976 dollars) for plant sizes of 10 MW_e and 100 MW_e as a function of turbine operation temperature for North-only (20 single boiler sections) and North/South (10 double boiler sections) concepts. The numbers in the columns titled MIN are the minimum number of boiler/superheat sections required to operate at 10 MW_e using turbine inlet steam at 6.9 mN/m^2 and 482°C.

TABLE XVI. NET BUSBAR COST IN YEAR 2 OF OPERATION
(Mils/kWh)

Plant Size		10 MW_e		100 MW_e		MIN	
Turbine Operating Temperature °C (°F)		North/South System	North-Only System	North/South System	North-Only System	North/South System	North-Only System
371	(700)	146	153	32	30	22	22
427	(800)	142	139	31	27	20	20
482	(900)	139	136	30	27	20	19
538	(1,000)	143	137	31	27	19	18

Heliostat Testing

Experimental Model

The experimental model employed the heliostat's basic triangular structure and width to accommodate four 5-ft mirrors (see Figure 49). This allowed experimental determination of function and frictional forces in the mirror focusing mechanism and a preliminary observation of mirror imaging. The experimental model heliostat allowed for elevation aiming and had a complete focus drive assembly and mirror focus mechanism. The tests were valuable in determining final heliostat configuration and demonstrated that mirrors can be successfully focused (see Figures 50 and 51) and automatically defocused.

A full-sized (18.7 m long) heliostat module is under construction (80 percent complete) for field testing. The module will contain 70 mirrors and will focus upon a computer-controlled moving target, as described in the following section.

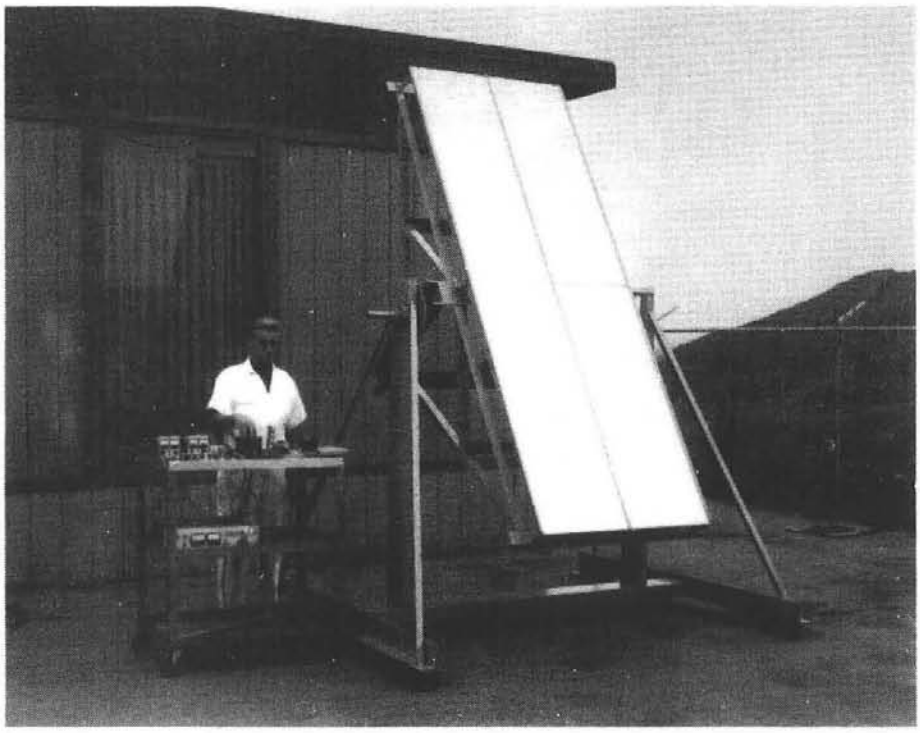

Figure 49. Experimental Model Heliostat

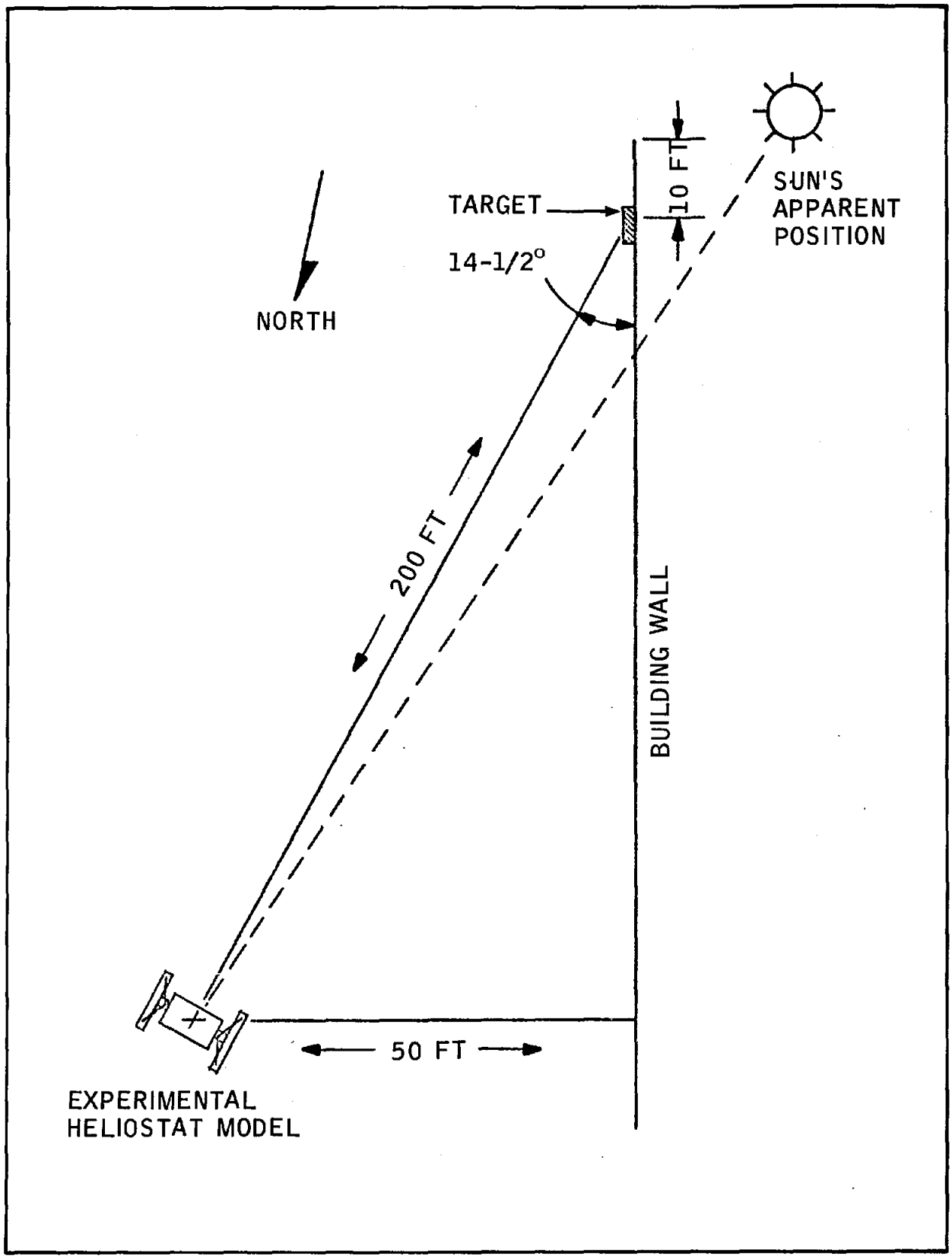

Figure 50. Layout of Experimental Model Heliostat Image Test

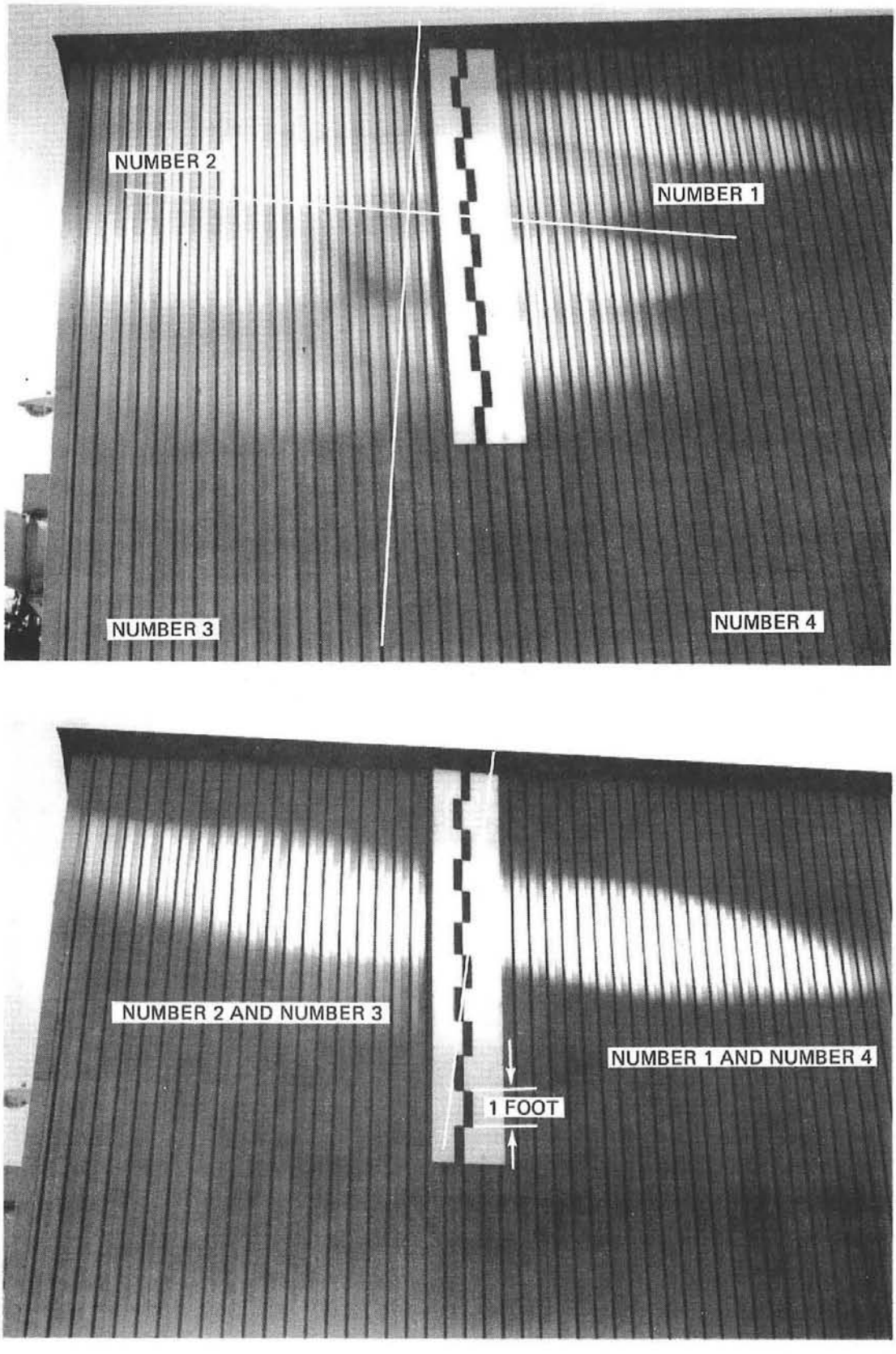

Figure 51. Experimental Model Heliostat Mirror Image

Target

A focused image of the sun will be reflected by the heliostat onto a driven target for analysis. As the sun's apparent position across the sky varies, the target will be moved to retain the image within its boundaries.

The initial design for the target and supportive mechanisms has been replaced by a more cost effective design which simplifies the test procedure and data acquisition. The new target is composed of eight 10-foot square louvered panels. The heliostat side of the target is painted with a high reflectance and temperature-tolerant aluminum paint. The louver angle is 30 degrees, which permits air flow through the panel to reduce normal wind velocity while reflecting the incident image from the heliostat down and in front of the target. The target and trolley are being fabricated and are 40 percent complete.

The target trolley will ride on eight steel casters along two concrete pads, as shown in Figure 52. The trolley will be driven by a friction wheel which bears against one side of the center guide rail. Two guide wheels will bear against each side of the guide rail at the front end of the trolley to restrict lateral motion. The drive motor and power train will be mounted on the trolley.

Heliostat Experiment

The experimental facility has been designed (see Figure 53), leased, surveyed, and construction will begin upon release of funds. The heliostat module reflects final configuration and will consist of 70 mirrors in a frame 60 feet long and 10 feet wide with elevation and focus drives.

The heliostat module will be mounted on a flat-bed trailer to transport the heliostat to the test site and to serve as the foundation platform for the heliostat during the experiment. The use of a flat-bed trailer as the heliostat foundation reduces the technical and logistics problem of moving the heliostat to a new position and eliminates the requirement for constructing (and dismantling) three concrete foundations. Leveling jacks on the trailer will be used for sighting the heliostat at the target plane.

The image from the heliostat will be scanned with a moving calibrated image intensity sensor. The sensor will be mounted on a frame which moves horizontally across the image plane while the sensor moves vertically to produce a sawtooth scan path. The sensor will make one complete scan (6 feet vertically by 60 feet horizontally) in about 10 minutes. About 1,170 scan pulses will be made in one complete scan (one scan for each 6 inches of vertical travel of the sensor).

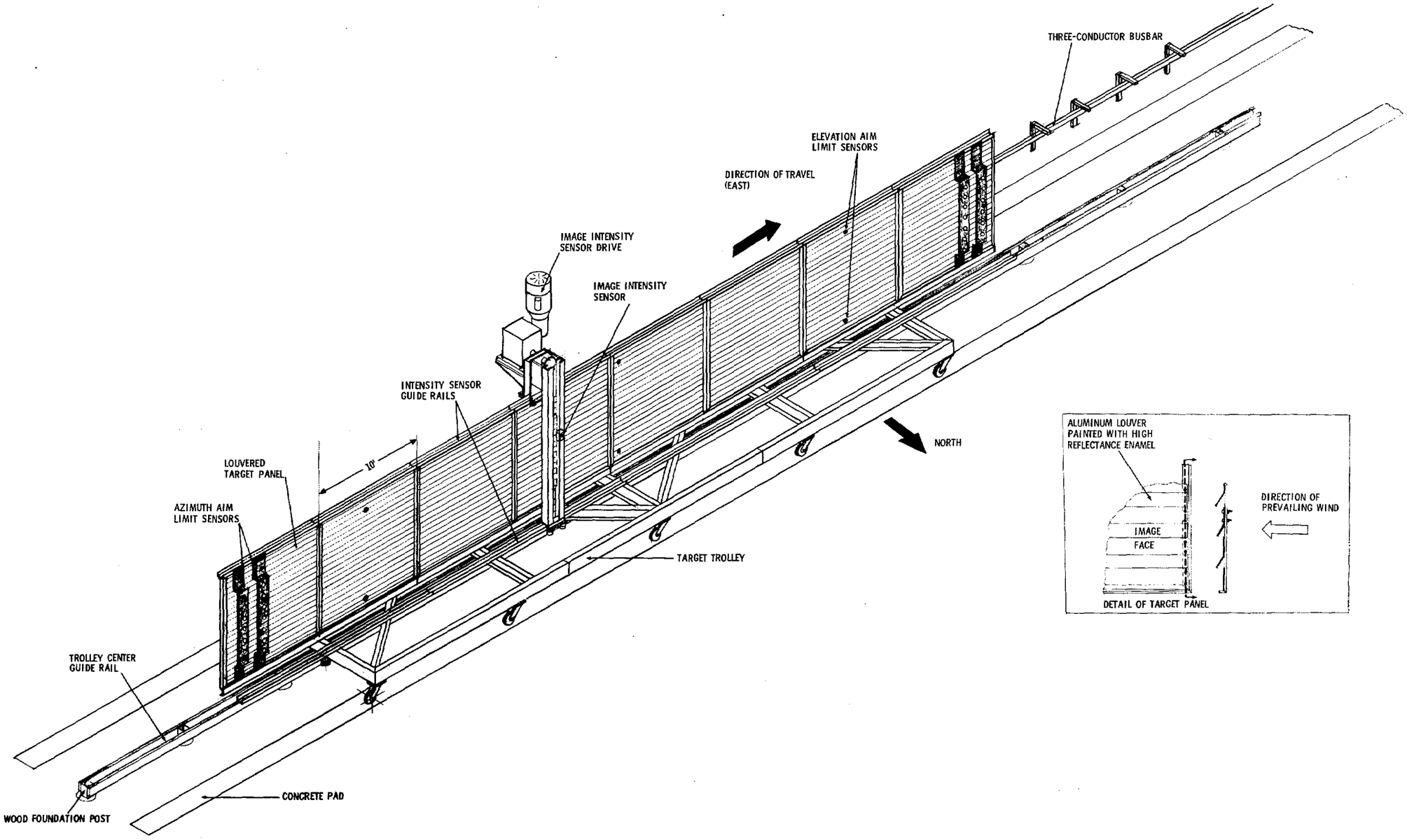

Figure 52. Layout of Target and Guidance Track

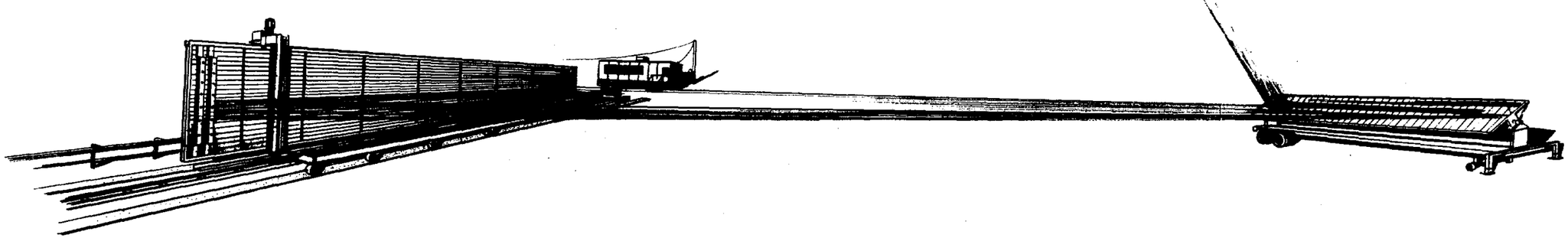

Figure 53. Layout of Test Site

Azimuth and elevation limit sensors provide feedback data to the computer for trolley movement and for focusing the reflected heliostat image onto the target. A three-channel busbar will be used to supply power to the trolley and to transmit all sensor signals from the trolley to the instrument van.

Control of the heliostat will be accomplished through the adjacent local controller receiving command signals from the test computer. The test heliostat local controller will simulate its final configuration (see Figure 54). The test computer and other control and environmental measuring devices are located in or about the instrumentation van.

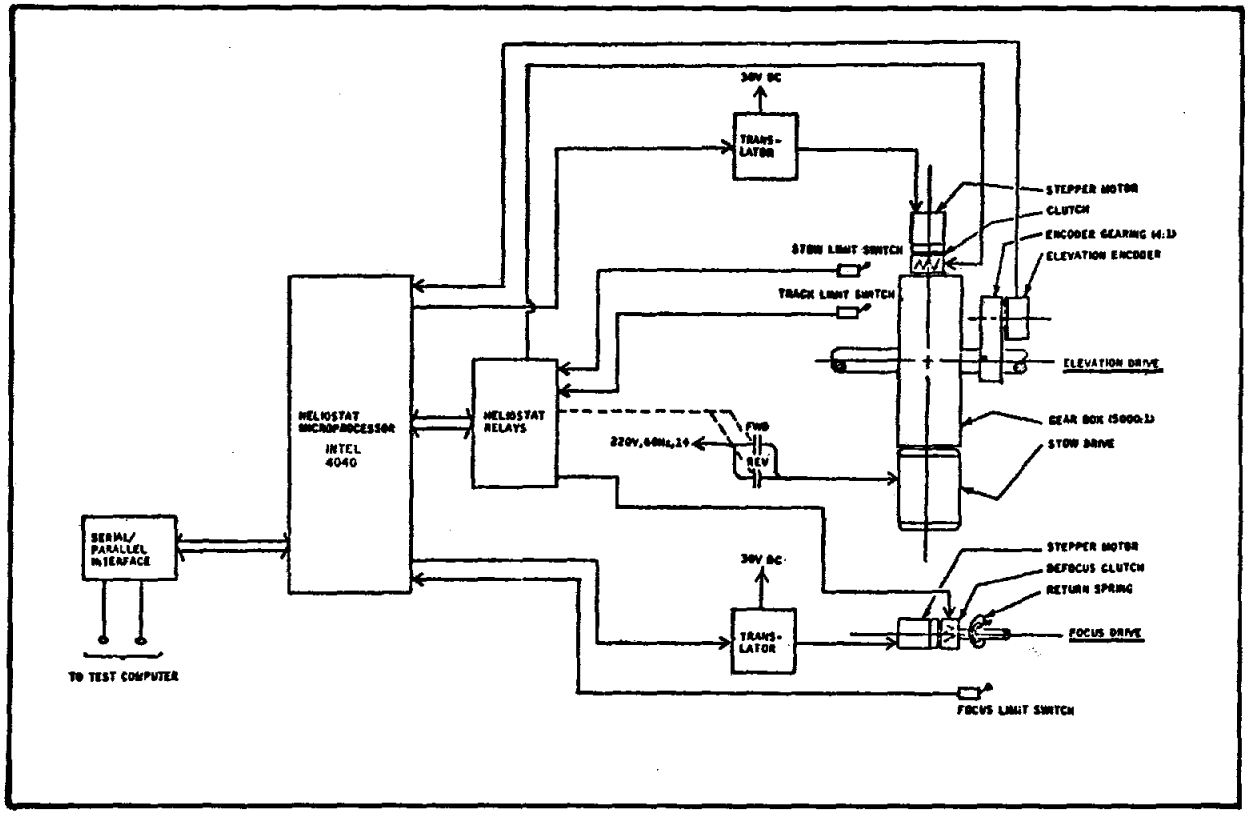

Figure 54. Heliostat Local Control Configuration (Test)

The specific objects of the heliostat experiment are to:

- Measure the spatial distribution of concentrated solar intensity under varying wind loads, insolations, degradation of the reflecting surface, and heliostat-to-target distance.

- Prove the performance of the emergency defocus system.

- Test the nutating mode performance and stability under varying wind load conditions.
- Test the focus geometry concept, performance, and wind load stability.
- Test the tracking mode performance and stability under varying wind load conditions and heliostat-to-target distances.

Future Developmental Objectives

Our initial research and analyses have shown that the cavity-type line central receiver is technically feasible and economically viable for solar thermal electric production at 100-MW_e plant capacity. We are confident that the heliostat experiment will verify our predicted collector performances. However, further system optimization, performance analysis, and tests of components are required to further improve system performance and verify subsystem predictions to the point where construction of a pilot plant is justified.

To reach this goal, we propose seven additional tasks to accomplish the orderly development of the system. Figure 55 shows the tasks, our time plan for accomplishing the tasks, and budgeting estimates of costs. A summary of each task follows Figure 55.

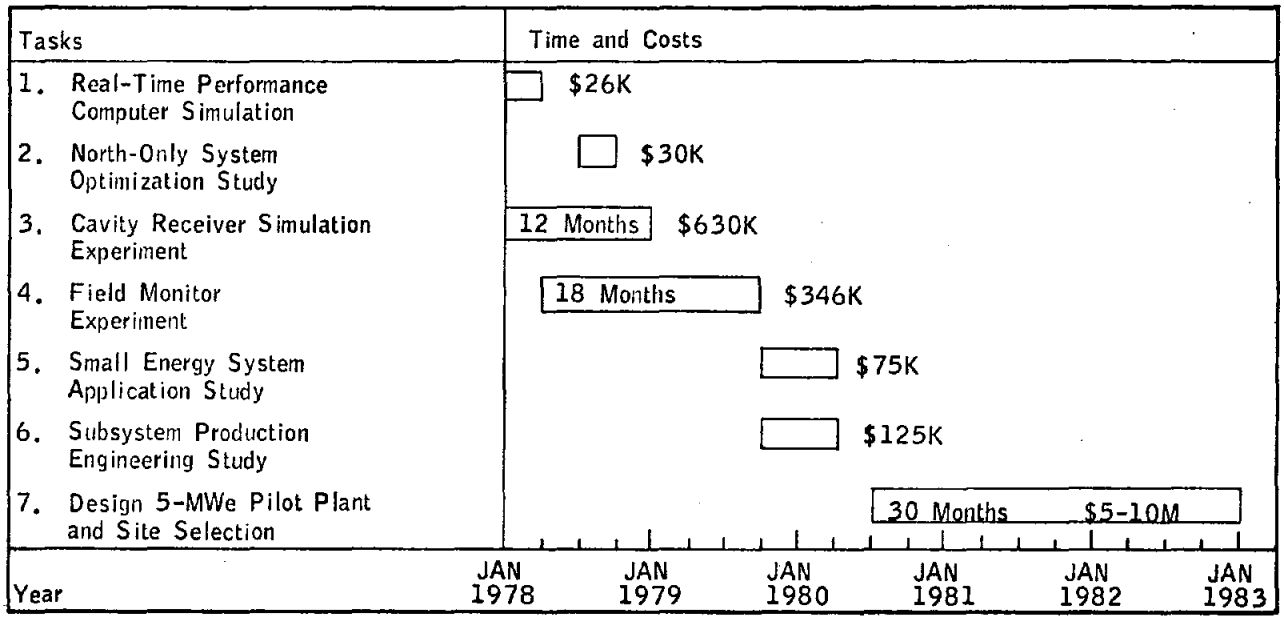

Figure 55. Proposed Line Central Receiver Development -- Solar Thermal Conversion Program

1. Real-Time Performance Computer Simulation

Part of the concept definition study for the line central thermal receiver included the development of a simulation model of the thermal performance of the once-through boiler/superheater receiver concept, and the use of this model to generate performance data to estimate busbar electric costs.

Performance simulations were made with insolation data for these solar days: winter solstice, vernal equinox, and summer solstice. The daily thermal energy output for these days was used to estimate annual busbar electric energy output.

Recent discussions with personnel from ERDA and JPL indicate the desirability of estimating the hourly performance of the receiver with standard weather/insolation data for Inyokern, CA. These data have been used by other contractors to estimate the performance of other central receiver concepts. It was concluded from these discussions that simulation of the annual performance of the FMC concept with the same weather/insolation data was necessary to further demonstrate the relative economic attractiveness of the FMC concept. Accordingly, a proposal has been submitted to accomplish this task.

2. North-Only System Optimization Study

In the initial study, an economic analysis of a north-only collector field was performed and the results were favorable. Therefore, a more detailed study is required to optimize heliostat size parameters, collector field configuration, receiver length, and configuration. The results of the heliostat experiment and the real-time performance computer simulation will be used in this study.

3. Cavity Receiver Simulation Experiment

We propose to construct a section of the circumferential cavity receiver of the once-through boiler design about 8.2 m long and apply a simulated solar flux with quartz lamps. The experiment will allow the measurement of fluid mass flow, heat transfer, thermal stresses, and receiver efficiency.

The test system for the proposed test of the once-through cavity receiver will consist of a section of the receiver itself and sufficient external test equipment to verify the thermal performance of the unit under design flux inputs and operating temperature conditions closely simulating those from a typical collector mirror field.

4. The field monitor experiment includes investigation, design, fabrication, and testing of the field monitor portion of the heliostat control subsystem. The purpose of the field monitor is to scan a specific portion of the collector field, measure the intensity profile of the focal line of each heliostat as it sweeps across the monitor aperture during its "jitter focus" cycle, and detect optical malfunctions of heliostats on a continuous basis. The monitor components will consist of electro-optic detection devices (TV cameras), hard wired analog signal conditioner with digital conversion, a data processor for evaluation correlation, and two-way communication with the central computer. Experimentation and conclusions obtained should confirm final design requirements for the monitor function and demonstrate suitability for inclusion as part of the proposed 5-MW_e pilot plant.

   To verify the operation of the field monitor sensor and to test the subsystem under operational conditions, a series of field experiments will be conducted wherein the subsystem will operate in conjunction with a test heliostat. The experiment would vary the heliostat-to-sensor distance and operate under various solar conditions. Test data will be analyzed to determine the degree of conformance to predicted operation.

5. Small Energy System Application Study

   In this task we propose to examine the use of a scaled-down version of the linear cavity receiver with single axis focusing heliostats for investigation of small energy system applications. System requirements for several configuration applications will be established. Typical applications would include small generating plants for agro-industrial complexes, low-temperature operation for localized supply of energy requirements for industrial complexes, and community-level supply of low-temperature energy for space heating and hot water. The modular design of our concept is ideally suited for development of such small-scale applications.

6. Subsystem Production Engineering Study

   A detailed production engineering study will be accomplished for the collector and receiver subsystems to develop automated fabrication and assembly processes, including the design of necessary tooling. Specific components to be included in this study are the heliostat, heliostat drive assembly, and the receiver tube array assembly. The results of this study will be a production data package for large-scale manufacture of the subsystem components.

7. Design 5-MW_e Pilot Plant and Site Selection

The results of the previous tasks will be incorporated into the design of a 5-MW_e power plant employing the FMC line central receiver concept. Plant design will be based on all data obtained from joint efforts, i.e., research studies, design and fabrications, test and evaluation of critical system components. Final system specifications will be established after consultation with key team members, which will include ERDA, a power utility, and a construction contractor. Site selection may be heavily influenced by the power utility team member. It is anticipated that this task will be a cost-sharing effort with a utility.

DESIGN CONCEPT CHOSEN FOR SOLAR ELECTRIC PLANT

ERDA/HQ

A conceptual design has been chosen for the nation's first experimental solar "power tower," a 10-megawatt electrical generating plant to be built near Barstow, California, at a cost of about $100 million.

The design is based upon the cylindrical "inside out" boiler (receiver), metal-glass mirrors (heliostats), and oil/rock thermal storage subsystems developed by a team headed by McDonnell Douglas Astronautics Company as part of a two-year development program.

"The successful completion of the conceptual design phase of the project is a major achievement toward meeting our cost goals for solar thermal electric power," said Dr. Henry H. Marvin, Director of the Division of Solar Energy at the Energy Research and Development Administration (ERDA). "We now have a good basis for confidence that these plants can be built on a commercial scale by 1990 at a cost which should make them attractive to the electric utilities."

The design concept chosen culminates a two-year development program by three industrial teams, one led by McDonnell Douglas and the others by Honeywell Incorporated and Martin Marietta Corporation. Additionally, the Boeing Corporation developed a conceptual design for the heliostats (sun-tracking mirrors) only.

All the teams submitted technically sound designs, Dr. Marvin said, but the concept chosen appears to be the least costly approach for future commercial-scale systems of 50 megawatts and larger.

The experimental plant at Barstow will generate electric power in the same way that a fossil or nuclear plant does, except that the steam which drives the turbine/generator will be produced from the heat of the sun. The chief solar components are the heliostats (sun-tracking mirrors) that concentrate sunlight, the receiver (boiler) that converts water into high-pressure steam, and a heat storage system that permits steam to be produced when there is no sunlight.

The conceptual design teams, all under contract to ERDA, submitted four different designs for heliostats and three for receivers. In the concept chosen, a cylindrical configuration of boiler-tubes sits atop an 86-meter (283 ft) tower and absorbs sunlight reflected from more than 1500 mirrors surrounding the tower. The heliostats will be multifaceted glass mirrors of approximately 40 square meters supported by a metal structure and mounted each on a single concrete pile foundation. The field of heliostats will be computer controlled to continuously reflect the sun's energy onto the receiver.

Steam from the receiver passes through a turbine and generator on the ground, generating more than 10,000 kilowatts of electrical power. Additional steam can be produced from this storage system to continue generating about 7,000 kilowatts electric for four hours without sunlight.

ERDA expects to award contracts to fabricate components and construct the plant within the next six to eight months and to place the plant in operation in late 1980 or early 1981. The plant will be built and operated under a partnership arrangement with the Southern California Edison Corporation, the Los Angeles Department of Water and Power, and the California Energy Resources Conservation Commission. Southern California Edison will provide the non-solar generating equipment, which is expected to cost approximately $20 million.

SOLAR THERMAL TEST FACILITY

John Otts
Sandia Laboratories

The Sandia STTF (Figure 56) will consist of a 200-ft central tower initially surrounded by 222 heliostats capable of directing 5 MW of thermal energy to various locations on the tower. Each of the 400-sq. ft. heliostats consists of 25 4' x 4' mirrors which are focused to produce a concentrated beam of solar radiation on a target test area. It is expected that peak thermal flux levels up to 250 W/cm will be available at the center portion of the beam. Approximately one MWth will be available within a one-meter diameter circle, 2.5 MWth within a two-meter circle, and 5 MWth within a three-meter circle.

The facility is designed to provide flexibility for a variety of solar receivers and various combinations of heliostats. The experiment tower is 200 feet high with test bays located at the 120, 140, 160, and 200-ft levels. Other test locations will also be available in the future for small experiments.

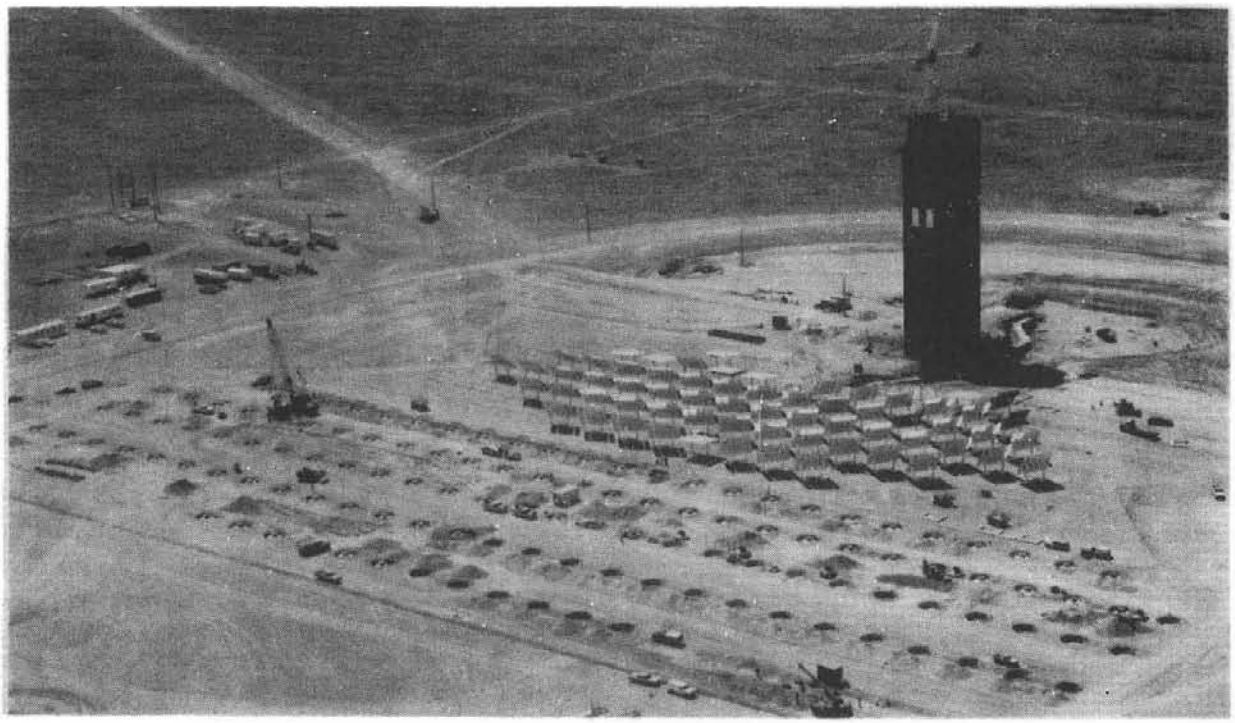

Figure 56. Solar Thermal Test Facility

The facility schedule is shown in Table XVII. Tests have already been scheduled for the 200-ft level for the first 19 months of operation. Tests have also been scheduled for the 140-ft levels for the 3rd through 16th month and for the 160-ft level for the 6th through 9th month.

TABLE XVII. TEST AND CONSTRUCTION SCHEDULE

Event	Target Date
ERDA selects first 5-MW receiver for STTF testing	August 1, 1977
Tower floors available for focus and alignment system installation	September 1, 1977
Tower construction to top completed	October 10, 1977
Beneficial occupancy of control building for computer move-in	October 25, 1977
Align first half of 144 heliostats	November 1, 1977
Complete heliostat foundations (north and circular)	November 10, 1977
144 heliostats installed in north field	November 18, 1977
Mount first 5-MW receiver on elevating module	December 15, 1977
Align remainder of 144 heliostats	December 23, 1977
Complete control building	January 1, 1978
Accept 144 heliostats	February 1, 1978
Initiate 5-MW solar test	April 1, 1978

400 kW SOLAR THERMAL TEST FACILITY AND STEAM GENERATING PLANT

Georgia Institute of Technology

Construction of the basic Georgia Tech Francia-type 400 kW solar steam generating plant is nearing completion. All major systems have been installed and are being checked out. Initial, low-power startup of the system is scheduled for the middle of September, and characterization of the basic facility will occupy most of the remaining 1977 calendar year. A south tower and experimental platform, to complement the existing central tower, will be installed by March 1978. The first user of the facility, Sanders Associates, will begin performance testing of a 250-kW air-cooled receiver in June 1978. Other users are being actively encouraged to explore possible test arrangements, and a facility users' manual has been prepared to outline relevant information and procedures.

The primary objectives of the current ERDA program are to: (1) perform a technology transfer of Giovanni Francis solar thermal technology from Italy to the United States, and (2) establish a major solar thermal test facility in the United States. The Georgia Tech facility was patterned after Francia's 135-kW St. Ilario solar steam plant and was designed and fabricated by ANSALDO*, a major Italian manufacturing organization. Installation of the facility on the Georgia Tech campus has been a Georgia Tech responsibility. The solar facility, consisting of a 400-kW collector system and a 350-kW high-pressure solar steam generator, will be the fourth solar steam plant designed and built under Francia's supervision.

The Georgia Tech Solar Thermal Test Facility (GT/STTF) consists of an hexagonal array of 550 mirrors driven mechanically to follow the sun and to focus its rays onto test objects positioned either atop the central tower or on the tower at the south end of the field. The heliostat drive system is operated open loop. An overview of the field with the initial startup mirrors in place is shown in Figure 57. The mirrors thermselves measure 43.7 in. in diameter, are constructed from 3-mm thick low-iron glass and may be operated either flat or focused. Concentrations to approximately 2200 will be possible with the mirrors focused. Measurements that have been made on the heliostat system include rms surface slop error of a representative set of mirrors, alignment errors associated with the installation of the heliostat support system, and pointing or tracking errors. Fifty-two mirrors are currently installed at the site for initial startup and checkout of the receiver steam system.

---

* ANSALDO Societa Generale Elettromeccanica S.p.A. Genoa, Italy.

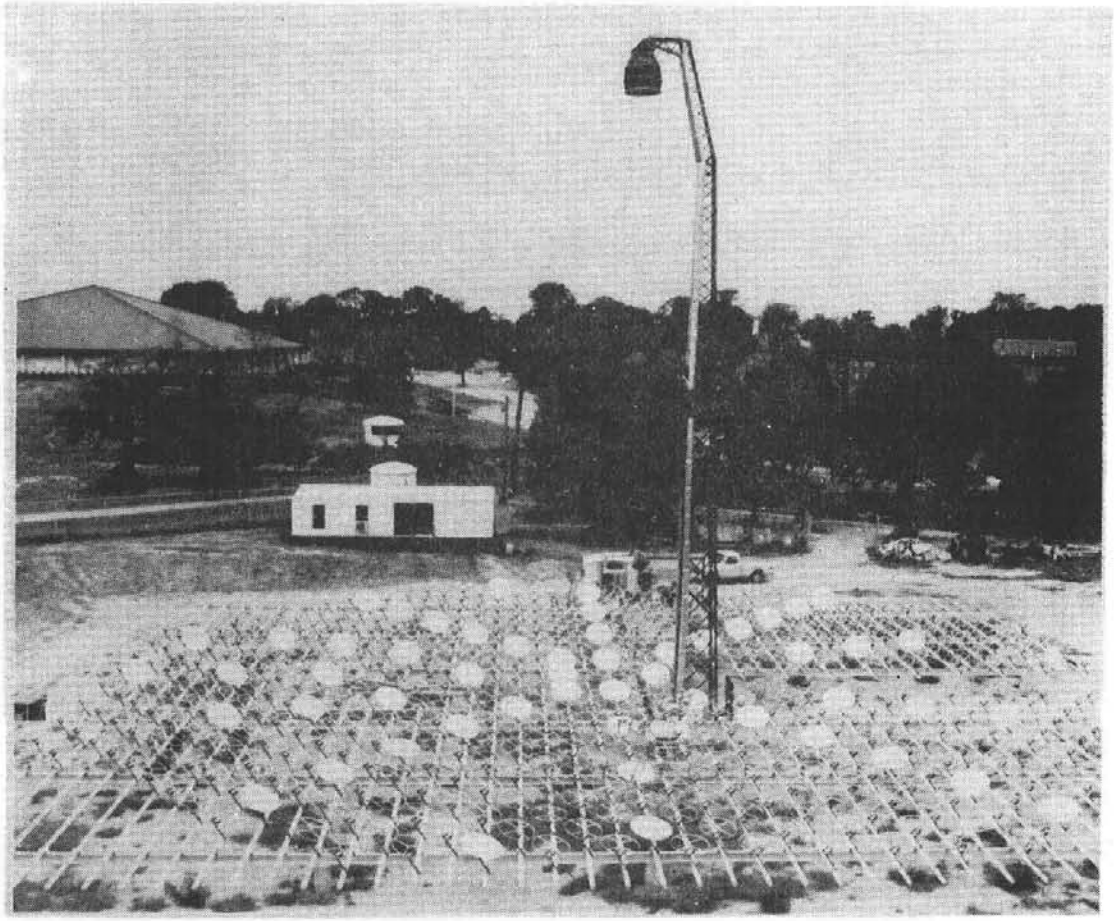

Figure 57. Georgia Tech Solar Thermal Test Facility

The steam generating plant is designed to generate 700 pounds/hour of 1112°F, 2200 psi superheated steam. In the present test facility, the steam will be throttled, desuperheated, and condensed, with all heat being disposed to a conventional wet cooling tower. The steam generator, which will be supported on the central tower, has been instrumented with thermocouples and high-temperature weldable strain gages.

The central tower is an open truss structure designed to support a maximum test load of 1500 lbs. It will articulate to allow easy attachment and maintenance of test objects. A second tower is being designed for the south end of the field. As illustrated in Figure 58, this tower will support a 20,000-pound cantilevered test load on the north face of the tower. Test objects can be supported by a general purpose 10 ft by 10 ft experiment platform furnished by Georgia Tech, or may be supported from four attachment points located on the north face of the tower. An elevator will be used to transport light equipment and personnel to the test area located 82 feet above the ground. Major test objects will be positioned on the tower by a portable crane. The south tower will include a 10 ft x 10 ft instrumentation and

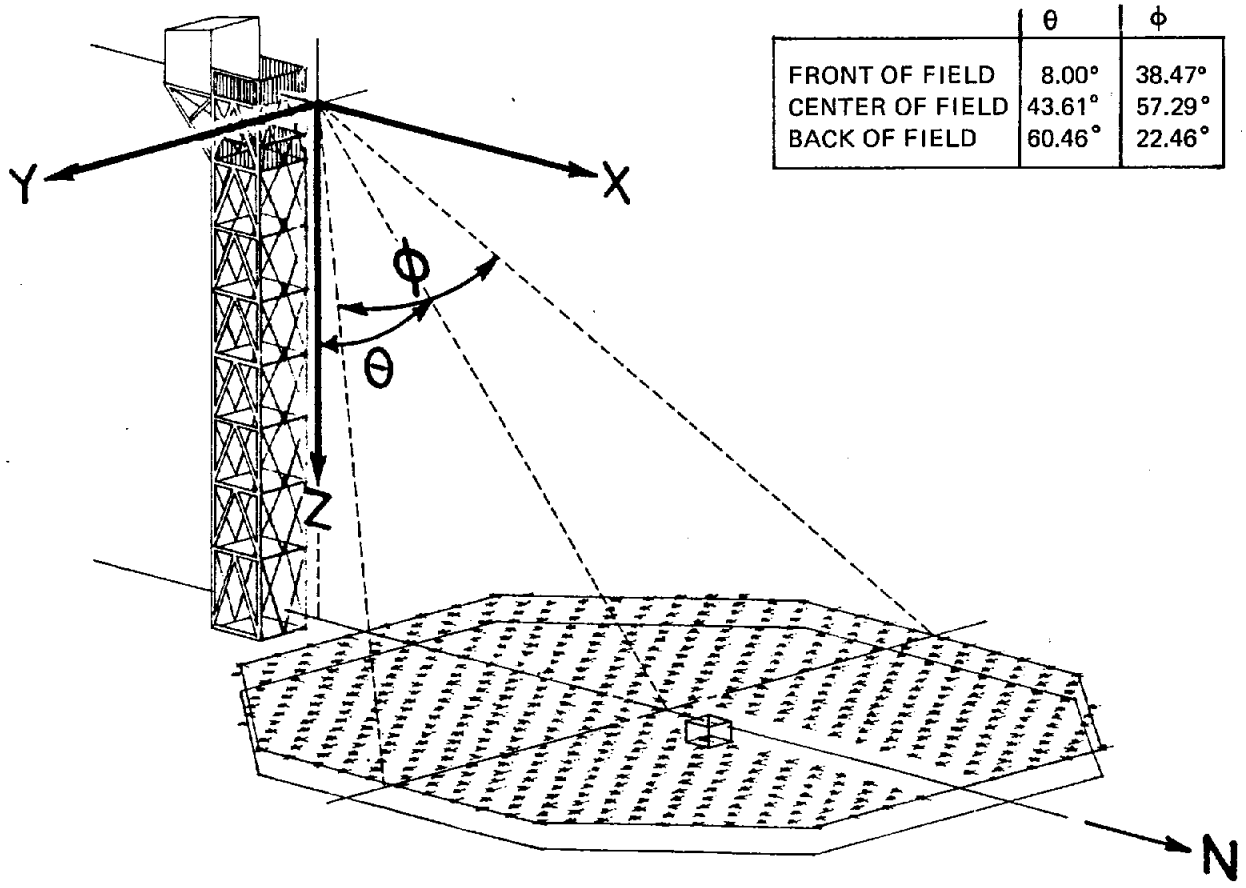

	θ	ϕ
FRONT OF FIELD	8.00°	38.47°
CENTER OF FIELD	43.61°	57.29°
BACK OF FIELD	60.46°	22.46°

Figure 58. Second Tower Being Designed For the South End of the Georgia Tech Solar Thermal Facility

equipment building cantilevered off of the south face of the tower. This room will be located outside of the radiation beam and will require no special thermal consideration.

The maximum radiation flux density available from the facility has been estimated to be on the order of 300 W/cm^2 for the central tower and 200 W/cm^2 for the south tower, given an insolation of 900 W/m^2. These irradiation flux densities are calculated values and await experimental verification once the facility is operational.

Installation of the computerized data acquisition system to service the central tower has been completed. This system is based on a Digital Equipment Corporation PDP-8/a minicomputer and includes disc storage on two different media, line printer hard copy, video display, and computer-to-computer commincations with the school's major computer system. The minicomputer and its peripheral equipment are housed in a central room at the western edge of the facility site. Additional data acquisition equipment will be located in the control room atop the south tower. Specifically, the

south tower control room will contain signal conditioning equipment and a second minicomputer that will digitize and transmit data to the main control room. Real time display and storage of the data will occur in this latter control room.

In summary, the tasks remaining to be completed at the STTF are as follows:

1. Construction of the south tower
2. Completion of a flux-scanning calorimeter now being built
3. Building of a total calorimeter
4. Final characterization of the facility to determine such parameters as heat flux and power, mirror field errors, and the performance of the receiver system
5. Installation of a materials test fixture to allow testing of a variety of high temperature materials without interim dismantling.

FRACTURE OF HELIOSTAT FACETS

V. D. Frechette
N. Y. State College of Ceramics
at Alfred University

Introduction

Essential to several systems for conversion of solar energy is the heliostat mirror, whose flatness or controlled curvature is critical to efficiency. Cracking of the glass in service can spoil its geometry to a degree depending on the glass support system used. Cracking permits access of moisture which degrades the silver, and cracks constitute an eyesore to those who expect perfection. It is the purpose of this paper to point out the factors in heliostat mirror design which invite disaster, to set forth principles for recognizing the cause of a particular crack, and to suggest principles of design and specification to minimize failures.

Glass Strength and its Degradation

Glass as a material is strong. But although measured strengths of very carefully prepared test specimens may exceed one million pounds per square inch in tension, normally handled specimens show strengths two to three orders of magnitude below that, i.e., in the 1000 to 10,000-psi range. The rougher the handling, the lower the strength. Impacts and abrasions provide flaws at whose tips applied stress becomes raised to values which lead to deepening of the flaws. Finally, if the load is sustained or repeated, a critical flaw depth may be reached, whereupon failure is catastrophic and a crack rapidly develops. Rate of loading is significant. Glass specimens may sustain three times the load for a few seconds that would break them if applied for a few hours. Glass failure always originates at surface damage sites (excepting rare cases of a gross manufacturing defect).

The presence of moisture can weaken glass, the more so the higher the relative humidity of the atmosphere. Exposure to moisture is not always detrimental. While moisture always degrades the strength during application of the load, attack by moisture following surface damage and prior to loading increases the strength as much as one and one-half times the value measured when damaged glass is loaded immediately.

Temperature also has its effect. At 50°C the time to failure under constant load is one-tenth of that at 20°C but the strength is affected very little.

Glass composition, within the range practical for window or mirror glass of either the drawn or plate glass variety, has almost no effect on strength.

In summary, the strength of glass is a tricky engineering parameter. Lowered a little by increasing temperatures and very much by high humidity, it is more than anything else a question of the condition of the surface in the region where tension is maximum.

Diagnosis of Cracks

When the worst happens and cracks appear in test installations, a great deal can be learned by reading the signposts in the cracks themselves. They indicate the sense and level of stresses in the system and the point of weakness from which the cracking began. Several types of marks appear on crack edges, i.e., on the new surface generated by cracking. Wallner lines are ripple-like marks which result from perturbation of the moving crack front by vibrations or stress pulses passing through the sheet. They indicate the approximate shape of the crack front as it passed; thus the crack can be inferred to have moved from the concave toward the convex side. Wallner lines also indicate the distribution of stresses through the glass sheet; tension is highest in the region where the Wallner line is advanced.

A smooth crack surface is the result of cracking at low velocity. High velocity crack surfaces show a mist which generally develops into coarser texture as a series of sharp markings, called velocity hackle, diverging in the direction in which the crack spread. Hackle can take several forms but always represents spread of the crack as a set of parallel elements offset from one another and joined up later to generate a continuous surface and accomplish separation of the material.

Twist hackle forms when the local stress field twists. Since cracks form perpendicular to the axis of principal tension, a twist in the direction of tension requires a corresponding twist in the crack plane. The transition from the initial crack plane and the surface corresponding to the new tension axis is accomplished in a way reminiscent of a Venetian blind which on opening maintains its original average plane although its slats rotate to a new direction. A crack that stops temporarily and starts to move again usually does so under a modified stress field and so it generates twist hackle. Figure 59 illustrates these features of the crack edge. Such details of the

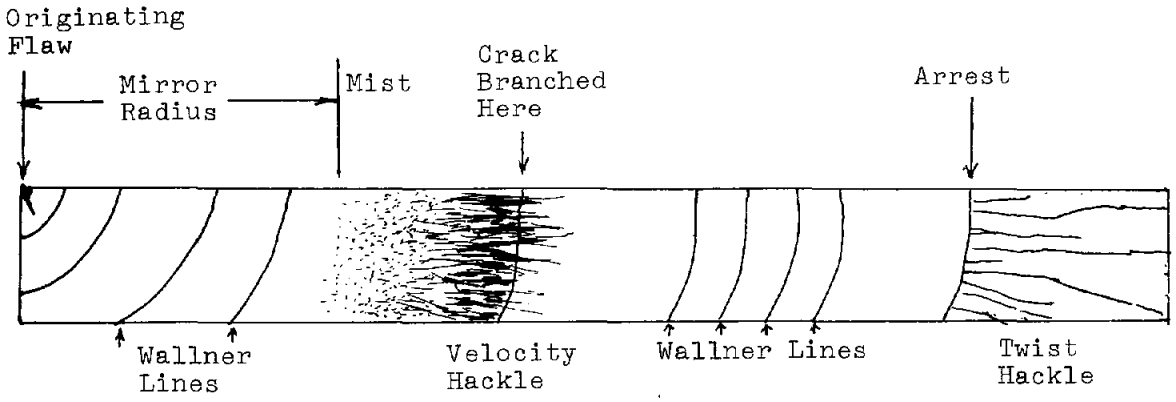

Figure 59. Features Typical of the Edge of a Crack Originating at a Rim Flaw
The mirror radius is inversely proportional to the square of the stress at failure.

crack surface may very often be seen with the naked eye but are more easily visible with the aid of a 6X hand lens or the lower magnifications of a stereoscopic microscope. Illumination is critical for effective examination; best results are obtained by arranging the direction of lighting and the direction of viewing so that the light is just on the borderline of being reflected by the crack surface. A frosted incandescent lamp held a few inches away from the crack is most convenient for the purpose.

Figure 60 shows how Wallner lines may be used to infer the distribution of stresses across the thickness of the sheet. Uniform tension across the

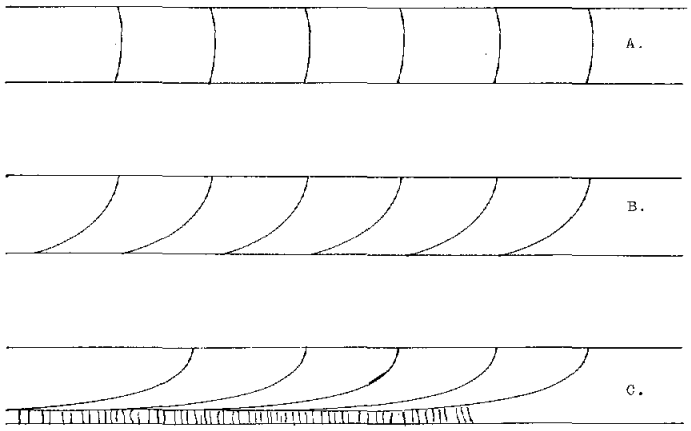

Figure 60. Wallner Lines Showing the Distribution of Stress Through the Glass Thickness
A. Tensile stress uniform across thickness
B. Tension is higher at the upper face
C. Tension at the upper face and compression at the lower, as when broken under cantilever stress or by a thermal gradient in which the top face is colder than the bottom face.

thickness leads to symmetrical Wallner lines. Higher tension at one surface causes the Wallner line to lead next to that surface. Where one of the surfaces is under initial compression, as in the case of a sheet broken in bending, the Wallner lines do not extend to that edge and the crack surface there is marked by fine hackle perpendicular to the sheet surface. Simple drumhead tension in the interior of a sheet yields cracks whose Wallner lines are symmetrical. Symmetrical Wallner lines are also characteristic of failure from the rim when the central area of the sheet is caused to expand relative to the edge, or when the rim is chilled and contracts relative to the interior.

The crack profile is also instructive and of course is very much more easily observed. Figure 61 shows the common rim-originated crack as its appearance is affected by stress at failure. Figure 62 shows three forms of centrally located crack systems. Cracking from simple drumhead tension is characterized by a radiating system of cracks originating in a short, straight segment and branching without spall. Cracking by impact from relatively heavy, low-speed objects originates at the back surface and radiates outward with the crack fronts leading at the back face, while circumferential cracks between the radiants have crack fronts leading at the front face. Spall may occur on the back surface of the radiants, and the area of contact with the projectile may be crushed. Where impact from a heavy, low-speed object occurs close to the rim of the sheet, a crack may be generated at the sheet rim; this crack will run inward to the point of impact and start a pattern of cracking identical with the above.

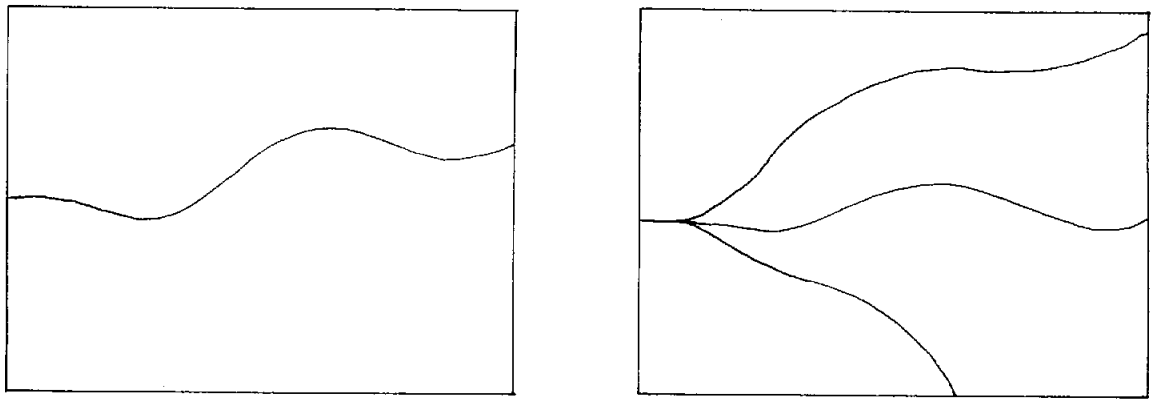

Figure 61. Profiles of Rim-Originated Cracks Caused by Thermal Gradient From Interior to Edge, the Edge Being Cooler. (The crack starts perpendicular both to the rim and to the face; it runs straight in for an inch or two and then meanders across the sheet. High stress at failure leads to branching, the sooner, the higher the stress.)

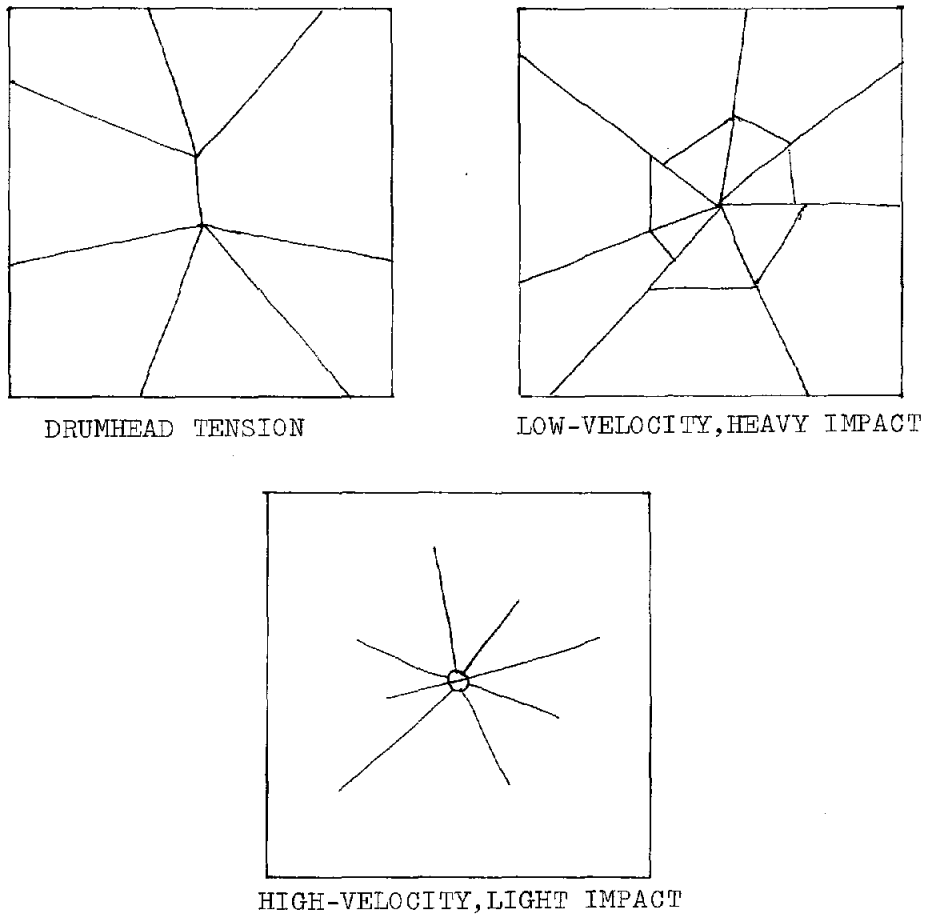

Figure 62. Centrally Originated Crack Systems
(Wallner lines on crack surfaces in drumhead tension are symmetrical; in low-velocity impact they lead at the back face in star cracks and at front face in circumferential cracks; in high-velocity impact they lead at the back face.)

Impact from a light, high-speed projectile originates at the front face in a circular crack or family of concentric cracks which extend into the glass and flare outward to the back face, generating a conoid. From this conoid a set of rather symmetrical cracks radiate, the crack fronts leading at the back face.

These are a few examples of simple stress systems which commonly cause cracking. More complex cases in which cracking occurs under combinations of stress systems may be dealt with in the light of these principles. Experiments with specimens simulating suspected stress configurations can be used to confirm such diagnosis.

Application to Heliostats

So far, the fundamentals of glass strength and crack interpretation have been considered in relation to flat glass or slightly curved sheet glass. To make the discussion more pointed toward current problems of heliostat facet design and specification, the following points are offered.

The crucial factor in a heliostat facet, or mirror, is its rim. On the one hand, stresses are likely to peak in the rim. Air flow is faster there and cools the rim relative to the central area, thereby placing the rim in tension; mismatch in thermal expansion between glass and substrate also tends to peak stresses in the rim. On the other hand, no part of the sheet is as vulnerable to the introduction of stress-raising defects as the rim.

The magnitude of stresses at the rim can easily be calculated by the routine methods of mechanics. The following discussion concentrates on reduction of rim stresses and on lessening the likelihood of defects in the rim region.

Reduction of Rim Stresses

If rim stresses are kept low, cracking will rarely occur. Some suggestions are:

1. The edge-effect of the facet should be reduced thermally by insulation. A strip of poor thermal-conducting material, such as plastic, should abutt the glass pane to prevent lateral thermal flux to or from the rim.

2. The mirror support should be designed so that no privileged path for thermal flux should exist, and no portion of the plane should be better insulated from heat exchange with the support than any other.

3. Shadows across the mirror should be avoided. (The more distant the shading object, the less will be its deleterious effect.) A shadow parallel to the mirror edges is not very dangerous, but combinations of diagonal shadows are to be avoided.

4. If a substrate differing in thermal expansion from that of the glass is inevitable, the mechanical coupling between the two sould be compliant.

Avoidance of Edge Defects

1. The edges of the sheet should meet the specifications for tinted (heat-absorbing) window lites. Such edges are formed by scoring the surface with a glass cutter's tool with light pressure and generous lubrication, then opening the crack with glass cutter's pliers. This is a highly exacting operation in which precise procedures must be used to avoid deviation of the crack from the score, generation of chips, "shark's teeth" (they look like shark's teeth, extending from the score across the edge surface), "serration hackle" (compression-edge hackle, as in Figure 60), and spall (Figure 63). Because of the critical importance of the edge to the resistance of heliostat facets to cracking, it may be best to have the facets cut to dimension by the manufacturer rather than to attempt cutting in the field. Edges should not be ground, stoned, sand blasted, bevelled, polished or otherwise disturbed after cutting.

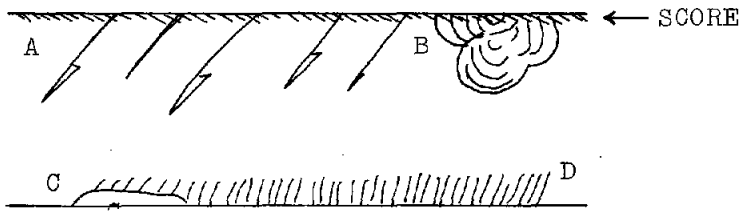

Figure 63. Edge Defects From Cutting

A. Shark teeth
B. Flake chip
C. Serration hackle
D. Spall

2. Specifications for the cut should be set and 100 percent inspection should precede acceptance.

3. The edges of the facets should be sedulously protected against damage in handling, installation, and service. An elastomer strip around the edge should be helpful but for thermal reasons should not extend above the plane of the front face of the glass.

4. Edge defects are prone to grow in size and effectiveness in the presence of water. The edges should therefore be sealed to prevent wetting. To avoid violation of the seal, detergents should not be used in cleaning the surface after mounting.

Conclusion

Cracking of heliostat facets is so largely dependent on the condition of the edges that proper precautions to assure freedom from edge flaws is the key to crack prevention.

Selected References

1. W. C. LaCourse, "The Strength of Glass," in Introduction to Glass Science, Pye, Stevens, and LaCourse, eds., Plenum Press, New York, 1972, pp. 451-512.

2. V. D. Frechette, "The Fractology of Glass," in Introduction to Glass Science, Pye, Stevens, and LaCourse, eds., Plenum Press, New York, 1972, pp. 433-450.

3. Leighton Orr, "Practical Analysis of Fractures in Glass Windows," Matls. Res. & Stds, 12, 21-3; 47 (1972).

4. PPG Industries, "Installation Recommendations - Tinted Glass," Tech. Service Report No. 104B.

AIR CYCLE SOLAR RECEIVER

Sanders Associates

Sanders Associates has recently contracted with ERDA to design, build, and test a 0.25-MW_t solar receiver using air as the heat transfer fluid. The receiver configuration is based on the use of a ceramic honeycomb heat exchanger element which absorbs solar energy and transfers it to the airstream at 2000°F. This type of receiver is applicable to an open cycle Brayton power system which offers the potential for a significant improvement in solar to electric conversion efficiency.

Under a previous ERDA contract, Sanders designed and tested a 10-kW solar receiver at the U.S. Army White Sands solar furnace. These tests showed that air cycle receivers could convert solar energy to heat in a high-temperature gas stream at efficiencies as high as 85 percent.

The objective of the current contract is to show the principles demonstrated at White Sands can be scaled to commercial receivers. The 0.25-MW_t receiver, which will be tested at the solar test facility at Georgia Institute of Technology, will be a scaled version of the envisioned commercial receiver. Several key issues have been identified (see Table XVIII) which need to be resolved during the development of the receiver. Most of the issues can be resolved during this program. The most important issues are the receiver convection losses, the ceramic heat exchanger lifetime, and the demonstration of an effective terminal concentrator.

The receiver is shown schematically in Figure 64. As currently envisioned, the honeycomb will be supported by a geodesic structure designed such that thermal expansion will be accommodated without damage to the honeycomb. Flow controls will be investigated as a means of providing constant output air temperatures under varying flux conditions. The receiver specifications are summarized in Table XIX.

One of the main concerns with any open cavity receiver is the potential loss in efficiency due to wind induced convective losses from the aperture. Since there is almost no background information with which to estimate these losses, an initial experiment will be conducted at Sanders to determine the magnitude of the losses and to make an initial effort to understand what scaling laws apply. Additional measurements will be made during the experiments at Georgia Tech.

The overall program schedule is shown in Figure 65.

TABLE XVIII. RECEIVER KEY ISSUES

Major Subsystem	Comment/Assessment	Actions	When
Effect of flux nonuniformity at aperture on collection efficiency*	Sanders computer model predicts that gross flux inhomogeneities up to 7:1 have only small effect on receiver performance.	Solar Facility - Test data is required to confirm this finding to determine if local flow control through the ceramic receiver is necessary or desirable.	0.25 MW_t RECEIVER PROGRAM
Terminal Concentrator*	Probably required to provide concentration ratios = 2000 economically. Sandia analysis confirms this.	Solar Facility - Exercise computer model - Test confirmation required.	0.25 MW_t RECEIVER PROGRAM
Ceramic Heat Exchanger material lifetime*	SiC best candidate - accelerated thermal cycling lab test desired.	Test at Sanders	0.25 MW_t RECEIVER PROGRAM
Structure geometry and supports	Evaluate several designs by analysis of commercial sized receiver.	Test best candidate	0.25 MW_t RECEIVER PROGRAM
Ceramic Cost	Manufacturer assures advantageous quantity costs	Continue dialogue with postential fabricators	0.25 MW_t RECEIVER PROGRAM
Dusting	Turbine blade life dependent on erosion if dusting from receiver and storage cannot be controlled.	Measure dusting during SiC lab life test - run storage media also	0.25 MW_t RECEIVER PROGRAM
Receiver heat loss due to free convection and wind*	First measurements	Solar Facility	0.25 MW_t RECEIVER PROGRAM
	Aerodynamic design will minimize loss	Wind tunnel test	RECEIVER SRE
	Computer model will yield sensitivities	Exercise computer	0.25 MW_t RECEIVER PROGRAM
Thermal insulation/ ceramic liners	Economic tradeoffs of heavy firebrick vs "exotic" lightweight insulation designs are straightforward	Apply kiln, furnace, checker stove experience to complete design	0.25 MW_t RECEIVER PROGRAM
		Run 2000°F heat loss and structural integrity testing without safety risk in Solar Facility	0.25 MW_t RECEIVER PROGRAM

*Critical item

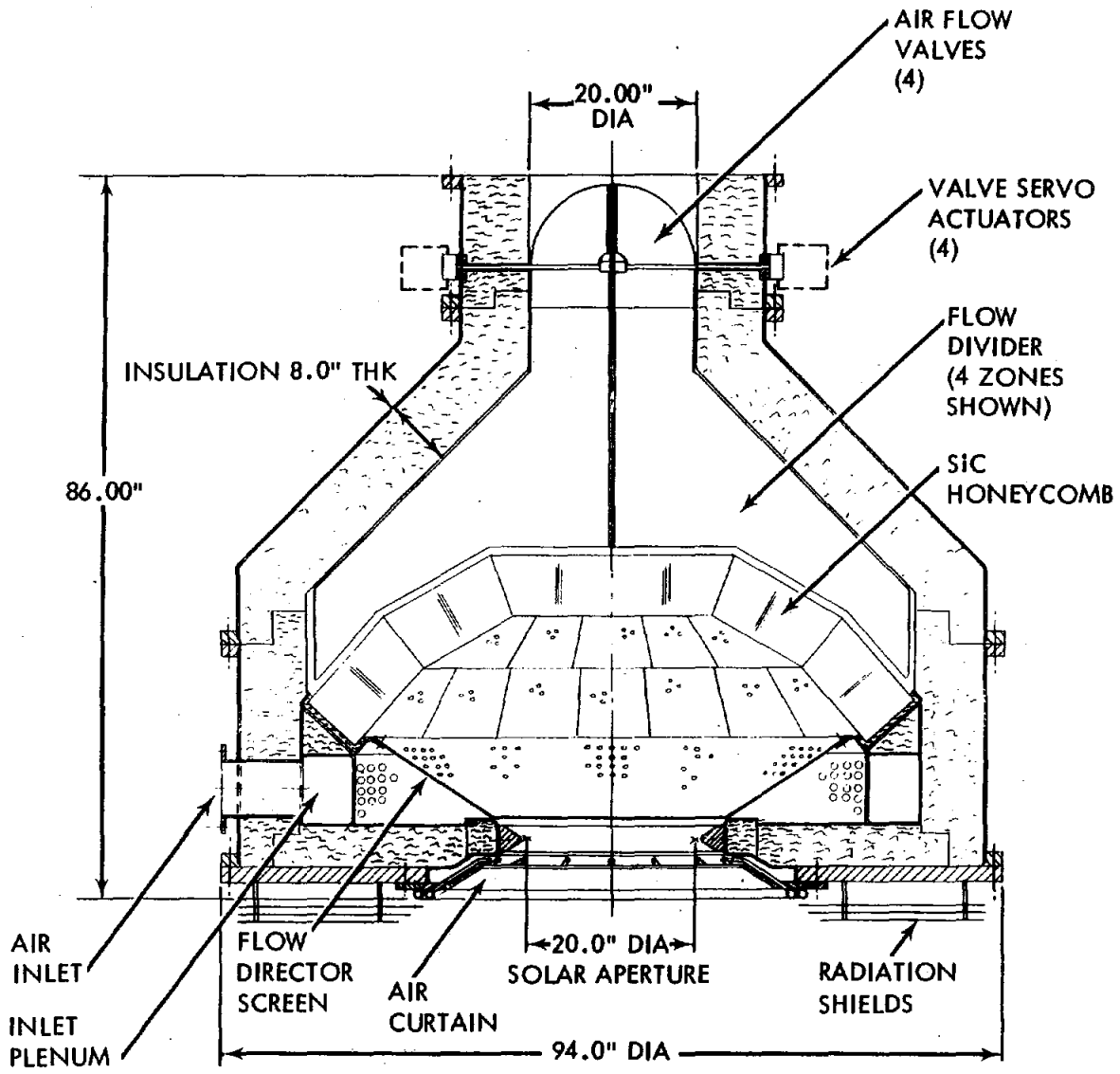

Figure 64. Receiver Schematic

TABLE XIX. RECEIVER UNIT OPERATING PARAMETERS

Input power	0.3125 MW_t
Output power	0.25 MW_t
Input air temperature	510°C (950°F)
Output air temperature	1100°C (2000°F)
Pressure	Atmospheric (at opening)
Efficiency	80% energy incident on cavity aperture converted to energy in the airstream at 1100°C (2000°F)
Air flow rate	1.7 lb/s

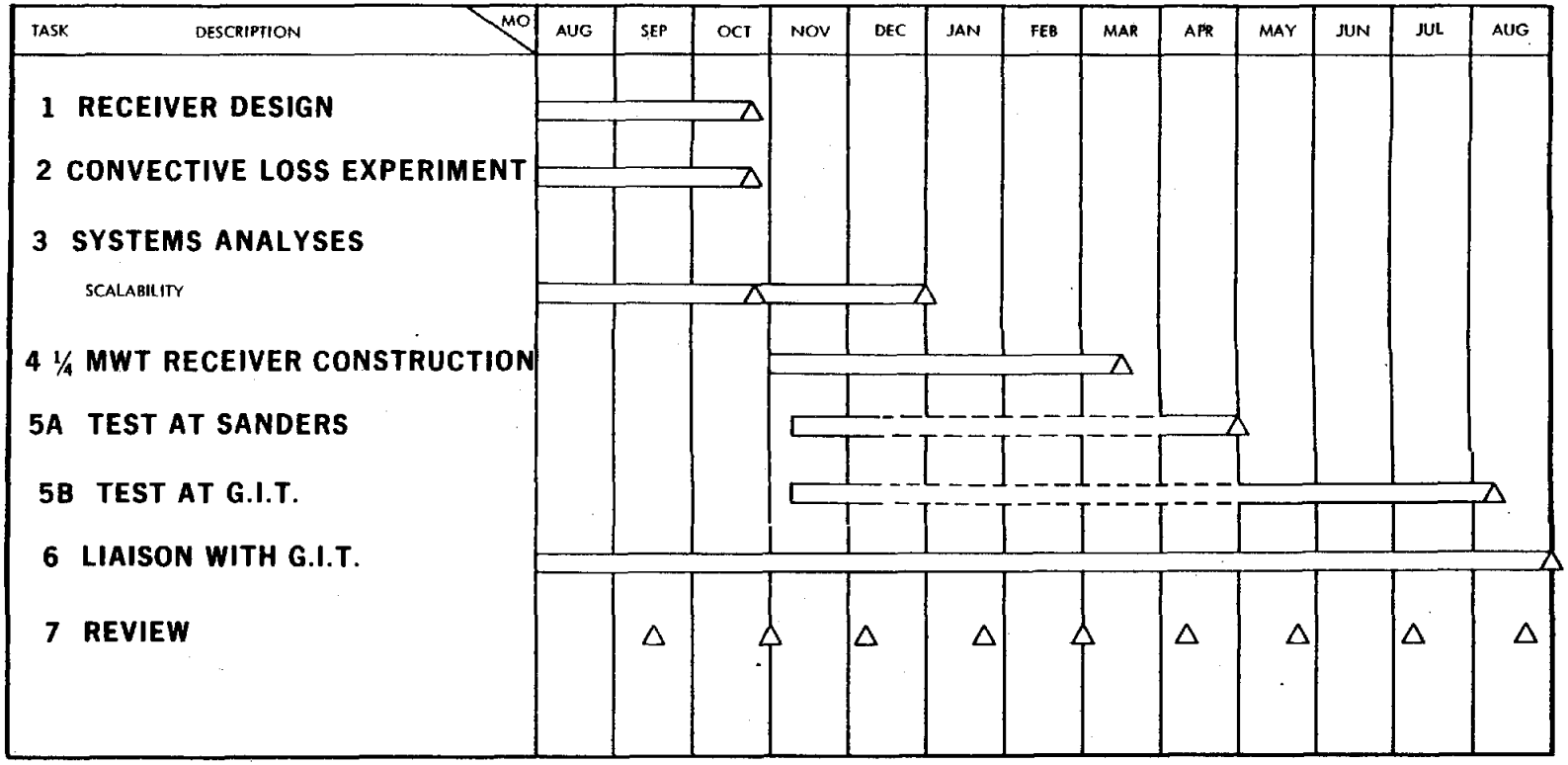

Figure 65. Schedule 0.25 MW_t Receiver

LIQUID METAL COOLED SOLAR CENTRAL RECEIVER FEASIBILITY STUDY AND HELIOSTAT FIELD ANALYSIS

University of Houston

Introduction

This study has two components. The first, which was completed in June, was to perform a high level conceptual design and feasibility analysis for a liquid metal cooled reactor. This system has advantages resulting from the excellent thermal properties of liquid sodium and from the ability to store all the collected energy directly as hot sodium, operating the turbine (with reheat) at full efficiency from storage at any time hot sodium is in the tank.

The second, continuing component involves analysis related to the water/steam central receiver systems. The first task is a net energy analysis, which we prefer to express as an energy amplification factor (EAF), i.e., the ratio of the energy sold by the facility over its useful life to the energy required to produce the facility from basic natural resources. A reasonable data base has been established, and transportation and fabrication energy costs have been evaluated. For a plant with a 30-year life, 1.1 years are required to produce enough electricity to satisfy all the energy requirements (0.37 years if credit is taken for fuel displacement) (see Table XX). The distribution is: collector field 91.4 percent, receiver and support 2.3 percent, riser and downcomer 0.3 percent, and tower 6 percent.

The EAF of 27 compares very favorably with nuclear (4). As all significant contributions have been considered, we expect that refinements of our analysis for this design will not change our numbers by as much as 20 percent. Other central receiver systems could vary by perhaps ± 50 percent from our value. In particular "low cost" heliostats and advanced receivers could lead to lower material content and higher system efficiency, particularly if the EAF is a consideration early in the design phase.

Solar direct beam data tapes have been obtained for Albuquerque and Fort Hood. These are being used to qualify our clear air insolation model (CAM). We find the model is good, but that a turbidity correction is essential to achieve nominal agreement with reality (Figure 66). For cloudless days at Albuquerque, variations in the daily integral from the CAM vary from 1.5 percent to 33 percent. With a simple exponential turbidity correction fit at noon, the +33 percent error is reduced to -3.5 percent. As a first approximation, a correction based on data from 20 cloudless days in 1962, which is exponential in air mass, will be used. This correction reduces the daily integral at equinox by 12 percent in optimization programs to more correctly weight morning and evening performance.

TABLE XX. NET ENERGY REQUIRED FOR 100-MW_e COMMERCIAL PLANT

Part	Item	Weight (Metric Tons)	Energy Required (MWH_t)	
Heliostat	(One complete)		19.72	
Heliostats	(22,940 complete)			452,147
Receiver	Incoloy 800 steel and steel	1,127	8,998	
	Transportation		652	
	Manufacturing and construction (15%)		1,448	
	TOTAL			11,098
Riser & Downcomer	Steel	182	1,135	
	Transportation		105	
	Manufacturing and construction (10%)		124	
	TOTAL			1,364
Tower (concrete)	Concrete	41,757	13,517	
	Steel	1,266	7,899	
	Transportation		5,170	
	Manufacturing and construction (10%)		2,659	
	TOTAL			29,245
				493,854
Number of days needed to provide equivalent energy (446K MW_e/Yr)		Thermal - 135 Electric - 405		

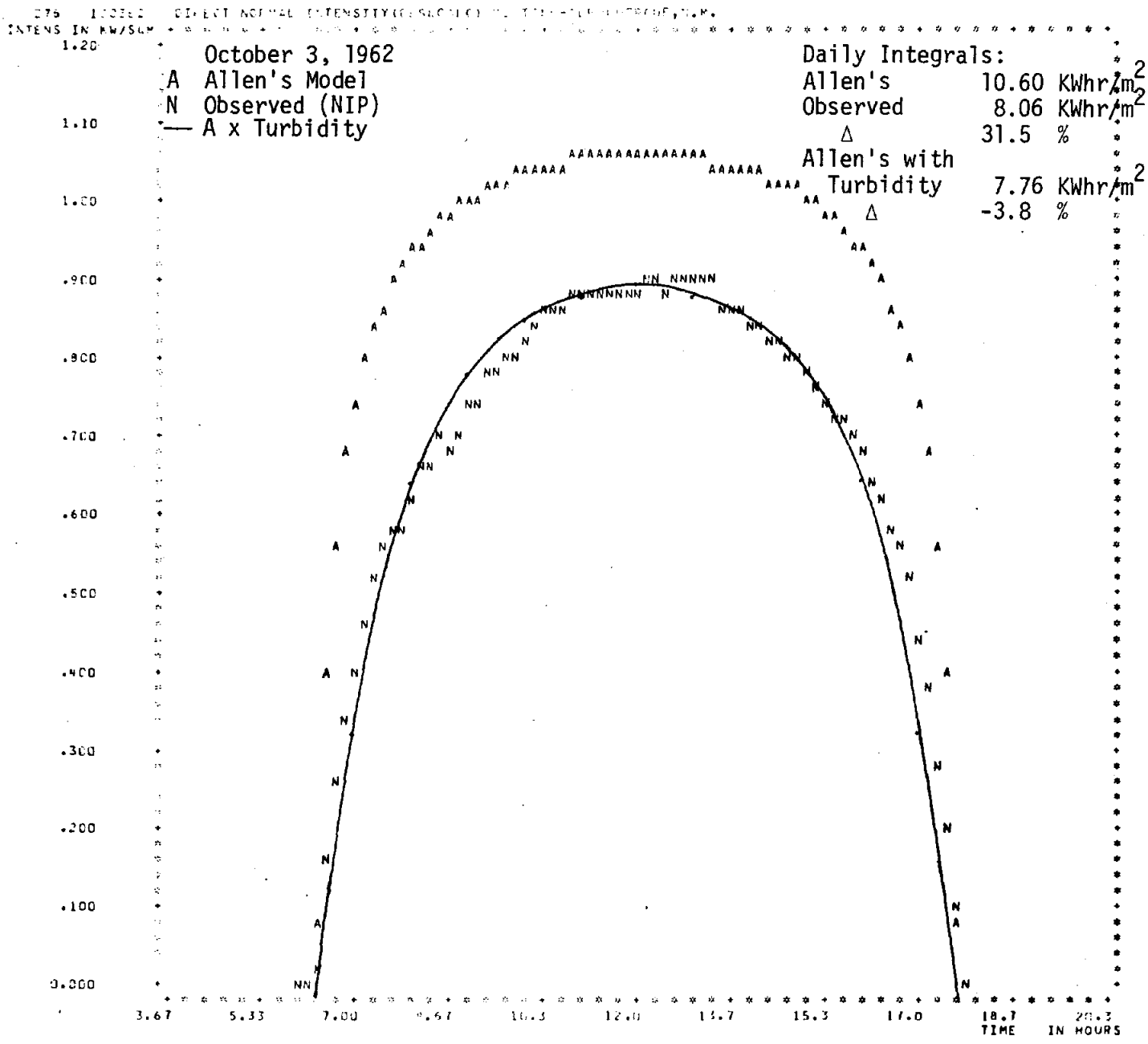

Figure 66. Clear Air Insolation Model, Showing Turbidity Correction

The third task involves the generation of heliostat fields optimized for various latitudes and ground slopes (Table XXI). Preliminary results were obtained for 1975 estimated costs using the RCELL iterative optimization approach. Modifications associated with the recently obtained 1977 cost figures led to extremely large rim angles and extremely poor interception factors for the boundary heliostats. Model modifications which lead to a more reasonable configuration as well as a closer approach to reality are as follows: move to seismic zone 2 - 8 percent reduction in tower and receiver costs; consider cloud cover - 15 percent reduction in operating hours; consider turbidity or haze - 12 percent reduction in mean solar intensity. Optical losses between the heliostat and the receiver corresponding to a 50-km visual range, differential costs of land and wire, and heliostat interception factors are the items currently in the optimization routine which tend to limit the extent of the field. Other than a conversion from Univac to a Honeywell computer, there are currently no obstacles to completion of this study.

TABLE XXI. OPTIMUM PERFORMANCE SUMMARY (PRELIMINARY)

Latitude (degrees)	25	35	45
Equinoon (MW)	796.	734.	616.
Annual (MMWh)	2.38	2.12	1.66
Fixed Cost (M$)	7.26	7.26	7.26
Tower Cost (M$)	6.56	6.56	6.56
Land Cost (M$)	5.09	5.09	4.63
Wiring Cost (M$)	2.45	2.40	2.12
Heliostat Cost (M$)	119.44	112.03	94.91
Total Cost (M$)	140.81	133.35	115.48
Figure of Merit ($/MWh)	59.08	62.82	69.44

An evaluation of the Ford sodium heat engine for use with the sodium central receiver is in progress. Current power densities are of the order of 10 to 20 kW/m^2, so either operation from stored sodium or use of an extended receiver surface (heat pipes and/or cavity receiver) will be required. Operation at 700°C to 800°C will also pose some interesting problems.

Liquid Sodium System Conceptual Design

ERDA's program to design and build the first 10-MW_e solar power plant is presently well under way and proceeding on schedule. The first generation solar plant has been designed around a superheated steam/water cycle in order to minimize technical, cost, and schedule risks. The potential for higher efficiency and lower cost has led to the consideration of second generation systems based on either a hot gas cycle or a liquid metal cycle. The hot gas cycle is presently under study by several EPRI contractors. Concurrently, a conceptual design study of an advanced liquid sodium solar power plant has been performed by the University of Houston, McDonnell Douglas, and the Atomics International and Rocketdyne Divisions of Rockwell International.

In accordance with the study guidelines, ERDA design criteria and subsystem designs resulting from the ongoing water/steam solar central receiver program were used wherever possible. This was done to permit the rather limited funds available on this study to be concentrated on the unique liquid metal aspects of the system while minimizing the duplication with other contract efforts. In addition, by maintaining similarities between the two systems, it was possible to make meaningful cost and performance comparisons.

The study confirmed the technical and economic feasibility of using the exceptional heat transfer capability of liquid sodium in a solar central receiver power plant to significantly improve plant efficiency. A conceptual design of a 100-MW_e commercial scale solar power plant was defined which would provide unique operational advantages. A summary schematic of the complete water/steam and sodium loops of the selected baseline configuration is shown in Figure 67. As indicated, the inlet receiver flow is drawn directly from the low-pressure, low-temperature sodium storage tank with a pump at the tank outlet providing the necessary head required for circulation. After absorbing the required heat energy in the receiver unit, the hot sodium travels through the downcomer, through a pressure-reducing device and into the low-pressure, high-temperature storage tank. A pump at the outlet of the high-temperature tank propels the sodium to the heat exchangers at the rate required to provide the nominal 100-MW_e output.

The heat exchanger assembly consists of a parallel superheater and reheater (from a sodium flow standpoint) followed by a preheater/boiler stage. The feedwater counterflows through the preheater/boiler and superheater stages and is passed to the turbine inlet as superheated steam at the conditions indicated. The steam which passes through the high-pressure turbine section exhausts to the reheater at the indicated temperature and pressure. The reheater raises the steam temperature to the original 538°C (1000°F) level at which point it is introduced into the low-pressure turbine section. The final exhaust steam is routed to the condenser where it is condensed and pumped through the feedwater heaters where it is heated and the cycle is repeated.

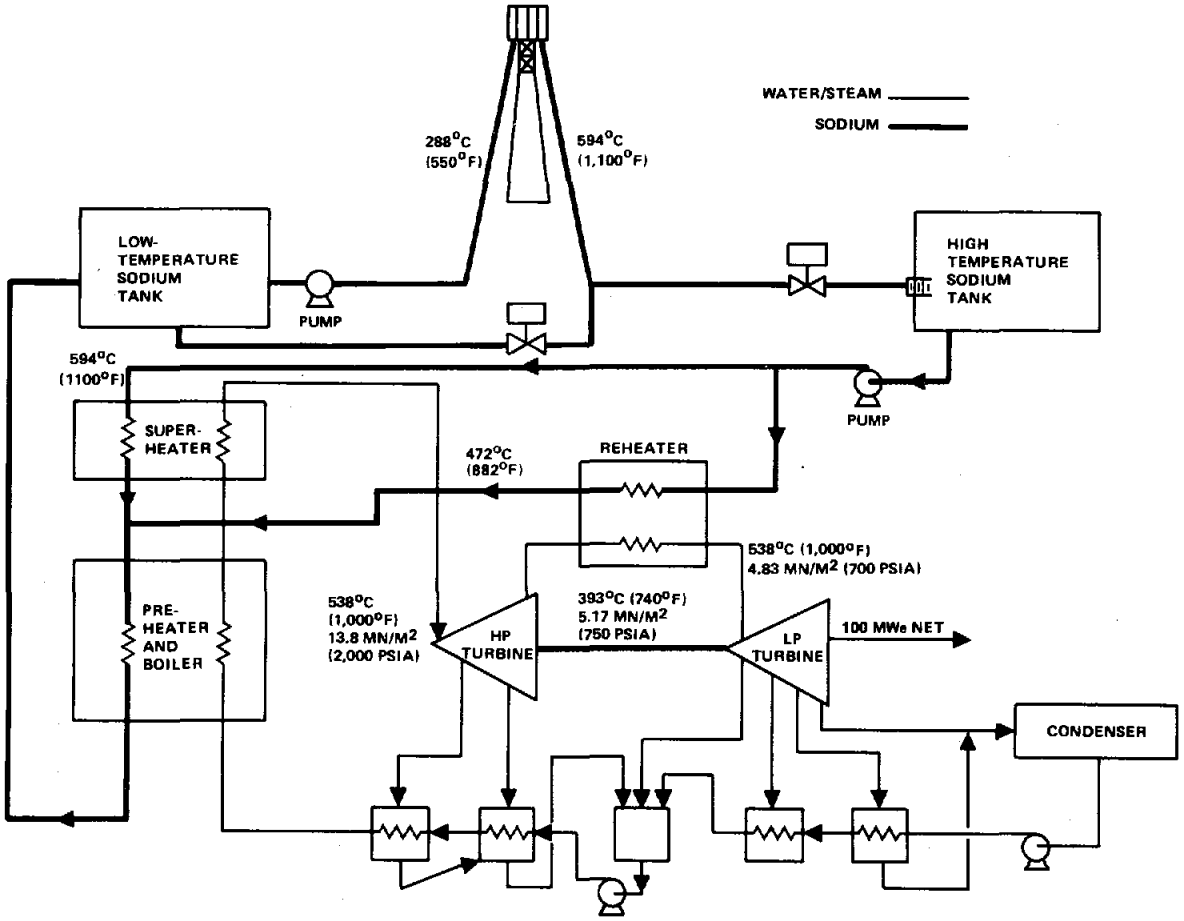

Figure 67. Liquid Sodium System Schematic (Revised Baseline)

Receiver Subsystem

The receiver subsystem includes all components and piping necessary to absorb the incident thermal energy from the solar collector subsystem and make it available to the turbine as superheated steam.

The receiver subsystem contains the receiver, the receiver pump, the steam generator units, and the main sodium piping including the riser and downcomer in the tower. The steam generator units are included with the receiver subsystem on the basis that the receiver loop could be connected directly with the steam generator without the thermal storage subsystem if operation were only during hours of sunshine. With the baseline configuration, however, direct operation of the steam generator with the receiver is by definition only since all liquid sodium passes through the storage tanks to reach the steam generators. This is a substantial advantage for this configuration since receiver operation is decoupled from the power generating activity.

Hence full rated power generation can continue as long as hot sodium is in the storage tanks without regard for the transient conditions at the receiver due, for example, to passing cloud fronts.

The receiver unit (Figure 68) is cylindrical in shape, 17 m x 17 m with an external energy-absorbing surface consisting of 24 panels. Each panel has 116 stainless steel 1.9 cm (0.75 in.) O.D. tubes connected to a common manifold. With a single point aim strategy, peak receiver heat flux is limited to 1.7 MW/m^2 to achieve a tube life of not less than 10,000 cycles.

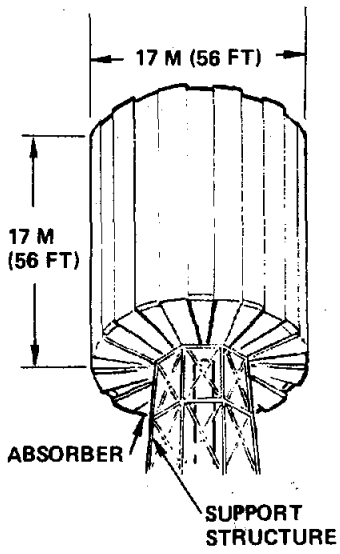

RECEIVER UNIT	
PEAK POWER	475 MW
SODIUM FLOW, Kg/h (lb/h)	4.47×10^6 (9.83×10^6)
SODIUM TEMPERATURE, °C (°F)	288 (550) – IN: 593 (1100) – OUT
SURFACE COATING	PYROMARK ($\alpha = .95$)
PANELS	
NUMBER OF PANELS	24
NUMBER OF TUBES/PANEL	116
PANEL WIDTH, M (FT)	2.2 (7.3)
PEAK HEAT FLUX, MW/M^2 (BTU/IN^2 – SEC)	1.67 (1.03)
TUBES, CM (IN)	1.91 (0.75) OD, 1.65 (0.65) ID (304H STAINLESS)

Figure 68. Receiver Subsystem Summary

The steam generator consists of an evaporator, a superheater, and a reheater. These units would be derived from current technology for the Clinch River Breeder Reactor program and test data available for the existing AI modular steam generator.

Thermal Storage Subsystem

The thermal storage subsystem contains the hot and cold storage liquid sodium tanks, a pump, a pressure reducing device, and interconnecting pipe. The subsystem characteristics are summarized in Figure 69. Liquid sodium from the receiver subsystem is stored in the hot storage tank at energy rates up to 475 MW_t, which corresponds to a flow rate of 4.47×10^6 kg/h (9.83×10^6 lb/h). Sodium is drawn from the hot storage tank at energy rates of up to 275 MW_t (2.68×10^6 kg/h (5.90×10^6 lb/h)) to generate steam for the

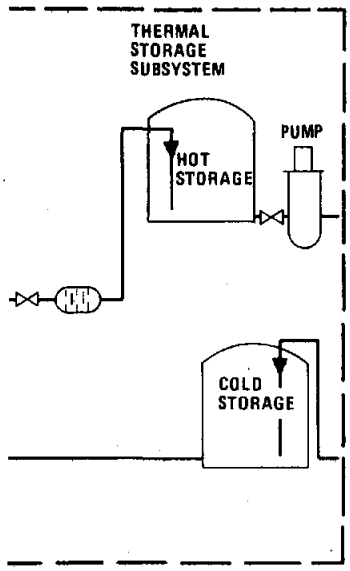

	HOT TANK	COLD TANK
ENERGY IN STORAGE, MWT-H	1,600	
TEMPERATURE °C (°F)	593 (1,100)	288 (550)
WEIGHT OF SODIUM KG (LB)	15.3 X 10^6 (33.6 X 10^6)	
VOLUME OF SODIUM M^3 (GAL)	18,925 (5.0 X 10^6)	17,910 (4.6 X 10^6)
STORAGE TANK SIZE M (FT)	38.14 X 17.2 (125 X 56)	38.14 X 15.6 (125 X 51)
MATERIAL	SS	CS
MAXIMUM FLOW RATE KG/H (LB/H)		
IN	4.47 X 10^6 (9.83 X 10^6)	2.68 X 10.6 (5.90 X 10^6)
OUT	2.68 X 10^6 (5.90 X 10^6)	4.47 X 10^6 (9.83 X 10^6)

Figure 69. Thermal Storage Subsystem Summary

electric power generating subsystem. Sodium from the steam generator units flows to the cold storage tank. During the day, hot sodium is accumulated by the hot tank in a sufficient quantity to store up to six hours of operation at 100 percent rated power. The thermal storage requirement of 1610 MW_t is satisfied with 15.3 x 10^6 kg (33.6 x 10^6 lb) of sodium operating with a temperature change from the hot storage to the cold storage of 305°C (550°F).

The storage tanks are 38.14 m (125 ft) in diameter with a height of 17.2 m (56 ft) for the hot storage tank and 15.6 m (51 ft) for the cold. The hot tank, which operates at 593°C (1100°F), is made of stainless steel; the cold tank, which operates at 288°C (550°F), is made of carbon steel. The tanks have a cover gas pressure of less than 0.0069 MN/m^2 (1 psi) to exclude air from contact with the sodium and to minimize cost. This cover gas requires a pressure reducing device to dissipate the tower static head.

Collector Subsystem

The principal elements of this subsystem are the heliostats, the field controllers, and the power distribution/data bus network. Since the principal hardware elements of the collector subsystem were defined in conjunction with the water/steam preliminary design effort, the task of the study was

primarily to determine the optimum collector field layout (based on the goal of minimizing the cost of energy on an annual basis) and size which satisfies the power flow demand for the rest of the system.

The heliostat configuration assumed for this study is of the type shown conceptually in Figure 70. The reference heliostat is composed of six reflector panel assemblies, a reflector support structure, drive assembly, and pedestal with buried foundation. As indicated in Figure 68, the panels are arranged so that a slot is created through the center of the reflector of sufficient width to permit inverting of the reflector assembly during nonoperating periods.

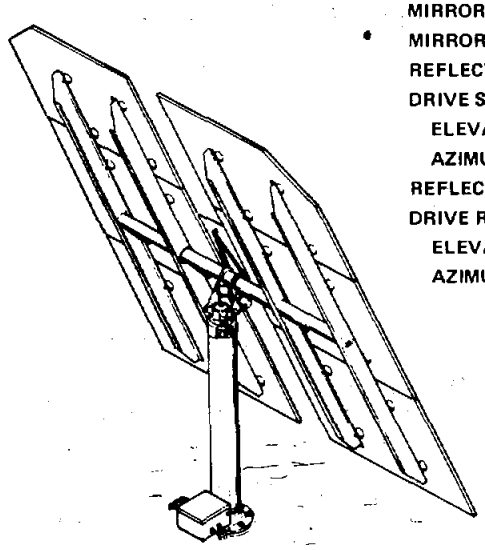

REFLECTOR SHAPE	SQUARE – 6.5 X 6.5 M (21.3 X 21.3 FT)
MIRROR TYPE	SECOND SURFACE SILVERED FLOAT GLASS
MIRROR AREA	37.95 M^2 (408 FT^2)
REFLECTIVITY	0.91
DRIVE SYSTEM	
ELEVATION	ORBIDRIVE, 3ϕ 230 VAC
AZIMUTH	ORBIDRIVE, 3ϕ 230 VAC
REFLECTED BEAM ACCURACY	3 MR (1σ)
DRIVE RATE	
ELEVATION	15°/MIN
AZIMUTH	5°/MIN

Figure 70. Heliostat Assembly

The drive unit incorporates two rotary drives which provide azimuthal and elevation tracking motions. The drives convert high rpm motor motion into the slow heliostat drive rates by means of a ~42,000:1 gear reduction. The motors are 230 V, 3-phase operated in a pulsed manner. Power pulses to the individual motors are controlled by the field controller, which continually calculates the heliostat pointing error based on the difference between perfect orientation and the input from the sensing equipment.

A plot plan of the optimized collector field is composed along with pertinent sizing data as shown in Figure 71. The collector field is composed of 20,580 heliostats and surrounds the central exclusion area which contains the tower, thermal storage, and balance of plant equipment. The exclusion area in turn is shifted slightly to the south of center in order to optimize the

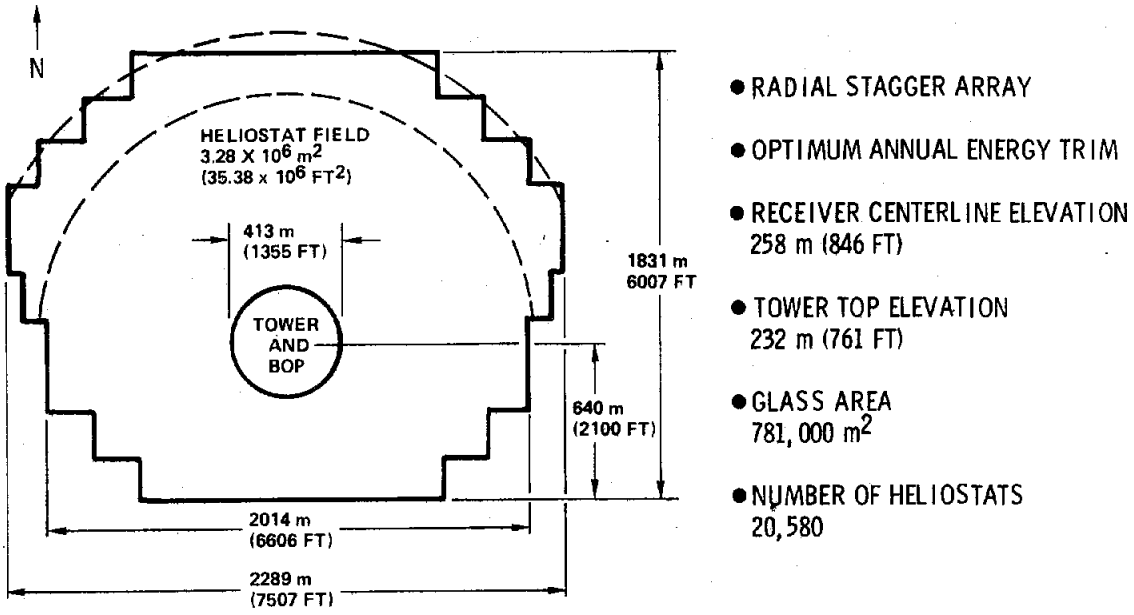

Figure 71. Sodium System Field Layout

annual collection of energy. The irregular field outline results from the cell-by-cell computational approach which deletes marginally performing cells. In reality, the field outline would be defined with a smooth curve which would approach an ellipse. The heliostats within the field would be arranged in a radial stagger layout which produces the maximum performance per unit glass area on an annual basis for most areas of the field. The field would actually be layed out along complete circles or continuous arcs with alternate rows being staggered relative to their neighbors.

Due to the high heat transfer capability of the sodium, the receiver is capable of accommodating the heat flux which would result from a one-point aim strategy; i.e., all heliostats aimed at the equator of the cylindrical receiver. The peak heat flux which results on the equator of the north-facing side of the receiver is ~1.67 MW/m^2. If excessive tube temperature conditions were to occur, it would be possible to reduce the flux peak by adopting a multiple aim strategy to distribute the flux vertically.

Electrical Power Generation Subsystem

The electrical power generation subsystem (EPGS) includes all of the equipment necessary to convert the incoming thermal (steam) power into electrical power output which is compatible with the utility grid. The basic turbine configuration selected for this system is a tandem compound, double-flow, extraction, condensing turbine designed to operate at a back pressure

of up to 16.92 kPa (5 in.-Hg). Machines of this type are capable of accepting a 10 percent overflow condition at the turbine inlet with a corresponding increase in electrical power output of ~9 percent.

The condenser design was developed in accordance with Heat Exchanger Institute Standards for Steam Surface Condensers. It was sized to condense the turbine exhaust at the daytime design point steam flow. The method of heat rejection selected for this system is a mechanical draft, wet, cooling tower. The specific configuration involves five cross flow cells, with the air circulation in each cell being provided by a 150-kW (200 HP) fan.

Master Control Subsystem

The master control subsystem (MCS) for the advanced central receiver power system will consist of the control and display hardware and software necessary for overall control and integration of the total system. The MCS will be similar in concept to the preliminary design reported in detail in MDAC Report MDC G6776, Volume VI, which is the preliminary design for a Master Control Subsystem for the water-steam central receiver system.

The baseline design features operator selectable manual or computer-based automatic centralized control. The central master control communicates with subsystem set point controllers, which in turn control the various individual pressures, temperatures, and flows.

HEAT PIPE CENTRAL SOLAR RECEIVER

Dynatherm/ Foster Wheeler

The objective of this program is to develop a solar-to-gas heat exchanger for a central solar receiver power plant. The concept employs heat pipes to transfer the concentrated solar flux to the gaseous working medium of a Brayton cycle conversion system. During early phases of the program, an open air cycle recuperator with a turbine inlet temperature of 800°C was selected as the optimum design. The predicted cycle efficiency is 33 percent, and the overall solar-to-electric efficiency is 20 percent.

Three potential receiver configurations were identified during the initial phases of the program (Figure 72). Optimum heat pipe diameter is approximately 5 cm for all three receiver configurations, and typical lengths are 2 to 3 meters. The required number of heat pipes for a 10-MW_e receiver ranges from 2000 to 8000. Heat transport requirements per pipe vary from 4 to 18 kW.

Several wick structures were developed and evaluated in subscale heat pipe tests. These wick structures and typical subscale heat pipe dimensions are shown in Figure 73. All heat pipes were tested with sodium. The best performance was achieved using the parallel tent artery for axial fluid transport and bias cut screen for circumferential fluid distribution. The axial and radial heat fluxes which were achieved meet the requiqements for the full-scale heat pipes.

Receiver evaluation and the heat pipe development effort have resulted in the selection of a baseline heat pipe design (Figure 74). The heat pipe evaporators, spaced on 10-cm centers, protrude from the wall of the pressure vessel and intercept the solar flux. The finned condensers are exposed to the compressed gas stream. Each heat pipe acts as an isothermal fin whose temperature is related to the local gas temperature.

Two heat pipes with the same general dimensions and wick design, but without fins, have been fabricated and tested. The working fluid was sodium. Typical test results for a horizontally and a vertically oriented heat pipe are shown in Figures 75 and 76. The open symbols represent limitations of the available power source or gas dynamic limits. The darkened symbols represent heat transport limits. The axial heat transport capability exceeds the performance requirements associated with the three receiver configurations over the operating temperature range (490-870°C) except below 550°C. Sonic limitations at these low temperatures may necessitate the use of potassium or a design modification to raise the heat pipe vapor temperature near the gas inlet. Radial flux capability exceeds 1 MW/m^2 at 600°C and is approximately 0.5 MW/m^2 at 800°C.

The test results indicate that horizontally or vertically oriented heat pipes will meet the stated requirements. If a receiver configuration is selected where the heat pipes are oriented vertically, simple wick designs may be used and heat pipe start-up is instantaneous. If the heat pipes are oriented nearly horizontal, arterial wicks must be used and controlled start-up procedures are required.

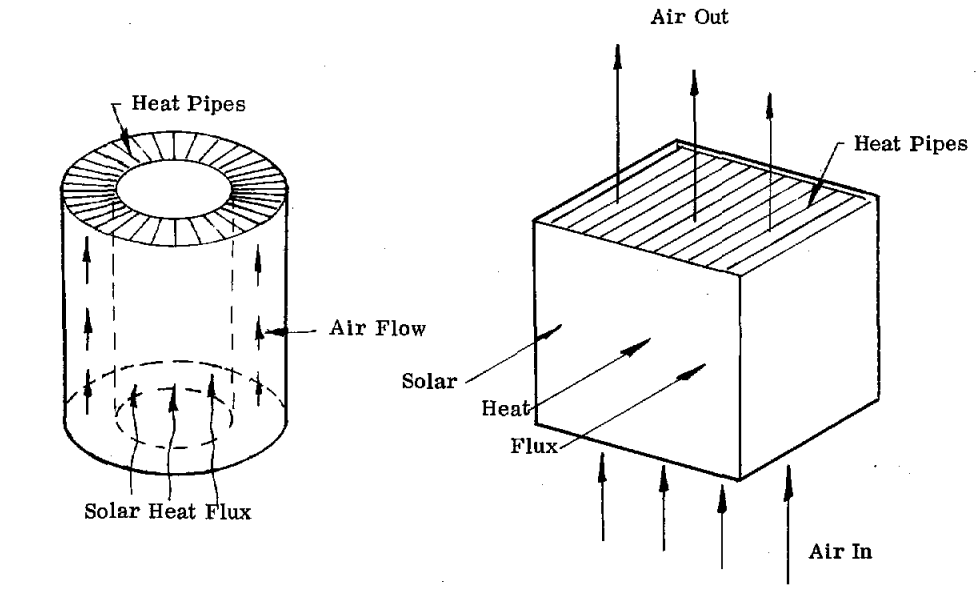

a. Cylindrical Cavity Receiver with Radial Heat Pipes

b. Square Box External Receiver

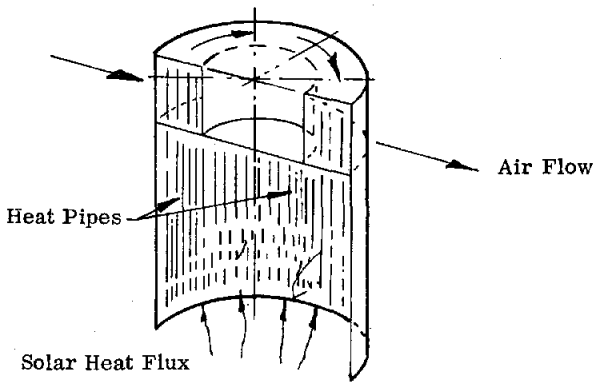

c. Cylindrical Cavity Receiver with Vertical Heat Pipes

Figure 72. Receiver Concepts

SUBSCALE HEAT PIPE TESTS

PURPOSE: Test many wick designs with smaller heat pipes (less expensive to fabricate and test) and extrapolate performance to full-scale heat pipe size.

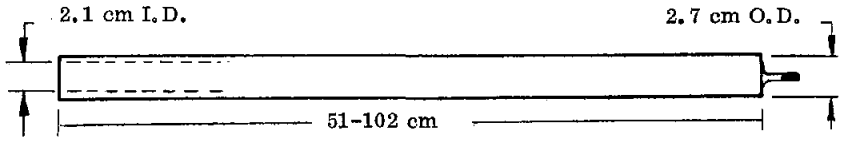

TYPICAL SUBSCALE DIMENSIONS

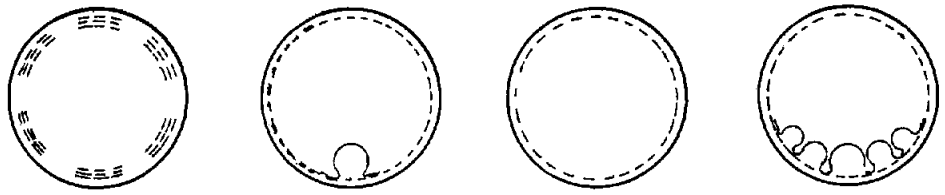

HOMOGENEOUS WICKS

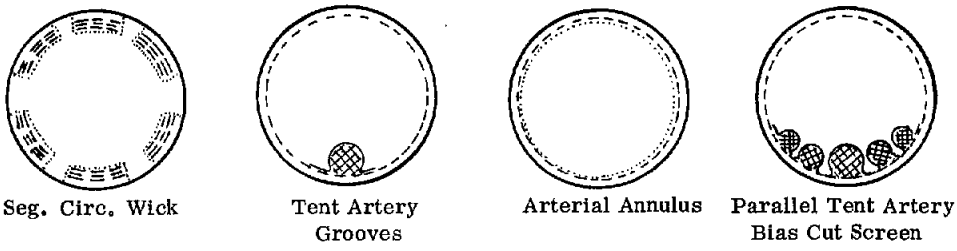

Figure 73. Arterial Wicks

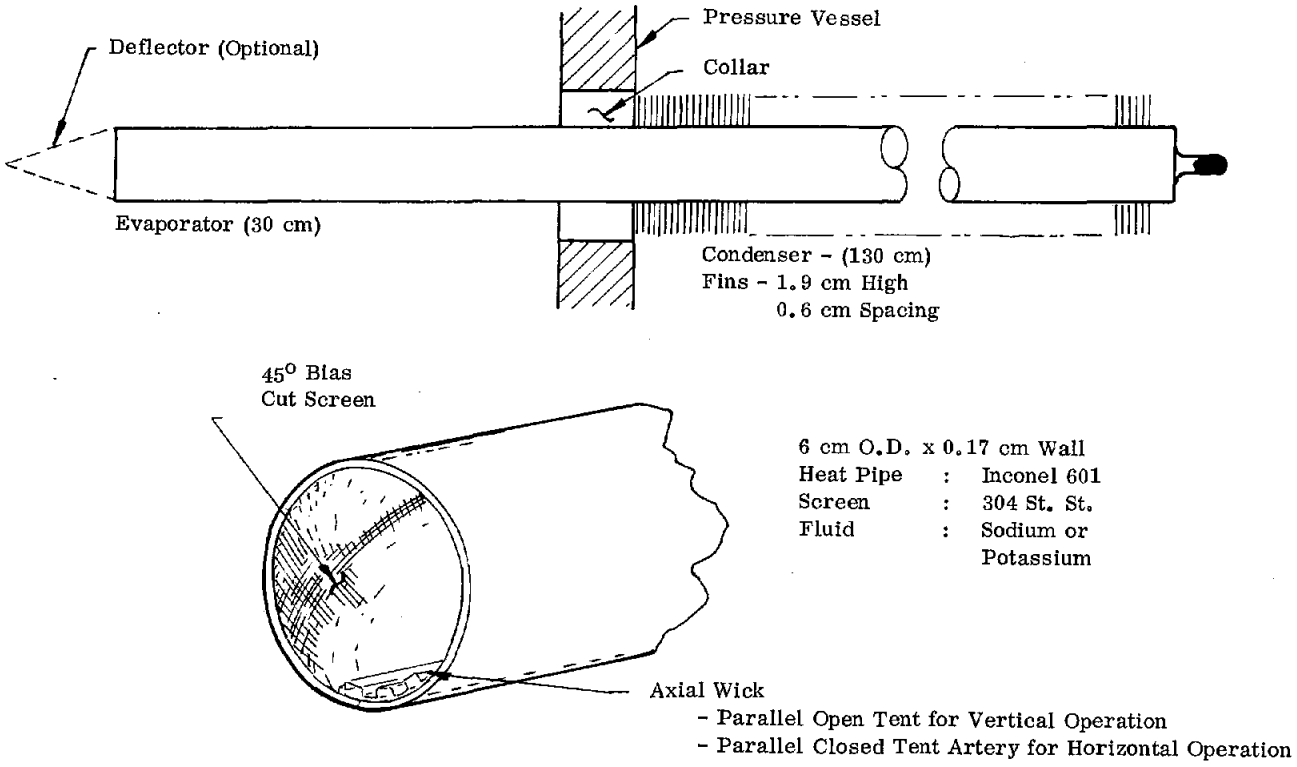

Figure 74. Baseline Design of Thermal Diffuser Heat Pipe

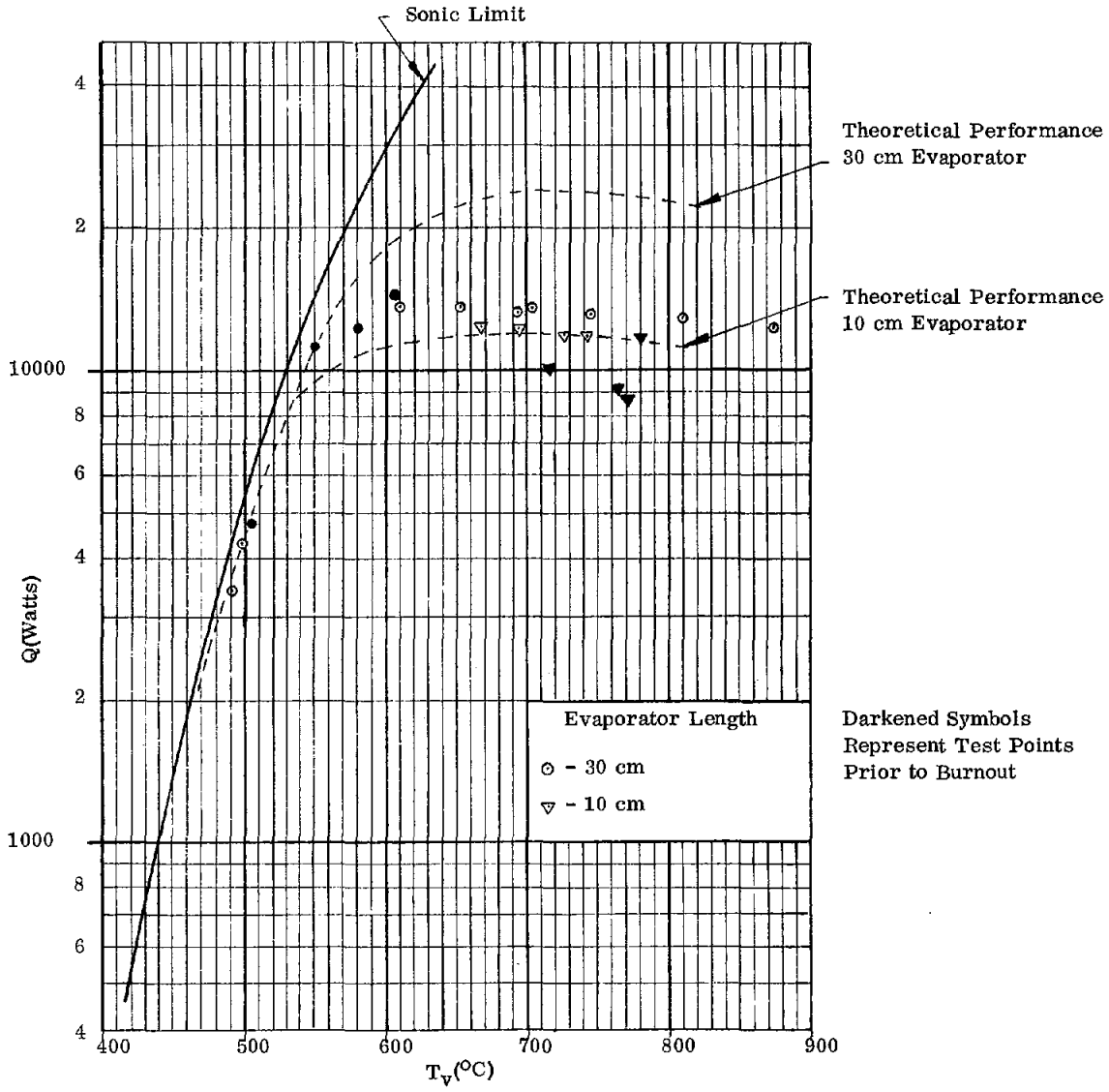

Figure 75. Horizontal Performance of Full-Scale Parallel Artery Heat Pipe

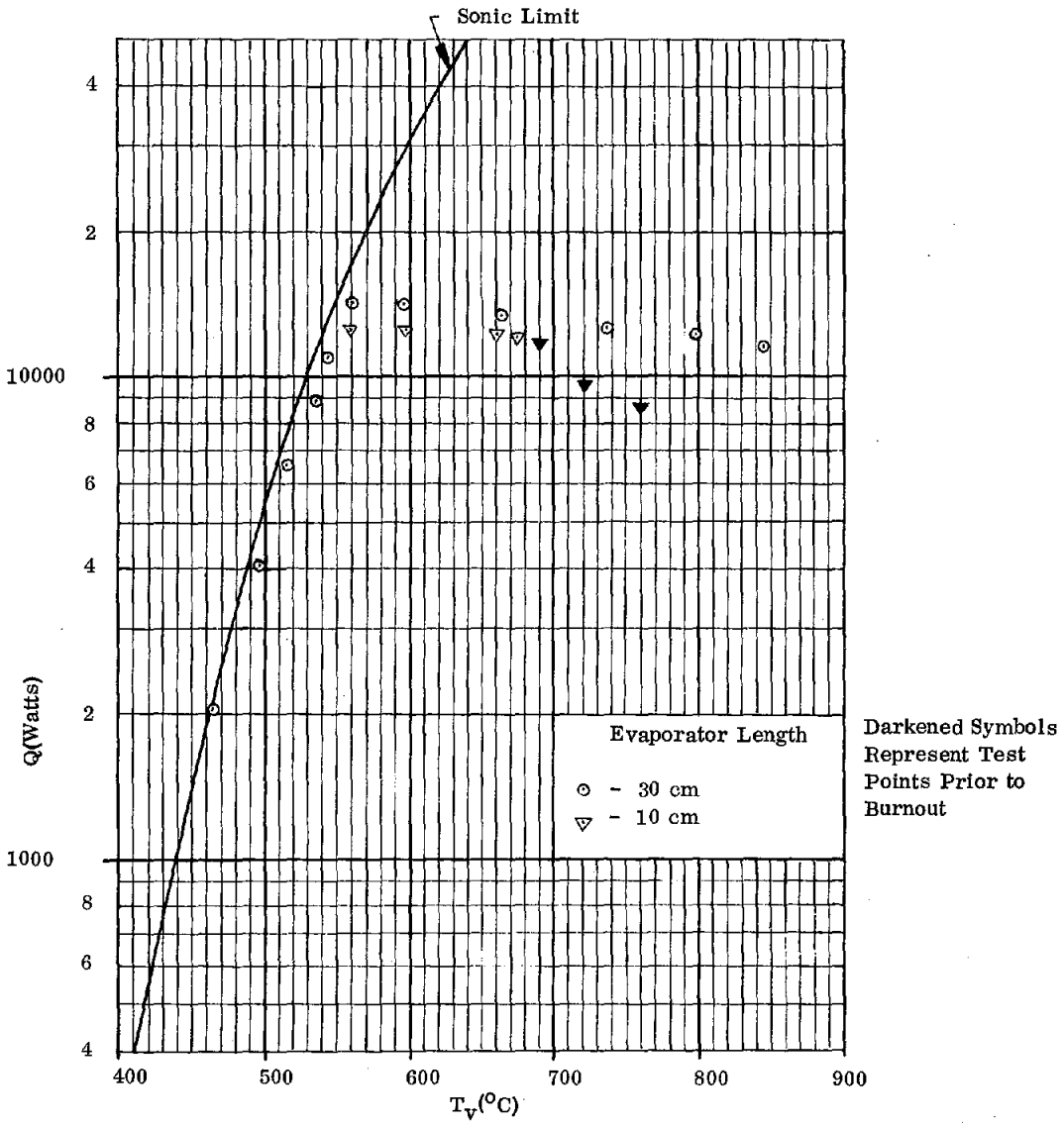

Figure 76. Vertical Performance of Full-Scale Parallel Tent Heat Pipe

HELIOSTAT DEVELOPMENT FOR A SOLAR POWER STEAM ENERGY SUPPLEMENT

J. G. Cottingham
Brookhaven National Laboratory

The "power tower" type collector configuration has been widely studied with most of the effort directed toward the generation of electric power on a utility scale. But this efficient collector configuration has many other applications some of which may be easier to engineer and some may be more accepted or accepted at an earlier date in a cost competitive market. All applications must be carefully investigated. The following is a brief list of some additional applications for the "power tower" collector.

1. Building heating and cooling
   a. Cluster residential
   b. Commercial
   c. Institutional
2. Process heat (300 to 1000°F)
3. Generation of electric power
   a. Community size
   b. Institutional size
   c. Energy feed to photovoltaic arrays

The object of any solar energy collecting system is to collect and deliver energy at a cost competitive with other forms of energy and so it should be for the "power tower." For only when cost-effectiveness has been attained will solar energy slow the rapid drain on the world's remaining store of fossil energy.

Solar energy storage is the first casualty to cost competitiveness. While it is comforting to think of an all-solar energy system free from the need of fossil auxilliaries, it is not economical to design to this extreme. Most solar cost analyses have indicated that the first increment of solar energy is the most cost effective. This fact creates the solar supplement concept in which the collector is sized to collect little or no surplus energy, thus eliminating the need for storage.

The "power tower" being a strong energy concentrator delivers solar energy in high temperature form. The commonly used working fluid in this temperature range is water-steam. While the utility industry use of steam is widespread, the use of steam for building space conditioning is regionally

confined to the northeastern part of the United States. Fortunately, this is the region of the country with the highest energy costs, and therefore the region of the country most easily penetrated with an alternate energy form.

The Brookhaven Heliostat Development Project is targeted for building space conditioning including both heating and cooling and makes use of the inplace steam technology in the northeast region.

The "power tower" collector configuration was chosen for the following reasons:

1. Higher concentration ratio--thus more efficient
2. Avoids distributed energy collection
3. Separation of receiver from heliostat yields lower cost
4. Less maintenance

What are the dominant cost factors in this type of collector? The heliostat cost represents approximately 70 percent of the total system costs. It is this cost that must be carefully controlled and reduced to an acceptable value. Wind, more than any other consideration, influences the heliostat cost. Without the wind the heliostat could be nothing more than a wire-supported reflective foil.

To minimize heliostat costs, Brookhaven proposed the fold-down design shown in Figures 77 and 78 which allows the heliostat to be exposed to the wind only under favorable conditions. Energy is lost by folding the heliostats down during sunny, windy hours. A nine-year wind-insolation history for Upton, New York is shown in Figure 79. If the heliostats were folded down all hours with wind speeds above 15 mph, only 5 percent of the available solar energy would be lost. However, the wind-insolation history for other locations is more demanding (see Figure 80). The first heliostat prototype built at Brookhaven will have a 20-mph design.

To permit a light-weight support structure, the reflecting skin of the heliostat must flex; otherwise a rigid and costly back structure is required. Glass, which can be made to flex, if segmented into facets, does not naturally lend itself to this requirement. A good reflecting plastic film would be much better in this application. However, there are two problems in using reflecting plastic films; specularity and weatherability. When films are bonded to supporting structures they often lose clarity, show waves, and other small defects. This reduction in specular quality is more important to the central tower configuration than it is to trough or other concentrating systems because of tighter angular requirements.

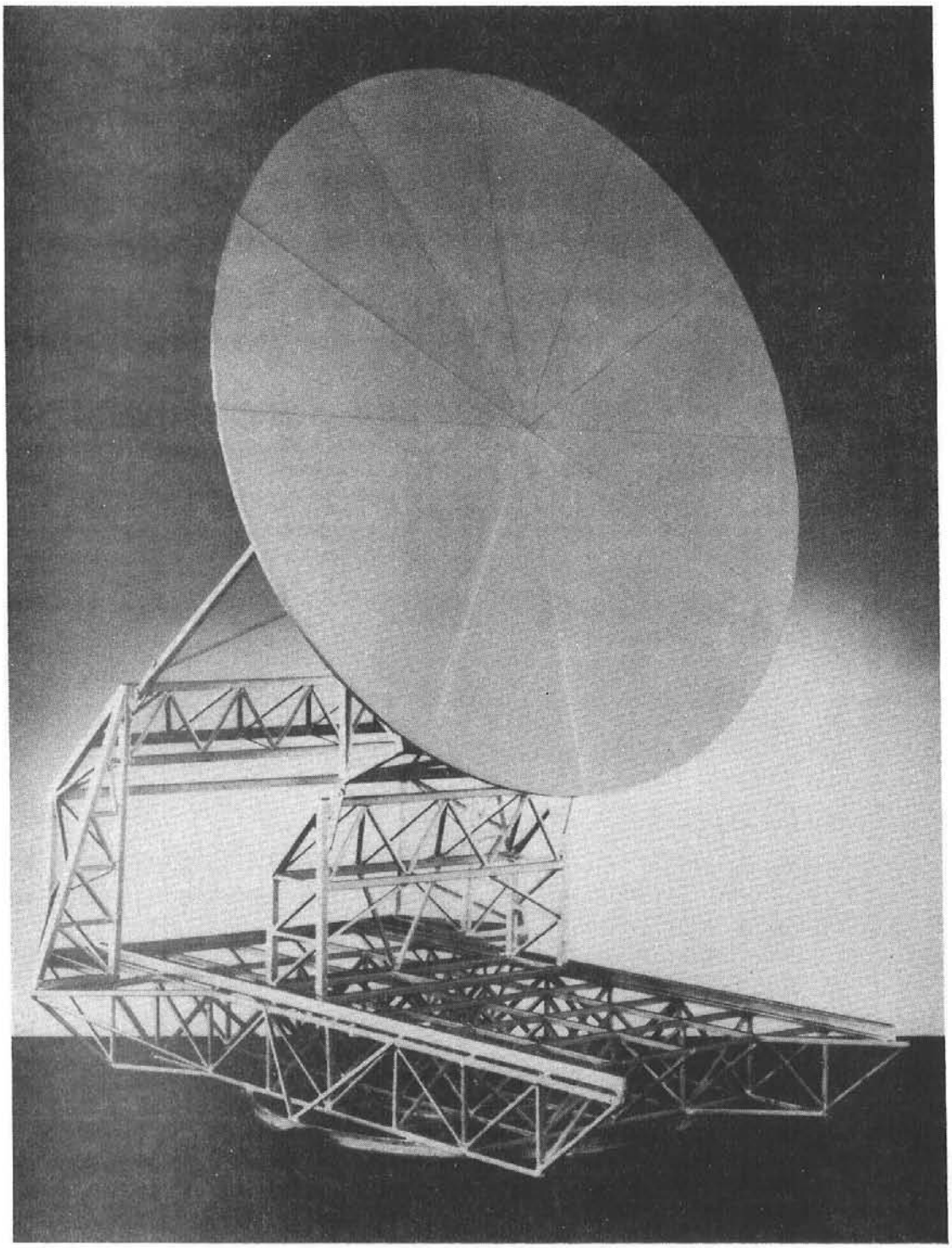

Figure 77. Heliostat, Operating Position

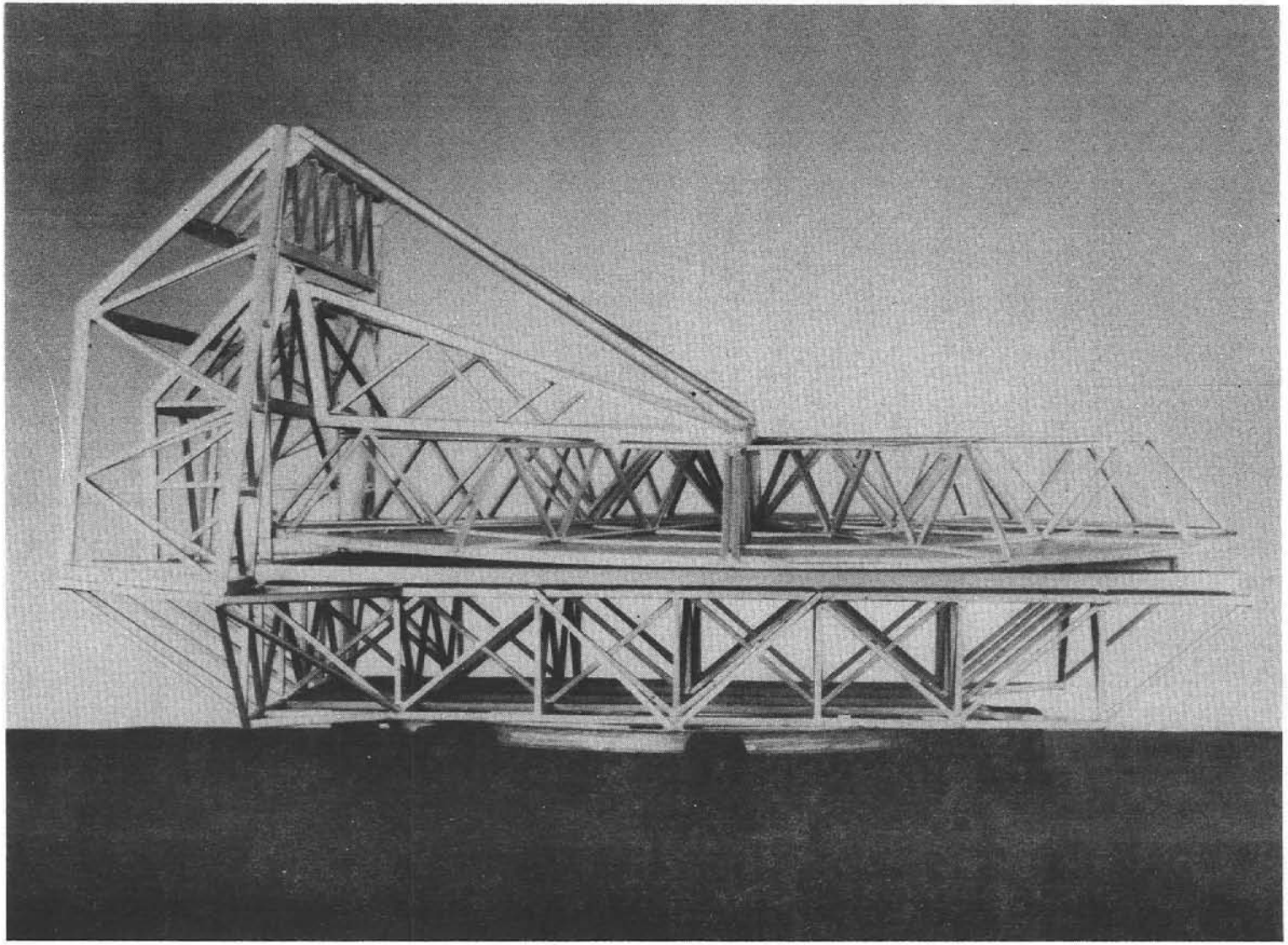

Figure 78. Heliostat, Folded Down Position

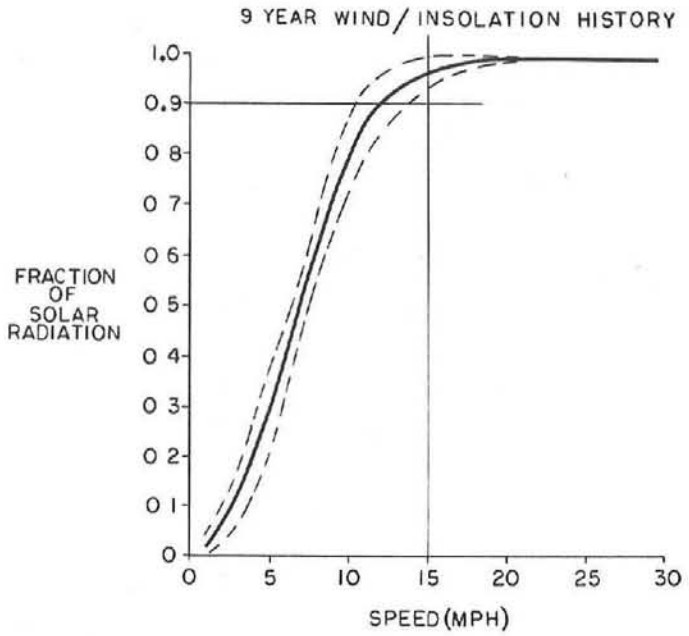

Figure 79. 9-Year Wind/Insolation History, Showing Extreme Years

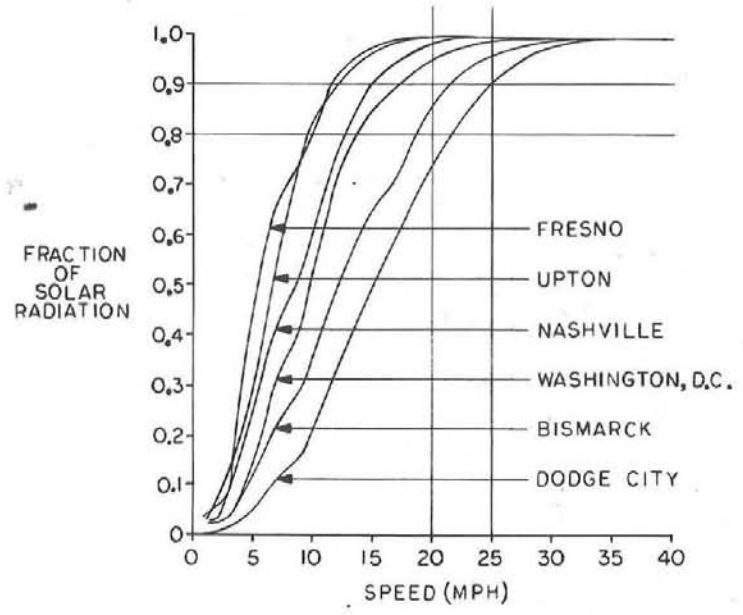

Figure 80. Wind/Insolation History, Other Locations

One of the major accomplishments of the early months of the Brookhaven heliostat program is the development of a plastic film bonding technique that produces excellent specularity ($\sigma \simeq 0.5$ mrad).* The method is simple and easy to employ in production. The film is laid reflecting side down on a quality glass surface using a soap-water surface adhesion. Excess soap-water solution is removed by rolling. While the reflecting film is held against the glass, it is bonded to the support structure using an epoxy agent. After curing, the finished product is removed from the glass tooling surface.

The reflecting film presently being worked at Brookhaven is a Dunmore product, Dunchrome 200, with a 393 first surface coating. This is an aluminized polyester product and at present does not have the desired weatherability. However, Brookhaven has entered into a contract with Dunmore to develop a cross-linked polymer coating which hopefully will have acceptable weatherability. The present film has a solar reflectance of 0.85, which is a little lower than desired. Efforts will be made to improve this coefficient.

The proposed support structure for the reflecting film is the sandwich shown in Figure 81, which consists of two aluminum sheets spaced by a piece of Styrofoam. Test sandwiches have met deflection requirements and are undergoing life tests. An alternate honeycomb type support is being studied in co-operation with Hexcel Corporation.

A heliostat field configuration is undergoing development. The configuration, shown in Figure 82 is tentative pending a computer refinement using the following guidelines:

	Worst-Case Heliostat	Whole Field
Shadowing	75%*	90%*
Optical Efficiency	70%	85%
Combined Shadow-Optical	65%	80%

*yearly average

The ratio of heliostat area to field area for the field arrangement shown in Figure 82 is 0.43.

*Specularity can be measured by measuring the fraction of light scattered from a collimated beam. Details of this technique have been described by Richard Pettit, Sandia Laboratories, (SAND76-0537).

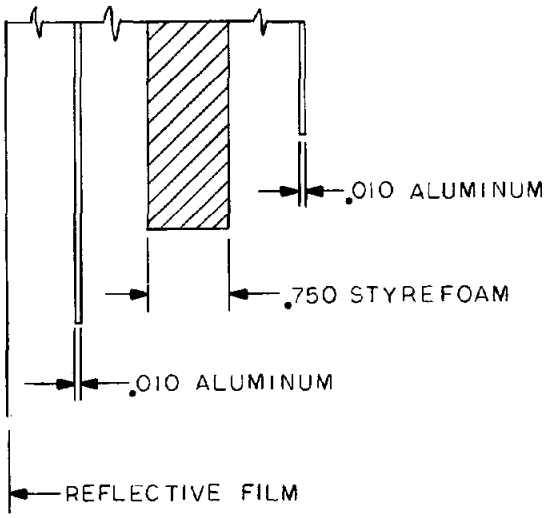

Figure 81. Reflecting Surface Support, Exploded View

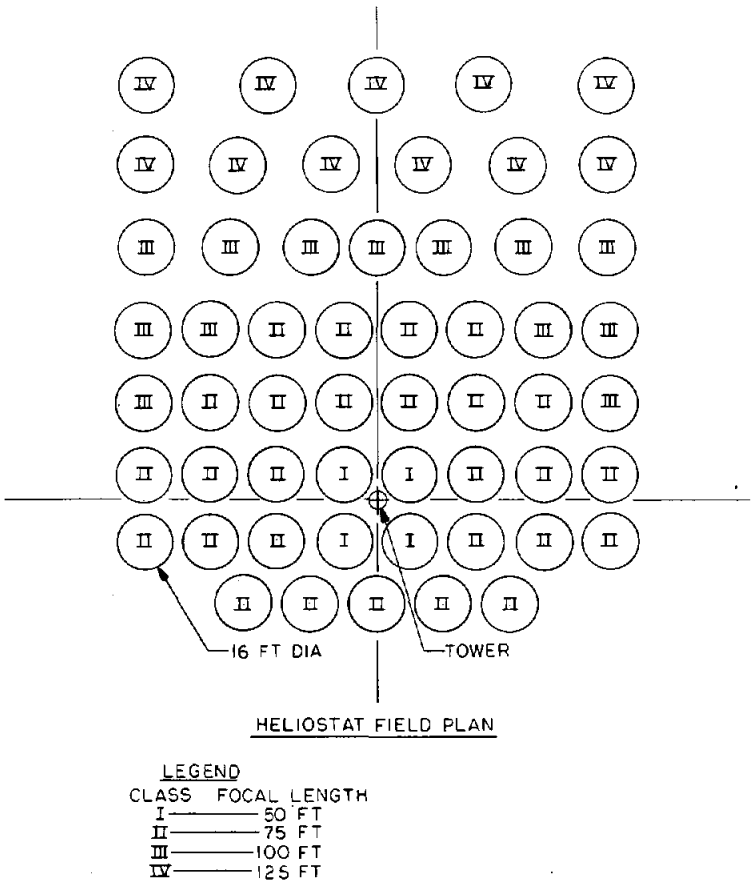

Figure 82. Heliostat Field Plan, Tentative

A preliminary estimate of the cost competitiveness of this solar energy collecting system relative to No. 6 fuel oil in the Northeast follows. Figure 83 is typical of the price history of No. 6 fuel oil in the target area. The price is expected to cross the 40¢/gal mark soon. The heliostat system costs are:

Power Tower System Costs

Heliostats, 55 units	$ 82,500
Boiler	12,000
Tower	15,000
Controls	1,500
Installation - checkout	7,500
	$118,500

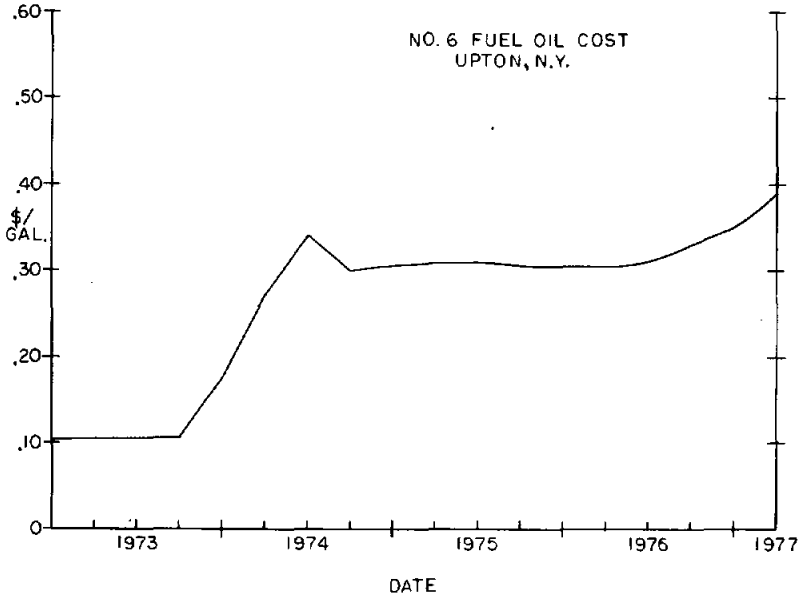

Figure 83. Fuel Oil Price History For Upton, NY

When used an an energy supplement, this system is expected to displace 44,500 gals of fuel oil as outlined below.

Fuel Displacement

Collector area	11,055 ft^2
Solar input per year	7.0×10^5 Btu/ft^2
System efficiency boiler losses, reflectivity	79%
Geometry factor shadowing, optics, cosine θ	80%
Energy yield	4.9×10^9 Btu
1 gal of #6 oil burned at 75% efficiency yields	1.1×10^5 Btu
Annual fuel savings	44,500 gal

The economic relationship between the invested sum and the operating saving is user dependent. Two balance sheets have been prepared; one for a tax exempt user such as a school, hospital, municipal or other nonprofit institution and a second balance sheet for a profit-making user in the 50 percent tax bracket. Different interest rates have been used in the two cases which reflect different financing environment. It is interesting to note that a greater first year return occurs in the high tax case.

Balance Sheet - Tax Exempt

	Price of Oil, #6	Fuel Savings 44,500 gal	$120,000 Amortized 8% - 7 yrs.	Maintenance	Net Return
1977	$ .38/gal	-	-	-	-
1981	.52	$23,140	$22,440	$2,140	-$ 1,440
1982	.56	24,920		2,290	+ 190
1983	.60	26,700		2,450	1,810
1984	.65	28,925		2,620	3,865
1985	.70	31,150		2,805	5,905
1986	.76	33,820		3,000	8,380
1987	.82	36,490	22,440	3,210	10,840
1988	.89	39,605	0	3,440	36,165
1989	.97	$43,165	0	$3,680	$39,485

Balance Sheet - 50% Tax Bracket

	Price of Oil, #6	Fuel Savings 44,500 gal	$120,000 Amortized 9% - 7 yrs.	Interest Credit	Capital Write-off	Maintenance	Net Return
1977	$ .38/gal						
1981	.52	$11,570	$23,170	$4,843	$8,571	$1,070	+$ 1,474
1982	.56	12,460		4,236		1,145	1,742
1983	.60	13,350		3,575		1,225	1,951
1984	.65	14,462		2,854		1,310	2,320
1985	.70	15,575		2,068		1,402	2,616
1986	.76	16,910		1,212		1,500	3,088
1987	.82	18,245	23,170	0	8,571	1,605	17,795
1988	.89	19,802	0	0	0	1,720	19,330
1989	.97	$21,582	0	0	0	$1,840	$21,110

INTERIM STRUCTURAL DESIGN STANDARD FOR SOLAR ENERGY SYSTEMS COMPONENTS

Foster Wheeler Development Corporation

This program is aimed at the development of a set of interim design rules and standards applicable to the central receiver solar thermal power system components that generally fall under the scope of the ASME Boiler and Pressure Vessel Code. Test programs and additional development work required in order to upgrade the interim standard will also be identified. The program was initiated in June 1977 and it is scheduled to be completed by the end of 1978.

Program Need

The conversion of solar energy to usable power involves pressure-containing components such as boiler tubes, pressure vessels, piping, and valves. The pressure requirements, the temperatures of operation, the fluids used, and the environment may vary. In each case there may be a potential hazard associated with the failure of a pressure boundary. To greatly reduce this hazard, a set of requirements may be imposed on material, design, fabrication, and testing of the pressure boundaries. The ASME Boiler and Pressure Vessel Code* is such a set of requirements.

Code Historical Background

Before considering the applicability of the Code to solar energy system components, it is instructive to briefly review some of the background of Code development. In 1914, in response to a series of pressure boundary failures and the loss of lives and property, an initial set of rules was issued. This set of rules has been updated over the years and is now called Section I Power Boilers. However, in the intervening years it was recognized that there should be different Code requirements for pressure boundary components in various industries because they may have special needs. Thus in 1921 a Section on Boilers for Locomotives was issued. By 1963 the original rules of Section I were sufficiently modified so as to cover the needs of Boilers for Locomotives, and the special Section was discontinued. A similar section on Miniature Boilers was issued in 1922 and discontinued in 1962.

---

* Subsequently referred to as the Code

Other Sections were issued that are in existence today. Section IV was issued in 1923 to inexpensively meet the special needs of Low Pressure Boilers. Section VIII was first published in 1925 for unfired pressure vessels. It underwent many changes and is applicable to all vessels not covered by Section I, III, and IV. It also now has two Divisions which allows the choice of design by rules or design by analysis. Design by analysis is more expensive in terms of carrying out the analysis but may be cheaper in hardware cost.

Section III was the result of the decision in the 1960's to make special provision for nuclear components. High reliability was sought by means of the explicit consideration of additional failure modes. These rules, however, only apply to applications in which material temperatures are below the creep range. It was recognized that the simplistic approach that other sections of the Code take to design at temperatures above the creep range would not be acceptable for the special conditions of nuclear design. However, it was also recognized that an acceptable Code at these creep temperatures required the development of analytical capabilities, materials information, and other advanced technology in addition to a massive effort from Code development bodies. Rather than delay the promulgation of a nuclear code, the high-temperature aspects were deferred. A substantial effort has gone into the development of a high-temperature Code for more than a decade. The current status is Code Case 1592-10 that is almost ready to be incorporated as part of Section III.

Legal Questions

Today the Code is legally binding in almost all jurisdictions of the United States as well as in many other countries. However, there is no legal obligation on the part of the ASME to change the Code or to write new Sections of it. It is not sponsored by any governmental agency, but rather is written by volunteers.

Impetus and Resources to Develop Code Rules

The decision to set up new Code Committees in order to develop Sections of the Code is the responsibility of the ASME Policy Board Codes and Standards. Once a basic Code is set up, the particular Code Committees develop and modify rules mainly in response to inquiries sent to them. The various resources available to the Code Committee upon which to base modifications and development of the Code are:

- Their own expertise and that of colleagues
- Published information
- Unpublished information sent to or available to the Committee

Packages of information sent to the Code Committee with the inquiry .

The resources of the Code Committee to develop new information are:

- Their own or colleagues work voluntarily done
- Work carried out or sponsored by organizations such as the Pressure Vessel Research Committee, the Material Properties Council, and the Electric Power Research Institute
- Work sponsored or carried out by governmental organizations, some of which have representatives on various Code Committees, i.e., Nuclear Regulatory Commission (NRC) and the Energy Research and Development Administration (ERDA)

Other than limited funds for consultants or recently allocated funds for computer computation, there are no Code funds available for technical studies to back up or develop new Code rules.

Supplementary Rules

Sometimes the legal jurisdiction, government agency, customer, or insurance company may impose supplementary rules and regulations. They may believe that certain conditions are not adequately covered in the current Code for their needs. An example of this is the establishment of the F9 Committee in 1972 by the Energy Research and Development Administration to develop additional design standards for elevated temperatures until acceptable rules become available in the Code. These rules and criteria of F9-4 are to be used in conjunction with the applicable parts of the Code. In addition, another document "Guidelines and Procedures for Design of Nuclear System Components at Elevated Temperatures" was written and is continuously updated. This document is a valuable adjunct to high temperature Nuclear Code users for design guidelines, design-analysis methods, and computer program verification.

Solar Application

The Code may be applied to solar components. From the nature of its use, Section I, Power Boilers seems to be applicable to the design of a receiver of a Central Solar Power System in which steam (or another vapor) is generated. However, there are conditions of loading and service that are unique to solar systems and are very critical in their design. For example, portions of the solar receiver will generally operate at a high temperature. It might be required to have a twenty to thirty year lifetime and withstand a very large number of severe thermal cycles. Section I does not consider thermal cycles either explicitly or implicitly because fossil fuel boilers do not sustain as many severe thermal cycles.

There are other aspects of Section I which may be questionable for solar applications. For economic reasons it may be important to change these. For example, the determination in Section I of the allowable loading for structural attachments to tubes is very dependent on the experience gained in fossil fuel boilers and is not very defendable on a stress analysis basis for general applications.

Other Sections of the Code do have methods which are applicable to many of the special conditions of solar receivers. Included are techniques for the direct evaluation of creep, low cycle fatigue, and the design by analysis of structural attachments to tubes. However, before we can use these methods and rules with confidence, they must be examined for their technical validity, consistency, and completeness in the solar design situation.

Program Objectives

The objectives of this program are directed toward the development of a set of design rules and standards applicable to the central receiver solar thermal power system. Specifically, the overall objectives of the program to be carried out in Phase II are:

1. Develop and recommend an interim structural design standard applicable to CRSTPS components that generally fall under the scope of the ASME Boiler and Pressure Vessel Code.

2. Identify test programs and other additional work required in order to upgrade the interim standard.

In Phase I the specific tasks leading to the attainment of the above objectives are:

1. Study the loading conditions, environment, and different possible failure modes in CRSTPS components that fall under the scope of the ASME Boiler and Pressure Vessel Code.

2. Survey the available design rules and criteria in the Code and other standards that deal with the possible failure modes in CRSTPS components.

3. Study the available literature on failure rates and service failure history of different power system components designed under various Sections of the Code. Define the levels of reliability and safety for CRSTPS components consistent with its conditions of loading, failure modes, failure consequences, and system requirements.

Approach

Matrix of Information

The three tasks of Phase I will be used to develop a matrix of information. This matrix will include:

a. List of Components - The CRSTPS systems with steam turbines that have been designed will be reviewed to determine those components which fall within the scope of the Code. Seven such systems have currently been identified.

Some of the components which will be considered are:

- Steam drum
- Storage tank
- Boiler tubes
- Valves
- Pumps
- Piping

For each component, the elements as they appear in the Code will be identified. For example: cylindrical components, heads, openings, flanges, and nozzles.

b. Loads and Conditions Associated With Each Component - These would include items such as pressure, seismic, wind, transient, and attachment loads. An initial survey indicates a range of maximum temperatures and pressures as shown in Figure 84.

c. Possible Failure Modes - These failure modes will be coupled with the loads and components for which they are applicable. Some possible failure modes are fatigue, excessive plastic deformation, and ductile rupture.

d. Failure Consequences - This list will help differentiate between the failures that may impact safety and those that impact availability.

e. Items Other Than Design That Impact Safety and/or Availability - These include accessibility to repair, component repair time, operational considerations, failure detection and past experience.

SYSTEMS WITH STEAM TURBINE		SYSTEMS WITH GAS TURBINE
WATER/STEAM COOLED	LIQUID METAL COOLED	
STEAM OUTLET: ~950 - 1000°F ~1300 - 1500 PSI	STEAM OUTLET: ~950 - 1000°F ~1300 - 3000 PSI	GAS OUTLET: ~1400 - 1600°F ~100 - 200 PSI
BOILER METAL: <800°F ~1700 - 2000 PSI	STEAM GENERATOR METAL: ~1100 - 1300°F ~1300 - 3000 PSI	RECEIVER METAL: ~1500 - 1800°F ~100 - 200 PSI
SUPERHEATER METAL: ~1200°F ~1500 - 1800 PSI	LIQUID METAL OUTLET: ~1100 - 1300°F ~100 - 300 PSI	
	RECEIVER METAL: ~1200 - 1400°F ~100 - 300 PSI	

1kPa = 6.89 psi
$T[K] = (T_1[^\circ F] + 459.67)/1.8$

Figure 84. Maximum Temperatures and Pressures in Various Systems

f. Code Information - For each combination of component load and conditions the requirements in each Section of the Code will be listed.

Recommendations

The matrix of information developed in Phase I will be used to complete the overall objectives in Phase II.

a. Interim Structural Design Standard - The major objective is the development and recommendation of an interim structural design standard. Rules and Criteria in the Code related to each component or the elements of each component will be evaluated on the basis of the information gathered in Phase I. This will be the core of the recommended standard. If modifications of the rules or criteria in the code are deemed necessary and the technical information to carry out such modification is available, then the modifications will be included in the recommended standard.

b. Identify Tests and Additional Work - When inadequate information is shown to exist and when Code modification is indicated, tests and other work necessary to upgrade the interim document will be identified.

Progress to Date

The attached schedule (Figure 85) indicates the direction of work on each task and the timeframe of work on the overall objectives. Task 1 indicated in the schedule was started in June 1977. The loading, environmental conditions, and failure modes of the MMC/FWC receiver system was investigated. A preliminary review of the MDAC/Rocketdyne and Honeywell/B & W systems has been initiated. Task 2 and Task 3 were initiated in July. The initial portion of Section I of the Code has been reviewed, including the design rules for tubes, pipes, headers, and drums. The basis of these rules are currently being reviewed. Seventeen references related to failure data and service failure history of pressure vessels and power and chemical processing systems have been collected and partially reviewed.

This work has begun with the study of the information that is available. Its level of success is highly dependent on that information and on the additional information that can only be obtained from the community of designers of CRSTPS systems.

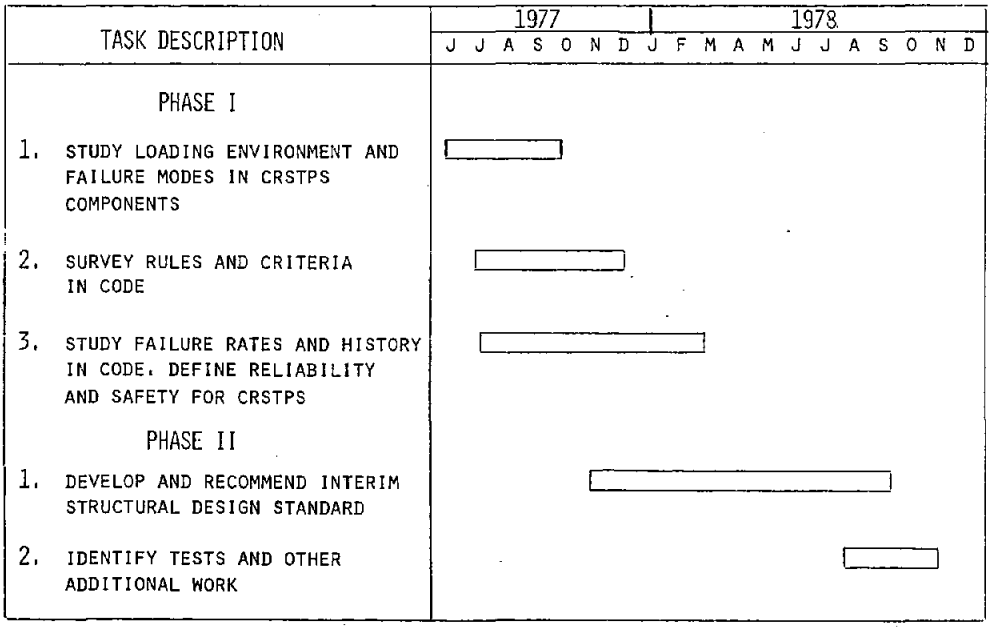

Figure 85. Program Schedule For an Interim Structural Design Standard For Solar Energy Applications

MATERIALS TESTING FOR CENTRAL RECEIVER SOLAR THERMAL POWER SYSTEMS

S. Majumdar and D. R. Diercks
Argonne National Laboratory

Background

The present program is concerned with the determination of specific elevated-temperature mechanical properties of materials used for critical components in solar central receiver power systems. Two general features of solar central receiver operating conditions are distinctly different from the operating conditions associated with fossil and nuclear electrical generating plants. The first is the highly cyclic nature of the thermal loading of critical components. Solar plants will undergo at least one major start-up and shut-down cycle per day, with the likelihood of additional thermal cycles being imposed by intermittent cloud cover and unscheduled maintenance and repair. Thus critical elevated-temperature components may be expected to accumulate of the order of tens of thousands of strain cycles over a 30-year design life. In addition, repeated thermal cycling of superheater tubing while under internal pressure can lead to incremental growth or ratchetting. The analyst must therefore design against structural failure due to thermal fatigue and creep-fatigue interaction and must also avoid excessive deformation due to incremental growth.

The second aspect of solar-plant operating conditions likely to cause design difficulties is that, during steady-state operation, the boiler and superheater tubing will be loaded nonaxisymmetrically at elevated temperatures (Figure 86). In particular, critical passes of the superheater tubing will be loaded during daytime operation such that the outer tubing wall on the high-temperature side will experience a large compressive axial stress and a moderate compressive hoop stress (Figure 87). On the other hand, the inner wall on the high-temperature side will be subjected to a compressive axial stress and a small tensile hoop stress. Considerable constitutive relation information under compressive and mixed tensile-plus-compressive creep conditions will be required to permit structural analyses of the components. In addition, failure criteria for nonaxisymmetric multiaxial tensile-plus-compressive creep-fatigue conditions must be developed. Finally, the nonaxisymmetric loading further complicates the ratchetting analysis.

Elevated-temperature design rules applicable to solar-power-plant boilers and piping are set forth in Section I of the ASME Boiler and Pressure Vessel Code. However, Section I was not developed with the highly cyclic and often complex loading conditions of solar-power-plant components in mind,

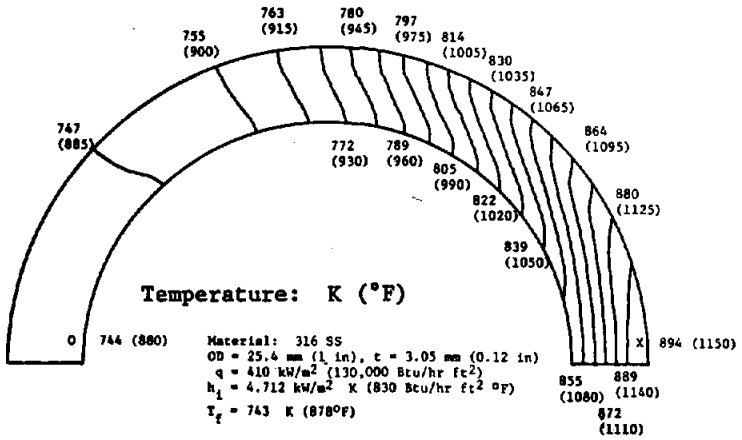

Figure 86. Temperature Distribution in Superheater Tube Pass 5A

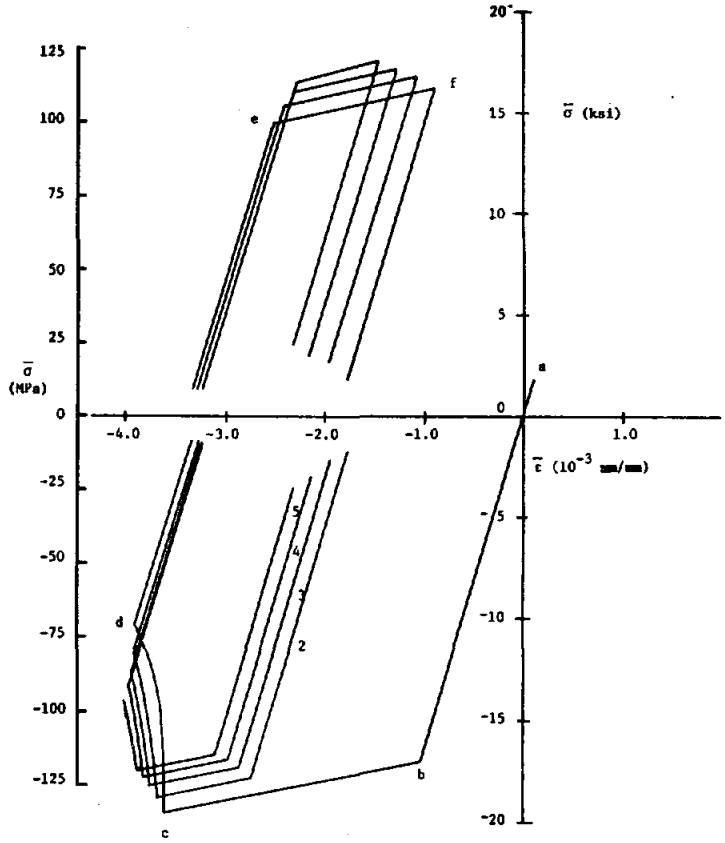

Figure 87. Effective Stress Versus Effective Strain for Element 5 of Pass 5A

and no specific design rules for treating fatigue, creep fatigue, or ratchetting are provided. Applicable design rules from the nuclear portions of the Code (Section III and Case 1592) are likely to result in excessively conservative designs. For example, Case 1592 would consider the compressive loading on the hot side of the superheater tubing to be as damaging as an equal tensile loading, although available data indicate that this is not the case for many materials, at least for uniaxial loadings. The ratchetting analyses rules of Case 1592 are also likely to be overly conservative when applied to the nonaxisymmetric multiaxial loading of superheater tubing. Thus a modified set of Code rules more appropriate to the design of solar components is needed. The development of these rules, in turn, requires the creation of a supportive base of mechanical-properties data.

In some of the more advanced designs for future solar central receiver systems, the use of liquid sodium is proposed as the coolant in the central receiver tower. The heated sodium would flow from the tower to a steam generator at ground level, where the steam to drive the turbines would be produced. Such an arrangement offers several advantages over the direct generation of steam in the receiver tower, including (1) the benefits of the superior heat-transfer characteristics of the sodium coolant, (2) the elimination of the high internal pressure in the receiver tubing, and (3) the elimination of problems associated with stress-corrosion cracking and departure from nucleate boiling in the receiver tubing. Considerable information has been obtained on sodium effects on structural materials in the Liquid-Metal Fast-Breeder Reactor (LMFBR) program. However, this information, particularly with respect to material sodium compatibility and sodium effects on elevated-temperature mechanical properties, needs to be reviewed and extended to the materials and anticipated operating conditions associated with solar central receiver systems.

Program Description

The present program has been developed in response to the needs outlined above and is divided into three subtasks. The first subtask is concerned with the biaxial creep-fatigue testing of Type 316H stainless steel superheater tubing. Current design procedure for the superheater tubing is to perform a creep-fatigue analysis using elevated-temperature nuclear rules (Code Case 1592) but to ignore creep damage due to compressive stresses. Thus hold times under compressive stresses are assumed to be nondamaging. As stated above, this assumption appears to be reasonable for austenitic stainless steels under uniaxial loading conditions (Tables XXII and XXIII), but it has never been verified for biaxial loading situations, particularly where the stress is tensile in one direction and compressive in the other. Furthermore, virtually no creep-fatigue data exist for Type 316H even under

MATERIALS TESTING FOR CENTRAL RECEIVER SOLAR THERMAL POWER SYSTEMS

S. Majumdar and D. R. Diercks
Argonne National Laboratory

Background

The present program is concerned with the determination of specific elevated-temperature mechanical properties of materials used for critical components in solar central receiver power systems. Two general features of solar central receiver operating conditions are distinctly different from the operating conditions associated with fossil and nuclear electrical generating plants. The first is the highly cyclic nature of the thermal loading of critical components. Solar plants will undergo at least one major start-up and shut-down cycle per day, with the likelihood of additional thermal cycles being imposed by intermittent cloud cover and unscheduled maintenance and repair. Thus critical elevated-temperature components may be expected to accumulate of the order of tens of thousands of strain cycles over a 30-year design life. In addition, repeated thermal cycling of superheater tubing while under internal pressure can lead to incremental growth or ratchetting. The analyst must therefore design against structural failure due to thermal fatigue and creep-fatigue interaction and must also avoid excessive deformation due to incremental growth.

The second aspect of solar-plant operating conditions likely to cause design difficulties is that, during steady-state operation, the boiler and superheater tubing will be loaded nonaxisymmetrically at elevated temperatures (Figure 86). In particular, critical passes of the superheater tubing will be loaded during daytime operation such that the outer tubing wall on the high-temperature side will experience a large compressive axial stress and a moderate compressive hoop stress (Figure 87). On the other hand, the inner wall on the high-temperature side will be subjected to a compressive axial stress and a small tensile hoop stress. Considerable constitutive relation information under compressive and mixed tensile-plus-compressive creep conditions will be required to permit structural analyses of the components. In addition, failure criteria for nonaxisymmetric multiaxial tensile-plus-compressive creep-fatigue conditions must be developed. Finally, the nonaxisymmetric loading further complicates the ratchetting analysis.

Elevated-temperature design rules applicable to solar-power-plant boilers and piping are set forth in Section I of the ASME Boiler and Pressure Vessel Code. However, Section I was not developed with the highly cyclic and often complex loading conditions of solar-power-plant components in mind,

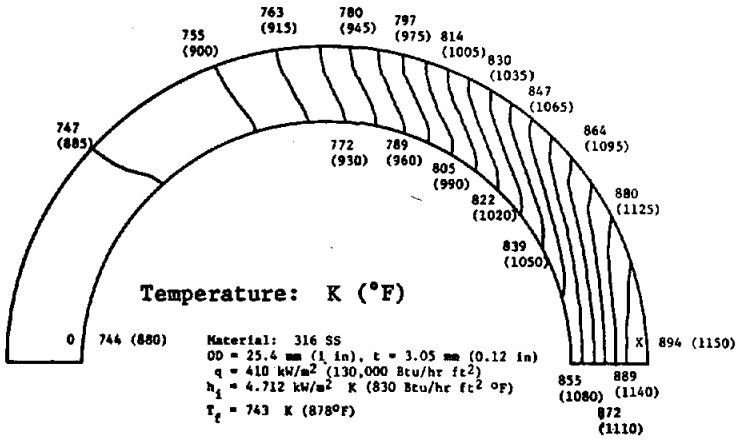

Figure 86. Temperature Distribution in Superheater Tube Pass 5A

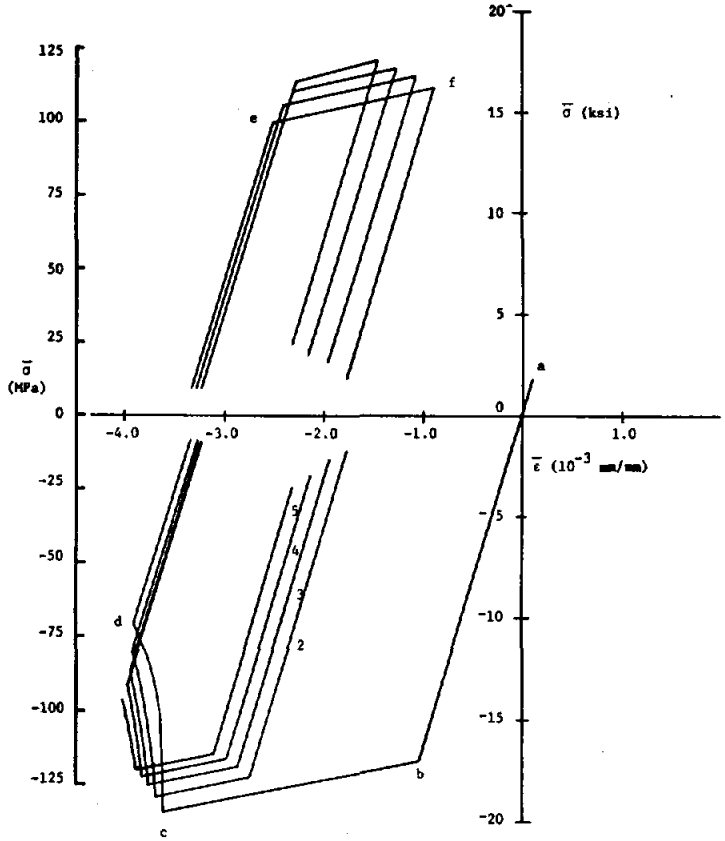

Figure 87. Effective Stress Versus Effective Strain for Element 5 of Pass 5A

and no specific design rules for treating fatigue, creep fatigue, or ratchetting are provided. Applicable design rules from the nuclear portions of the Code (Section III and Case 1592) are likely to result in excessively conservative designs. For example, Case 1592 would consider the compressive loading on the hot side of the superheater tubing to be as damaging as an equal tensile loading, although available data indicate that this is not the case for many materials, at least for uniaxial loadings. The ratchetting analyses rules of Case 1592 are also likely to be overly conservative when applied to the nonaxisymmetric multiaxial loading of superheater tubing. Thus a modified set of Code rules more appropriate to the design of solar components is needed. The development of these rules, in turn, requires the creation of a supportive base of mechanical-properties data.

In some of the more advanced designs for future solar central receiver systems, the use of liquid sodium is proposed as the coolant in the central receiver tower. The heated sodium would flow from the tower to a steam generator at ground level, where the steam to drive the turbines would be produced. Such an arrangement offers several advantages over the direct generation of steam in the receiver tower, including (1) the benefits of the superior heat-transfer characteristics of the sodium coolant, (2) the elimination of the high internal pressure in the receiver tubing, and (3) the elimination of problems associated with stress-corrosion cracking and departure from nucleate boiling in the receiver tubing. Considerable information has been obtained on sodium effects on structural materials in the Liquid-Metal Fast-Breeder Reactor (LMFBR) program. However, this information, particularly with respect to material sodium compatibility and sodium effects on elevated-temperature mechanical properties, needs to be reviewed and extended to the materials and anticipated operating conditions associated with solar central receiver systems.

Program Description

The present program has been developed in response to the needs outlined above and is divided into three subtasks. The first subtask is concerned with the biaxial creep-fatigue testing of Type 316H stainless steel superheater tubing. Current design procedure for the superheater tubing is to perform a creep-fatigue analysis using elevated-temperature nuclear rules (Code Case 1592) but to ignore creep damage due to compressive stresses. Thus hold times under compressive stresses are assumed to be nondamaging. As stated above, this assumption appears to be reasonable for austenitic stainless steels under uniaxial loading conditions (Tables XXII and XXIII), but it has never been verified for biaxial loading situations, particularly where the stress is tensile in one direction and compressive in the other. Furthermore, virtually no creep-fatigue data exist for Type 316H even under

TABLE XXII. AVAILABLE COMPRESSIVE HOLD-TIME FATIGUE DATA FOR TYPE 316H STAINLESS STEEL (SA)

Temperature (°C)	$\Delta\epsilon_t$ (%)	$\dot{\epsilon}_t$ (s^{-1})	Hold Time[a] (min)	Cycles to Failure	Data Source[b]
566	2.0	0.004	0	564	ANL
			0	473	BCL
			6T	163	BCL
			6C	665	BCL
593	1.0	0.004	0	2040	ANC
			0	2241	ANC
			0.6T	1170	ANC
			0.6C	2134	ANC
			6T	393	ANC
			6C	1938	ANC
650	1.0	0.004	0	1122	ANL
			0	1721	ANL
			1T	460	ANL
			1C	1690	ANL
	2.0	0.004	0	354	BCL
			0	459	ANL
			6T	81	BCL
			6C	386	BCL

a - T indicates tension hold time; C indicates compression hold time
b - ANL is Argonne National Laboratory, Argonne, Illinois
GE, General Electric Company, Everdale, Ohio
BCL, Battelle Columbus Laboratories, Columbus, Ohio.

TABLE XXIII. COMPRESSIVE HOLD-TIME FATIGUE DATA FOR TYPE 304 STAINLESS STEEL (See Ref. 2)

Temperature (°C)	$\Delta\epsilon_t$ (%)	$\dot{\epsilon}_t$ (s^{-1})	Hold Time[a] (min)	Cycles to Failure	Data Source[b]
593	1.0	0.004	0	3826	ANL
			0	3740	ANL
			1T	1171	ANL
			1C	3344	ANL
			10T	706	ANL
			10C	2810	ANL
650	2.0	0.004	0	765	GE
			0	724	ANL
			30T	146	GE
			30T	165	GE
			30C	480	GE
			30C	409	GE

a - T indicates tension hold time; C indicates compression hold time
b - ANL is Argonne National Laboratory, Argonne, Illinois
GE, General Electric Company, Everdale, Ohio

uniaxial loading conditions. Under this subtask, biaxial creep-fatigue tests (constant tensile hoop stress and cyclic axial strain with hold times in compression) will be performed on Type 316H superheater tubing material. Times-to-failure will be accelerated by increasing the magnitude of the axial strain range over that expected in service and by using considerably shorter compressive hold times.

Under the second subtask, a comprehensive survey of available information on sodium effects on candidate materials for solar thermal electric piping and steam generators will be conducted. The survey will include information on sodium effects on mechanical properties, sodium compatibility, and mass-transfer, as well as recommendations for future testing.

The third subtask is concerned with mechanical-properties data generation in support of the ASME Code development. This work interfaces directly with a program being conducted by Foster Wheeler Energy Corporation entitled "An Interim Structural Design Standard for Solar Energy Applications." In the Foster Wheeler program, design standards and criteria are to be established for solar central receiver systems that will eventually lead to the development of a set of ASME Boiler and Pressure Vessel Code rules. A critical phase in this development is the formulation and execution of an extensive mechanical-testing program to generate the required design-limits data. This mechanical-testing program is to be conducted by Argonne National Laboratory under this

subtask. The details of the test matrices have not been established by Argonne and Foster Wheeler; however, the mechanical-testing effort is expected to focus on elevated-temperature fatigue testing in the medium-to-high cycle range and on uniaxial and biaxial compressive creep testing.

Projected schedules and levels of effort for the three subtasks are as follows:

Subtask	Begin	End	Total Man Years
1	7/77	8/78	1.5
2	10/77	6/78	0.5
3	12/77	11/79	4.0

Status of Subtask 1

Approximately 30 feet of Type 316H stainless steel tubing (1 in. OD and 0.12 in. nominal wall thickness) have been procured from Pacific Tube Company, Los Angeles. The biaxial fatigue testing will be conducted in a closed-loop servo-controlled MTS biaxial test system (axial push-pull and internal pressure) that is available at Argonne National Laboratory. The specimen design is shown in Figure 88. A 0.5-in. gauge length axial extensometer for measuring axial strain and a diametral extensometer for measuring diametral strain have been designed and built. Heating of the specimens will be achieved by induction coils located at the center 3 in.

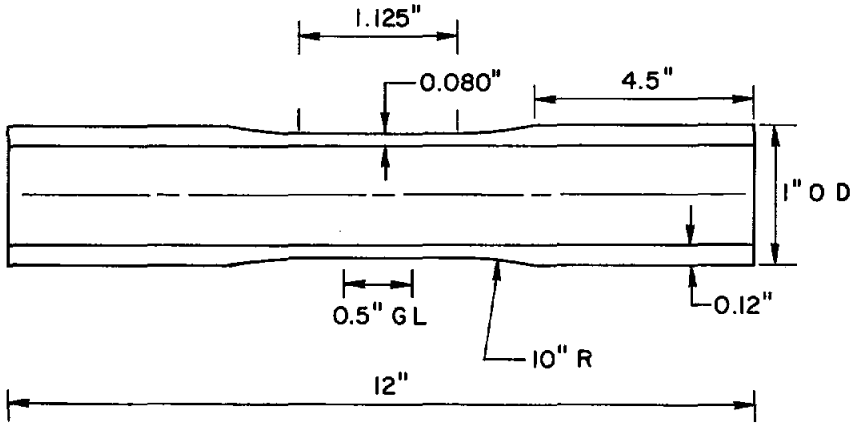

Figure 88. Biaxial Fatigue Specimen (Not to scale)

The proposed test matrix is shown in Table XXIV. The internal pressure has been chosen to produce a hoop stress in the specimen representative of that present in a superheater tube under service conditions. The axial strain range has been increased from the expected prototypic values in order to complete the tests in a year. Several reference tests with zero internal pressure are also planned. The test temperature has been tentatively selected as 1100°F, which approximates the highest temperature expected at the inner surface of the tube. We propose to test the tubing in the as-received condition.

Currently, we are awaiting delivery of specimens that are being machined at Argonne National Laboratory. Barring unforeseen difficulties, testing should commence within two months.

TABLE XXIV. PROPOSED TEST MATRIX FOR SUBTASK 1

Temperature = 1100°F
Cyclic Axial Strain Rate = 0.004 s^{-1}

Axial $\Delta\epsilon_t$ (%)	P_i (psi)	Hold Time (min)	Expected Life	
			N_f	t_f (h)
0.5	0	0	30,000	20
	1100	0	20,000	14
	1100	1C	20,000	350
	1100	5C	20,000	1680
	0	1C	30,000	520
0.75	0	0	7,000	7
	1100	0	5,000	5
	1100	1C	5,000	90
	1100	10C	5,000	840
	0	1C	7,000	124

Total Time = 3650
Add 50% for Duplicate Tests = 1825
Total Testing Time = 5475 h

References

1. Central Receiver Solar Thermal Power System, Phase I, Progress Report for the Period Ending December 31, 1975, SAN/1110-76/T1, Martin Marietta Corporation, Denver, Colorado.

2. D. R. Diercks and D. T. Raske, "Elevated-Temperature, Strain-Controlled Fatigue Data on Type 304 Stainless Steel: A Compilation, Multiple Linear Regression Model, and Statistical Analysis," Argonne National Laboratory, ANL-76-95 (1976).

EXPERIMENTAL STUDY OF CONVECTIVE LOSSES FROM SOLAR RECEIVERS

A. M. Clausing
University of Illinois

The objectives of this study, which has just been initiated, are: (1) to establish techniques by which the combined influences of natural and forced convection on the convective heat loss can be modeled and experimentally studied, (2) to design and build a cryogenic facility for the experimental investigation, and (3) to test models of solar receivers and obtain expressions which enable the prediction of the convective loss. The motivation for this study is:

1. Our poor understanding of the interaction between free and forced convection and our inability to estimate the convective loss with any degree of confidence.

2. The inability to obtain accurate convective loss data from receiver subsystem research experiments because energy balances cannot be effected with sufficient precision.

3. The inapplicability of data from scaled receivers due to the change in the relative importance of natural convection with the size of the receiver.

An examination of the ratio of the characteristic velocity due to buoyant influences to typical wind velocities at receiver elevations has indicated that the effects of both natural and forced convection have significant influences on the convective losses from pilot plant and commercial size solar receivers.

Part of the experimental study utilizes a water table to determine the behavior of separated flows in and around solar receivers. Both still pictures and color movies are being used to record the separated flow patterns. The main portion of the experimental program consists of designing and constructing a cryogenic wind tunnel, and performing tests of receiver models in this facility. The cryogenic environment is being used to enable perfect modeling of both the Grashof number and the Reynolds number in order to examine the interaction between, and the relative importance of, both natural and forced convection. The design of the cryogenic facility is partially completed at this time.

HYDRAULIC STABILITY OF SOLAR BOILERS

Herbert S. Isbin
University of Minnesota

At the University of Minnesota, we are initiating a modest program to study the hydraulic stability of heated channels connected in parallel arrays. My discussion will present an overview of what we intend to do, and therefore your comments at the start of our studies should be most helpful.

All of us, I am sure, are aware of possible oscillations in the flow of fluids in heated parallel channels. Flow instabilities are highly dependent upon system geometry and will vary to various degrees as flow parameters are changed. An effective way of minimizing or even avoiding such flow oscillations is to introduce a major throttling pressure drop in the inlet section, particularly for forced convection loops. A variety of dimensionless parameters has been introduced to delineate possible regions for stable and unstable flows. Unfortunately, the uncertainties in the model developments are too large and only trends in flow behaviour might be anticipated.

Much of the early work done on flow excursions and oscillations in boiling, two-phase flow systems was motivated by studies seeking to define thermal-hydraulic stability criteria for nuclear reactor cores cooled by forced convection of water. Additionally, for a given flow geometry, coolant, and system conditions, limits could be determined experimentally for the maximum heat flux, frequently labelled the critical heat flux or the burnout flux. The present designs for the solar boilers recognize this limitation too, and the intent of the design for the steady-stage operations and for the transient operations is to provide a reasonable safety margin between operational heat fluxes and the critical heat fluxes. Flow oscillations also may be undesirable from the standpoint of producing forced vibrations and possibly cycling of wall temperatures.

We suggest that the federal agency sponsoring the development of solar boilers should have effective and independent methods for predicting thresholds for unstable or oscillatory flows in parallel heated channels and for confirming safety margins related to the critical heat fluxes. The methods should be based upon models which can be verified by tests already undertaken. The progress of these studies should be helpful in determining what, if any, additional tests need be made to ascertain confidence in the predictive tools developed. The analytical tools should be helpful in determining what geometrical changes and operating conditions enhance stable flows in the solar boilers. We appreciate that several companies may have proprietary bases for their model developments and for their codes. Our model developments and code work should be helpful to all parties if we can coordinate an exchange of basic information.

Our analysis starts with the types of conservation equations already established for one-dimensional geometries taking into account some of the observed characteristics of steam-water flows. The mixture continuity and energy equations, and the mixture momentum equation are written in terms of the center-of-mass of the mixture. The vapor velocity may differ from the liquid velocity, and the velocity and void fraction profiles may be non-uniform at a cross section. Drift flux constitutive equations take these phenomena into account and are available for a variety of flow conditions. The drift flux is used in the mixture momentum equation and in the continuity equation for the vapor phase. With some simplifications and with available empirical correlations, a modest degree of thermal nonequilibrium between vapor and liquid phases may be taken into account.

Whereas an accounting will be made of the axial nonuniformity of the heat flux, our initial work will use only a simplified approach to the radial flux distributions. In general, we would seek to add complexity to the model in stages to determine and to better understand what phenomena need to be modelled to yield satisfactory results. As examples, we might ask what sophistication is needed in specifying flow regimes and flow regime transients? It should be remembered that the transients being considered for the flow regimes are relatively slow ones with expected periods of the order of magnitude of one second. We would expect that steady state correlations for two-phase flow phenomena would be applicable for these slow transients. The fluid enters the heated channels with a specified flow rate, inlet subcooling, and a given system pressure. The heat flux is specified as a function of axial position. In our first studies, we would neglect the effects of heat storage in the channel walls. The outlet system pressure is also specified so that the flow through the parallel channels is taken to be under a constant pressure drop condition. We will then examine the effects on the flow is a perturbation, for example, is made in the heat flux. We would seek to determine under what set of system and flow conditions that the dynamic effects involved with the gravitational, frictional and acceleration components of the pressure drop produce excursions or oscillating flows. The steady-state conditions used in the initialization conditions need to adequately describe the flow behavior starting with a subcooled liquid progressing to saturated boiling, and providing for increasing steam voids through film boiling to steam flows with entrained water droplets. Those of you who have already carried out the steady-state calculations know that even these calculations could entail varying degrees of sophistication to approximate the progressive change in the steam void fractions and the thermal nonequilibrium effects in subcooled nucleate boiling, as well as in the regions involving water entrainment in superheated steam. The two-phase flow regimes may involve bubbling, slug churn, and annular patterns. The flow regimes are illustrated in Figure 89, and in Figures 90 and 91, as examples, we show the predicted flow pattern maps which might be applicable for the Honeywell solar boiler tubes and for the riser. The modelling approach was developed by A. E. Dukler and Y. Taitel (NUREG-0162, "Flow Regime Transitions for Vertical Upward Gas Liquid Flow," Jan. 1977). In Table XXV,

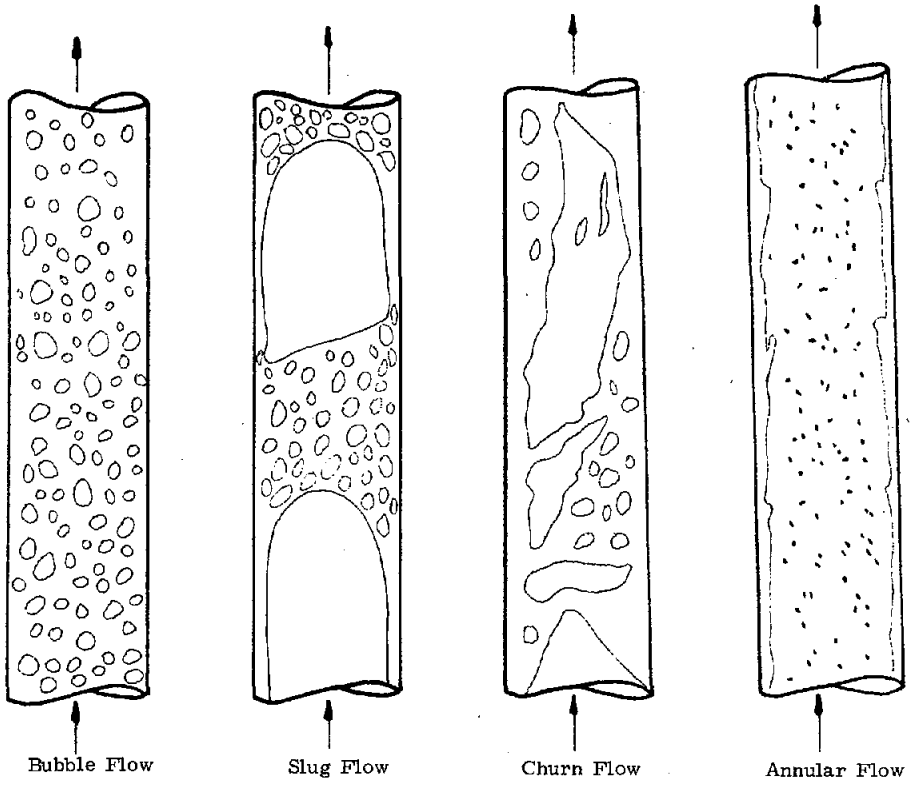

Figure 89. Flow Patterns in Vertical Flow

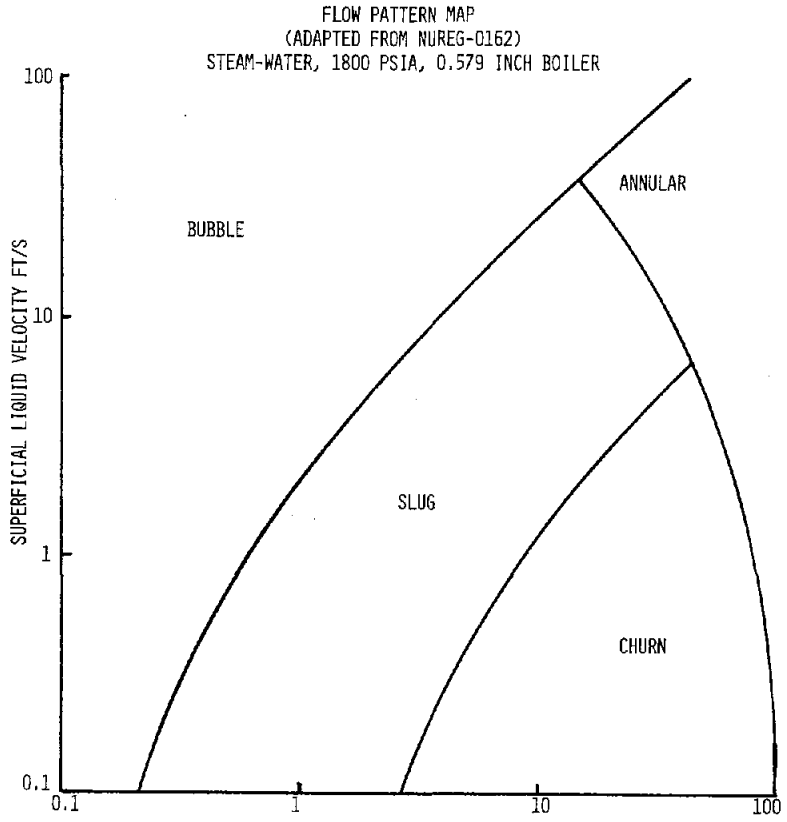

Figure 90. Superficial Steam Velocity (ft/s)

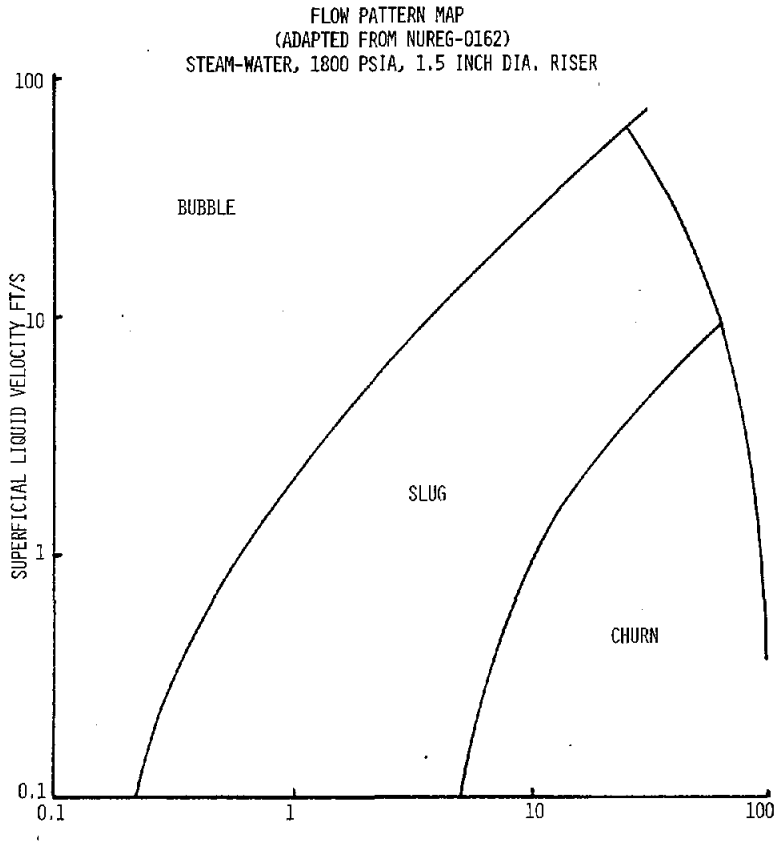

Figure 91. Superficial Steam Velocity (ft/s)

TABLE XXV. ESTIMATION OF VOID FRACTIONS STEAM-WATER FLOWS, 1800 PSIA, 1.5 INCH DIAMETER RISER STEAM FLOW 1.1×10^6 lb/h-ft^2

	Void Fraction			
Quality	Japanese (1)	Chisholm (2)	Martinelli (3)	Hughmark (4)
0.33	0.62	0.77	0.71	0.73
0.50	0.71	0.86	0.81	0.80
0.67	0.79	0.92	0.88	0.84
0.91	0.83	0.97	0.97	0.88

(1) Y. Yamazaki and K. Yamaguchi, J. Nuclear Science and Technology, 13 (12), pp. 701-707 (December 1976).

(2) D. Chisholm, Int. J. Heat and Mass Transfer, 10, pp. 1767-1778 (1967).

(3) From original curves.

(4) G. A. Hughmark, Ind. Eng. Chem., 2, No. 4, pp. 315-320 (1963); Chem. Eng. Prog., 58, p. 62 (1962).

for a given steam flow in the riser at a given pressure, and for varying qualities in the steam-water flow, several methods were used to estimate the void fractions. Two-phase frictional pressure drop relationships are available and many two-phase heat transfer correlations need to be examined. Applications appropriate for the conditions selected will be pursued.

Our work on formulating numerical solutions for the transient analyses is just beginning and we have no results to report. Figure 92 is an adaption from E. R. Quandt (WAPD-T-1134, March 1960) illustrating possible flow oscillations in a heated channel due to step increases in the power input.

With reference to the flows in the parallel channels, we need the details of the flow systems being used in the solar towers and the system input parameters. It would be helpful to obtain the steady-state flow conditions in whatever details are available for the initialization states. We would like to exchange information on selecting appropriate correlations so that we may compare values we would calculate with project predicted values and with whatever measurements may have been made or planned.

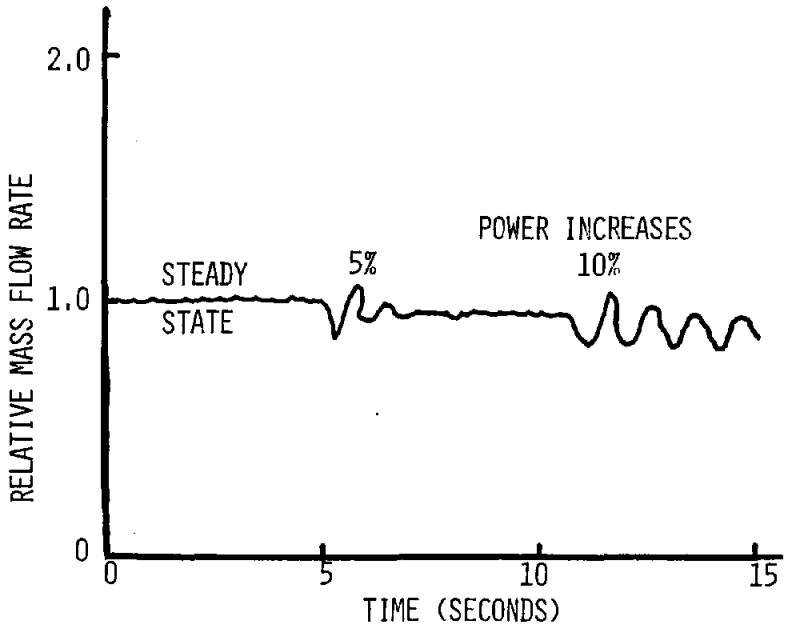

Figure 92. Flow Oscillations

DISTRIBUTION:

TIC/UC-62 (298)
A. C. Skinrood, 8132 (200)